

AD-A119 729

MINNESOTA UNIV MINNEAPOLIS DEPT OF MECHANICAL ENGIN--ETC F/6 21/5
CURVATURE EFFECTS ON THE HEAT TRANSFER PERFORMANCE OF THREE-DIM--ETC(U)
AUG 82 E R ECKERT; R J GOLDSTEIN DAA629-79-C-0117

UNCLASSIFIED

ARO-16595.6-E6

NL

1-1
ADA
1-1

END

DATE

FILED

14-82

DTIC

REPORT DOCUMENTATION PAGE		READ INSTRUCTIONS BEFORE COMPLETING FORM
1. REPORT NUMBER 16595.6-EG	2. GOVT ACCESSION NO. AD-A119729	3. RECIPIENT'S CATALOG NUMBER
4. TITLE (and Subtitle) "Curvature Effects on the Heat Transfer Performance of Three-Dimensional Film Cooling of Gas Turbine Blades"	5. TYPE OF REPORT & PERIOD COVERED Final Report 6/25/79-6/24/82	
7. AUTHOR(s) E. R. G. Eckert and R. J. Goldstein	6. PERFORMING ORG. REPORT NUMBER	
8. PERFORMING ORGANIZATION NAME AND ADDRESS Dept. of Mech. Engr. University of Minnesota Minneapolis, Minnesota 55455	9. CONTRACT OR GRANT NUMBER(s) DAAG29-79-C-0117	
11. CONTROLLING OFFICE NAME AND ADDRESS	10. PROGRAM ELEMENT, PROJECT, TASK AREA & WORK UNIT NUMBERS	
14. MONITORING AGENCY NAME & ADDRESS (if different from Controlling Office)	12. REPORT DATE August 1982	
	13. NUMBER OF PAGES 58	
	15. SECURITY CLASS. (of this report)	
	15a. DECLASSIFICATION/DOWNGRADING SCHEDULE	
16. DISTRIBUTION STATEMENT (of this Report) Approved for public release; distribution unlimited.		
17. DISTRIBUTION STATEMENT (of the abstract entered in Block 20, if different from Report)		
18. SUPPLEMENTARY NOTES THE VIEW, OPINIONS, AND/OR FINDINGS CONTAINED IN THIS REPORT ARE THOSE OF THE AUTHOR(S) AND SHOULD NOT BE CONSTRUED AS AN OFFICIAL DEPARTMENT OF THE ARMY POSITION, POLICY, OR DE CISION, UNLESS SO DESIGNATED BY OTHER DOCUMENTATION.		
19. KEY WORDS (Continue on reverse side if necessary and identify by block number) film cooling, heat transfer, gas turbine		
20. ABSTRACT (Continue on reverse side if necessary and identify by block number) Film cooling is used extensively for the blades of high-performance high-temperature gas turbines, especially for aircraft gas turbines. In this method, a film of coolant is injected into the boundary layer covering the skin of the blades and creating a cool layer which separates the blade surface from the hot gas stream and, in this way, reduces the blade temperature. For best performance the coolant should be injected through a slot or a strip of porous ma-		

DD FORM 1 JAN 73 1473

EDITION OF 1 NOV 65 IS OBSOLETE
S/N 0102-LF-014-6601

SECURITY CLASSIFICATION OF THIS PAGE (When Data Entered)

AD A119729

DTIC FILE COPY

DTIC
SELECTED
SEP 29 1982
H

Abstract (continued)

terial. This, however, is not possible for turbine blades because of strength considerations, and the coolant is injected through one or several rows of holes. For aircraft gas turbines, air is used as a coolant.

The present investigation, therefore, is concerned with the cooling performance of film cooling when cooling air is injected into the boundary layer through one or two rows of holes. A standard configuration of the coolant holes is used because it has been used in previous investigations and because configurations in actual turbine blades are close to it. The cooling holes are arranged at a distance apart equal to three times the hole diameter. For injection through two rows of holes, the two rows are staggered and the centers of the holes are on the corners of equilateral triangles. The channels which end at the blade skin in the cooling holes are inclined by an angle of 35° against the skin surface in the downstream direction.

All experiments were conducted with air in the mainstream and as a coolant. The velocities were of the order of 20 m/s and temperature differences were kept small. The effects of Mach number and aerodynamic heating are, therefore, not included. In a gas turbine, the highest temperature is that in the mainstream, the cooling air is the lowest, and the skin temperature has values in between. The heat flux at the skin surface is directed from the boundary layer into the skin. The experiments are performed with the cooling air having the highest temperature and the heat flux having the direction from the skin into the boundary layer. This results in better experimental arrangements. Film cooling effectiveness values and heat transfer coefficients are independent of the direction of the heat flux as long as temperature differences involved are sufficiently small to consider the transport properties involved as constant.



Accession For	
NTIS GRA&I	<input checked="" type="checkbox"/>
DTIC TAB	<input type="checkbox"/>
Unannounced	
Justification	
By _____	
Distribution/	
Availability Codes	
Dist	Avail and/or Special
A	

HEAT TRANSFER LABORATORY

FINAL REPORT

"CURVATURE EFFECTS ON THE HEAT TRANSFER PERFORMANCE OF
THREE-DIMENSIONAL FILM COOLING OF GAS TURBINE BLADES"

Submitted to:

Army Research Office
P.O. Box 1211
Research Triangle Park, North Carolina 27709

Contract # DAAG 29-79-C-0117

by

E. R. G. Eckert
Regents' Professor Emeritus

and

R. J. Goldstein
Professor and Head

August 1972

UNIVERSITY OF MINNESOTA

INSTITUTE OF TECHNOLOGY

School of Mechanical and Aerospace Engineering
Department of Mechanical Engineering

MINNEAPOLIS, MINNESOTA 55455



82 09 28 019

FINAL REPORT

"CURVATURE EFFECTS ON THE HEAT TRANSFER PERFORMANCE
OF THREE-DIMENSIONAL FILM COOLING OF GAS TURBINE BLADES"

Submitted to:

Army Research Office
P. O. Box 1211
Research Triangle Park, North Carolina 27709

Contract # DAAG29-79-C-0117

by

E. R. G. Eckert
Regents' Professor Emeritus

and

R. J. Goldstein
Professor and Head

Department of Mechanical Engineering
University of Minnesota
111 Church Street SE
Minneapolis, Minnesota 55455

August 1982

INTRODUCTION

Film cooling is used extensively for the blades of high-performance, high-temperature gas turbines, especially for aircraft gas turbines. In this method, a film of coolant is injected into the boundary layer covering the skin of the blades and creating a cool layer which separates the blade surface from the hot gas stream and, in this way, reduces the blade temperature. For best performance the coolant should be injected through a slot or a strip of porous material. This, however, is not possible for turbine blades because of strength considerations, and the coolant is injected through one or several rows of holes. For aircraft gas turbines, air is used as a coolant.

The present investigation, therefore, is concerned with the cooling performance of film cooling when cooling air is injected into the boundary layer through one or two rows of holes. A standard configuration of the coolant holes is used because it has been used in previous investigations and because configurations in actual turbine blades are close to it. The cooling holes are arranged at a distance apart equal to three times the hole diameter. For injection through two rows of holes, the two rows are staggered and the centers of the holes are on the corners of equilateral triangles. The channels which end at the blade skin in the cooling holes are inclined by an angle of 35° against the skin surface in the downstream direction.

All experiments were conducted with air in the mainstream and as a coolant. The velocities were of the order of 20 m/s and temperature differences were kept small. The effects of Mach

number and aerodynamic heating are, therefore, not included. In a gas turbine, the highest temperature is that in the mainstream, the cooling air temperature is lowest, and the skin temperature has values in between. The heat flux at the skin surface is directed from the boundary layer into the skin. The experiments are performed with the cooling air having the highest temperature and the heat flux having the direction from the skin into the boundary layer. This results in better experimental arrangements. Film cooling effectiveness values and heat transfer coefficients are independent of the direction of the heat flux as long as temperature differences involved are sufficiently small to consider the transport properties involved as constant.

Parameters Describing the Heat Transfer Performance

The temperatures determining convective cooling of a boundary layer are the temperature of the mainstream and the wall surface temperature. Sometimes the heat flux from the surface into the airstream is prescribed instead of the surface temperature. Film cooling performance depends on an additional temperature --namely, that with which the coolant leaves the injection holes. Various methods are possible to systematically describe the effect of these parameters on the heat transfer performance of film cooling. One way, which is extensively used in publications on film cooling, is based on two parameters: a film cooling effectiveness and a specially-defined heat transfer coefficient. The film cooling effectiveness parameter is

$$\eta = \frac{T_{aw} - T_{\infty}}{T_e - T_{\infty}} \quad (1)$$

In this equation, T_{∞} is the mainstream temperature (the recovery temperature has to be used when the effect of aerodynamic heating becomes important). T_e is the temperature at which the cooling air enters the boundary layer. T_{aw} is that temperature which a location of the cooled surface under consideration assumes in film cooling provided no heat passes through the surface.

Gas turbine blades are equipped with internal cooling in addition to the film cooling and, correspondingly, in general, heat passes through the skin surface and is picked up by the internal cooling air flow or is conducted away within the skin. A heat transfer coefficient is introduced to describe this situation and is defined by Eq. 2

$$q = h (T_w - T_{aw}) \quad (2)$$

in which q denotes the heat flux through the skin surface per unit time and area and h is the heat transfer coefficient. It can be seen that it is defined with the difference between the actual wall temperature, T_w , and that temperature which the wall surface assumes under adiabatic conditions. Equation 2 has the advantage that it makes the heat flux zero when the wall temperature, T_w , is equal to the adiabatic wall temperature, T_{aw} , as required by definition. Many experiments have also established that the heat transfer coefficient defined by this equation differs little from the heat transfer coefficient which exists on a surface exposed to a boundary layer flow without film cooling as long as one ex-

cludes conditions in the close neighborhood of the injection holes. This makes it possible to use the extensive amount of information which is available on normal convective cooling in predicting the heat transfer performance of film cooling. Equations 1 and 2 are obtained by superposition of solutions for the energy equation describing film cooling which is linear in temperature when the properties determining the flow and heat transfer can be considered as constant and having the same value for the mainstream fluid and the coolant.

A different method has been proposed and is used for full-coverage film cooling in which all of the surface to be cooled is provided with a regular pattern of holes through which a coolant is injected. The process approaches in the limit of an infinitely-large number of infinitely-small holes the transpiration cooling method, and the parameters which have been used in transpiration cooling are being used to also describe full-coverage film cooling. For the normal film cooling processes which are considered here, the method using Eqs. 1 and 2 has the advantage listed above and is therefore preferable.

The Effect of Curvature of a Turbine Blade on Film Cooling Performance

The majority of research papers published on film cooling describe the results of experiments in which a flat plate is used as the film-cooled wall. Experiments obtained in this way were used in design calculations for gas turbine blades based on the reasoning that the heat transfer process in a boundary layer is

influenced by surface curvature only indirectly through the pressure variation in the main stream as long as the boundary layer thickness is small compared to the radius of the surface curvature. For three-dimensional film cooling this may not apply because the jets leaving the holes sometimes penetrate deep into or through the boundary layer. A series of experiments, which are described in detail in Appendices 1 and 2, have, therefore, been performed in our laboratory to study the effect of surface curvature on film cooling with injection through holes.

The experiments were performed in a cascade tunnel described in Appendix 1. Six blades with the shape shown in Fig. 1 are located in the channel and the two central blades are equipped with either one or two rows of cooling holes. The blade shape is the same for the experiments with one row of holes. The following parameters determine the film cooling performance. The main flow Reynolds number, Re_D , is defined with the freestream velocity, V_∞ , at the outer edge of the boundary layer, the density and viscosity of the main flow, and the diameter, D , of the cooling holes. This Reynolds number had a value of approximately 3000, which is close to the value in actual gas turbines; the ratio of the displacement thickness of the boundary layer to the hole diameter was approximately 0.09 in our experiments; the ratio, $M = \rho_e V_e / \rho_\infty V_\infty$, of the mass flux of cooling air leaving the injection holes to the mass flux in the main stream had values between 0.2 and 2. The effectiveness also depends on the laminar or turbulent condition of the boundary layer and in the injected air as

shown in Appendix 3. Both streams were turbulent in the present study.

A heat-mass transfer analogy was used in the present experiments. The mainstream air and the cooling air were at the same temperature. Mass transfer was created within the boundary layer in a way that a different gas (helium, freon) was mixed with the "cooling" air and was injected into the interior of the hollow blade shown in Fig. 1 through a tube with a number of holes. This gas mixture then left the blade through the cooling holes and the local concentration in the boundary layer close to the blade surface was measured by samples which could be withdrawn through small holes located downstream of the cooling holes. Film cooling effectiveness values can be determined from the measured concentrations through the heat-mass transfer analogy, the validity of which is well proven by previous experiments.

A sample of the results obtained for one row of cooling holes is shown in Fig. 2. The effectiveness values $\bar{\eta}$ averaged in a spanwise direction are plotted in this figure for two values of the ratio of the distance, X , downstream from the cooling holes to the hole diameter, D . The parameter $I \cos^2 \alpha$ used on the abscissa is defined in the following way:

$$I \cos^2 \alpha = \frac{\rho_e V_e^2}{\rho_\infty V_\infty^2} \cos^2 \alpha \quad (3)$$

in which ρ denotes the density, V the velocity, and α the angle under which the coolant passages are inclined towards the blade

surface. The index e refers to the exit of the coolant passages and the index ∞ to conditions in the mainstream at the outer edge of the boundary layer. This parameter compares the component of the momentum flux of the fluid leaving the cooling holes parallel to the film-cooled surface with the momentum flux in the mainstream and can be shown to be an important parameter describing the flow interaction between the coolant jet and the mainstream (Appendix 1). In Fig. 2, the density ratio is close to 1 and $\cos^2 \alpha$ has a value of 0.671. For this density ratio, V_e^2/V_∞^2 is equal to the square of the blowing parameter, M , which is conventionally used in film cooling. Results are presented in the figure which has been obtained on the concave (pressure) wall and on the convex (suction) wall of the turbine blade. Results are also added which were previously obtained on a flat film-cooled wall. The figure demonstrates a large effect of curvature on film cooling such that the effectiveness is up to twice as large on a convex wall and only one-half as large on a concave wall as on a flat plate for values of the momentum flux ratio $I \cos^2 \alpha$ smaller than 1. The relative position of the effectiveness values is reversed for values of the momentum flux ratio larger than 1 but the difference is not as large. The effect of curvature is smaller for film cooling with injection through two rows of holes, as shown in Fig. 3, but it is still sufficiently large that it has to be included in design calculations for gas turbine blades. A discussion of the physical processes which lead to this effect of curvature is contained in Appendices 1 and 2.

Laminar Versus Turbulent Boundary Layer and Coolant Injection

Data on film-cooling effectiveness and heat transfer coefficients found in the literature agree qualitatively but sometimes show considerable quantitative differences. This will be shown later on. In addition, most of the experiments on film cooling have been performed in such a way that the boundary layer approaching the point of injection was intentionally made turbulent. On the other hand, film cooling on turbine blades is usually provided close to the nose region of the blade where the flow is strongly accelerated and often laminar.

The following experimental investigation was carried out as a contribution to both of the questions raised in the preceding paragraph. The results are discussed in detail in Appendix 3. The most significant findings will be outlined in the following.

The study was concerned with film cooling by injection of coolant through a single row of circular holes inclined at an angle of 35° in the mainflow direction and with a lateral spacing between the holes of three diameters. The velocity of the main flow was nearly constant along the film-cooled flat plate downstream of the holes. The Reynolds number of the mainstream and of the injection flow were sufficiently small to make the approaching boundary layer and the coolant flow through the injection channels laminar. Both flows, however, could be made turbulent by trips in the boundary layer approaching the coolant injection or in the tubes through which the coolant approached the injection holes. The mainstream Reynolds number based on the hole di-

ameter had a value of 3.4×10^3 and the injection Reynolds number was 6.0 to 6.7×10^3 . The ratio of boundary layer displacement thickness to the hole diameter 2 mm upstream of the leading edge of the injection holes was kept approximately equal for the laminar and for the tripped turbulent boundary layer and had values between 0.14 and 0.16. Air was used in the main stream as well as for the injected fluid. The temperature of the mainstream and of the injected fluid were kept almost equal so that the density ratio for both fluids was close to 1. Electric heating was used for the heat transfer experiments generating a heat flux which was nearly constant along the surface downstream of the coolant injection.

Laterally-averaged local heat transfer coefficients, h , were measured without injection and the results are presented in Fig. 4. Two solid lines present the results representing an established relation (Eq. 1) for convective heat transfer on a plane surface with a laminar boundary layer and for convective heat transfer in a flow with a turbulent boundary layer over a flat plate (Eq. 2). Experimental results are listed as square and triangular symbols for a laminar boundary layer (no trips) and a boundary layer which was made turbulent by trips. In some of the experiments the holes were closed by a thin tape to avoid a disturbance of the flow by a cavity effect of the holes. The experimental results for the laminar boundary layer and closed holes follow closely the line describing laminar convection except far downstream where some transition to turbulence occurred. The

open holes, however, caused a transiting of the boundary layer to turbulent flow and created a heat transfer coefficient close to the relation for turbulent convection regardless of whether the approaching boundary layer was laminar or turbulent.

Laterally-averaged film effectiveness values are presented in Fig. 5 over the dimensionless downstream distance X/D for two blowing rates $M = 0.50$ and 0.99 . The lines identified by a capital letter present the results of earlier published investigations listed in Table 2 of Appendix 3. They confirm the statement made earlier that a considerable difference exists between the effectiveness values measured by various investigators, especially at $M = 0.50$ and at values X/D smaller than 20. A partial explanation of these differences follows from the measurements obtained in the present investigation which are listed as full and empty symbols in the figure. It is observed that the main differences occur at the blowing rate $M = 0.50$ and that they are caused by a laminar flow in the injection tubes versus a tripped turbulent flow in these tubes. The influence of a laminar or turbulent condition in the approaching boundary layer is less significant and can only be observed for X/D ratios smaller than about 15.

The ratio of the laterally-averaged heat transfer coefficient \bar{h} measured without injection is plotted in Fig. 6 over the dimensionless distance X/D , again, for a blowing rate $M = 0.50$. The upper two curves indicate that this ratio is close to 1 for the whole range of X/D as long as the approaching boundary layer

is turbulent regardless of whether the jet is laminar or turbulent. For a laminar boundary layer approaching the injection, the ratio of heat transfer coefficients is again close to a value of 1 for X/D larger than 30. This points, again, to the advantage of defining a heat transfer coefficient for film cooling with Eq. 1. However, the ratio \bar{h}/h_0 deviates from this value for smaller X/D ratios. The flagged symbols use for h_0 a heat transfer coefficient without injection as reported in Fig. 4 for the initially-laminar boundary layer. For this situation, the ratio of heat transfer coefficients is always larger than one in the range X/D smaller than 30. Use of the heat transfer coefficient without injection for an approaching turbulent boundary layer makes the ratio of heat transfer coefficients in Fig. 6 somewhat smaller (unflagged symbols) and leads, in some cases, to values smaller than 1.

In summary, it can be stated that the laminar or turbulent condition in the approaching boundary layer, as well as in the film cooling jets, has an influence on film-cooling effectiveness and on heat transfer in some range of Reynolds numbers when film cooling is obtained by injection from a single row of holes.

Local Heat Transfer in the Neighborhood of Cooling Holes

Effectiveness values as well as heat transfer coefficients reported in the literature as well as the ones described in the previous section have been made for the ratio X/D larger than about 5. Failure of turbine blades is often caused by local thermal stress concentrations and it can be expected that tem-

perature gradients causing thermal stresses have especially large values close to the cooling holes. For this reason a study was performed which is described in detail in Appendix 4.

Local transfer coefficients have been measured on a flat plate equipped with one row of cooling holes. The mainstream Reynolds number, Re_D , based on the hole diameter had a value 11×10^3 with a velocity in the tunnel of 15 m/s. The boundary layer and the flow in the injection channel was turbulent. The method of naphthalene sublimation was used to obtain local mass transfer coefficients and the heat-mass transfer analogy then can be used to convert those to heat transfer coefficients. Fig. 7 shows contours of the ratio h/h_0 in which h denotes the local heat transfer coefficient with film cooling and h_0 the heat transfer coefficient for forced convection on a surface covered by a turbulent boundary layer. It can be recognized that two regions of large values of this ratio exist. One is on the sides of the cooling holes. It is probably caused by a horseshoe vortex which wraps around the jet at the location of injection. A second region of large gradients is located downstream of the holes and is probably caused by a separated flow region.

The temperature gradients in the skin of a turbine blade will surely be smaller than the gradients of heat transfer coefficients which can be obtained from the figure. They may, however, still assume values leading to high stresses because of the relatively poor conductivity of the heat-resistant steels used for the blade skin. The gradients of the heat transfer coeffi-

cients along the surface of the skin of the turbine blade taken from Fig. 7 may be used for an analysis of the temperature distribution in the blade skin which has to consider the heat convection at the skin surface, in the cooling air passages, as well as heat conduction in the skin in the neighborhood of the cooling holes. A stress analysis can then be based on this temperature distribution.

Local Heat Transfer Near the Intersection of a Plane Surface and a Cylinder Normal to It in Flow Parallel to the Surface

A system was designed to study the heat transfer in the vicinity of film cooling holes along the leading edge region of a turbine blade. For simplicity, a circular cylinder was used. The design permits injection holes to be placed in the cylinder which have a radius of hole diameter to cylinder diameter similar to that which occurs in the stagnation region of a blade. Because considerable detail was desired in the heat transfer distribution, the mass transfer analogy is used. This makes use of the sublimation of a naphthalene surface and permits very precise local measurements of the mass transfer coefficient--particularly true when one wants to find the relative effect of injection on the transport coefficients.

Before the holes were put in the tube, preliminary measurements were made for mass flow from a cylinder in crossflow. It was possible to make very precise local measurements. Figure 7 shows the distribution of mass transfer around the cylinder in the region of two-dimensional flow (for large Z/DEL_1) well away

from the wind tunnel walls. In these experiments, the Sherwood number can be considered equal to the Nusselt number. Theta denotes the angular distance from the stagnation lines.

A very interesting phenomena was observed in these tests. A deep trench was found close to the wall--that is, on the cylinder but well into the boundary layer along the wall (for $Z/\Delta L_1 \ll 1$). Figure 9 shows the variation of mass transfer coefficient with distance from the wall at specific angles, θ , around the periphery of the cylinder. Note that a very large increase is found close to the wall. In this region, near the normal separation point, the mass transfer coefficient increases by a factor of about 7 over the value in the two-dimensional flow region. Even close to the forward stagnation region, where the mass transfer coefficient is normally quite high, there is an increase of almost a factor of 2. This large increase in mass transfer is related to the horseshoe vortex that forms around a cylinder in crossflow within the boundary layer along a wall through which the cylinder protrudes. The intense nature of this increase in mass transfer in the small region in which it occurs indicates that this may not be due to the main horseshoe vortex but to a very small but very intense vortex within the horseshoe vortex. This phenomenon can have a significant effect on a number of heat transfer situations, particularly near the base of a turbine blade. It may lead to very high local heat transfer coefficients and, consequently, to very high thermal stresses. Conduction would tend to equalize the temperature in the blade but the poor

conductivity of normal high-temperature blades can still cause significant variations in the temperature distribution and high stress.

Survey of Film Cooling Performance on Gas Turbine Blades

Studies at this laboratory performed on film cooling and their application to design calculations for gas turbine blades have been discussed in a survey paper which is attached to this report as Appendix 5. The study describes all of the significant findings, including some of those reported here.

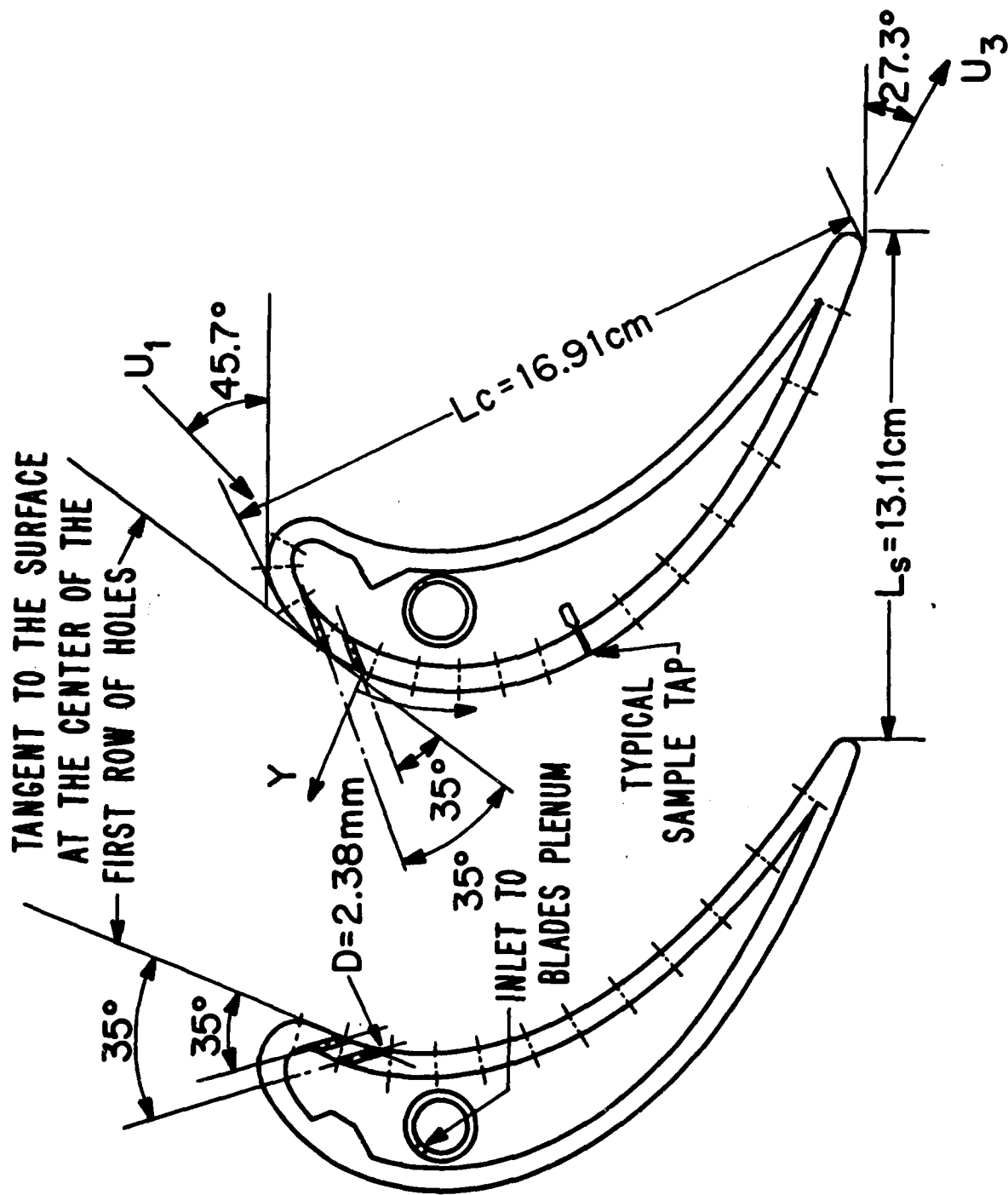


Fig. 1 CENTRAL TEST BLADES IN CASCADE

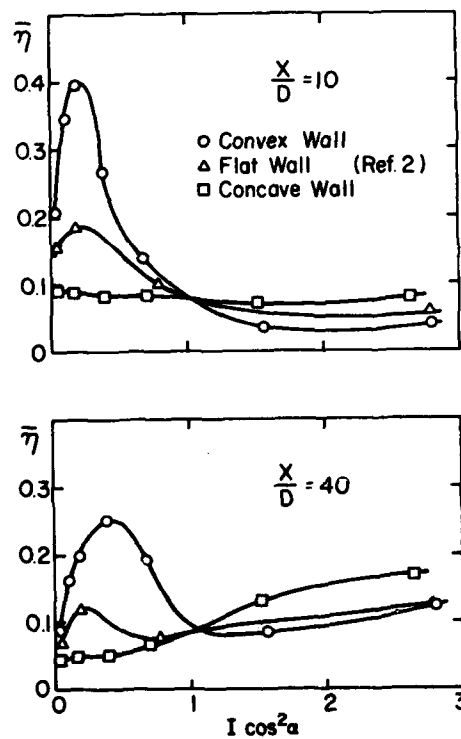


Fig. 2 Variation of lateral average effectiveness with $I \cos^2 \alpha, \rho_2 / \rho_\infty = 0.95$

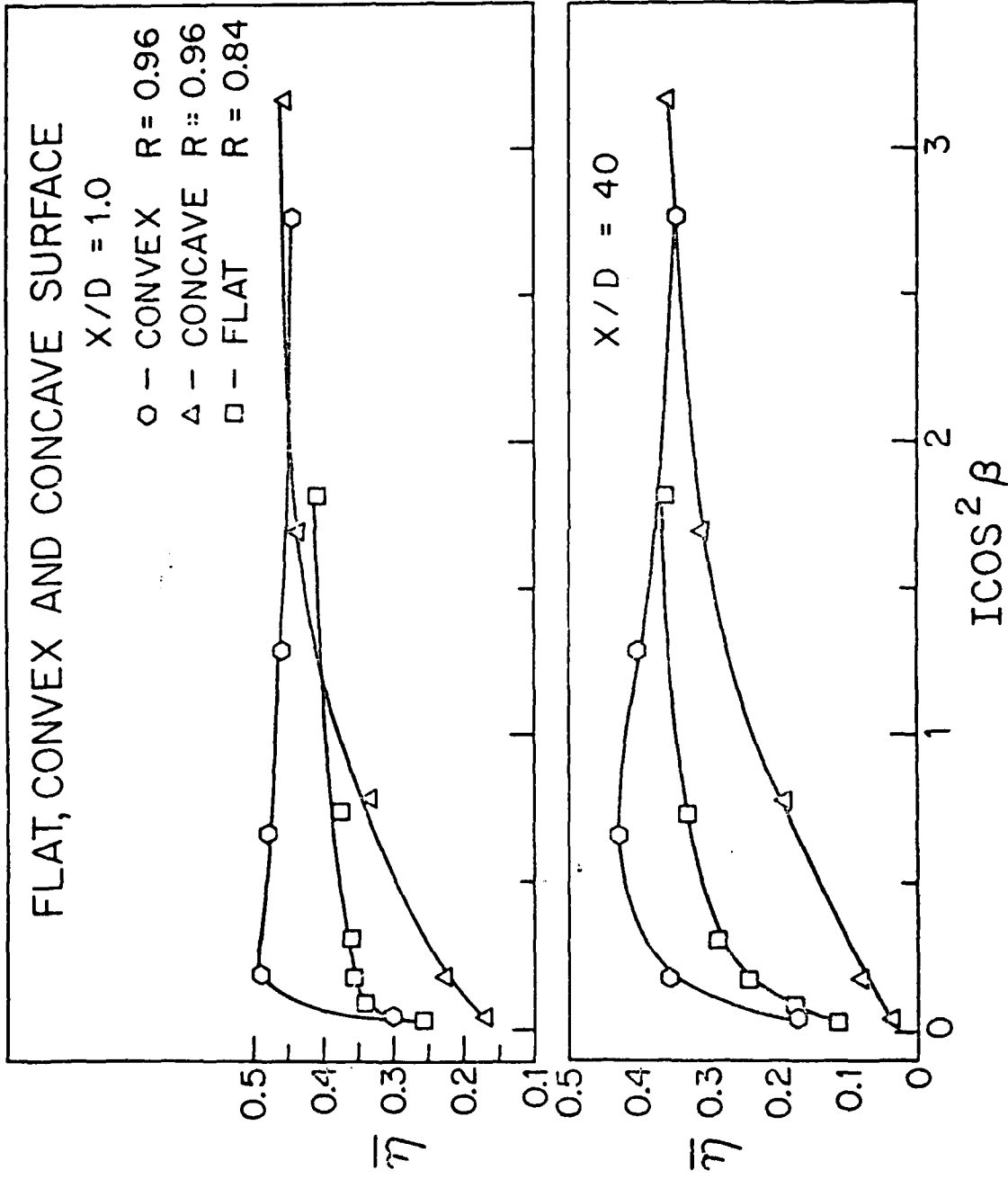


Fig. 3 Comparison of average effectiveness with film cooling results obtained on a flat surface

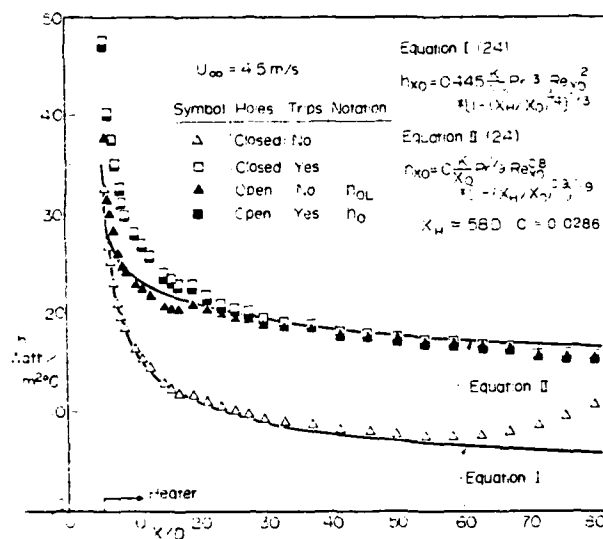


Fig. 4 Laterally-averaged heat transfer coefficient without injection

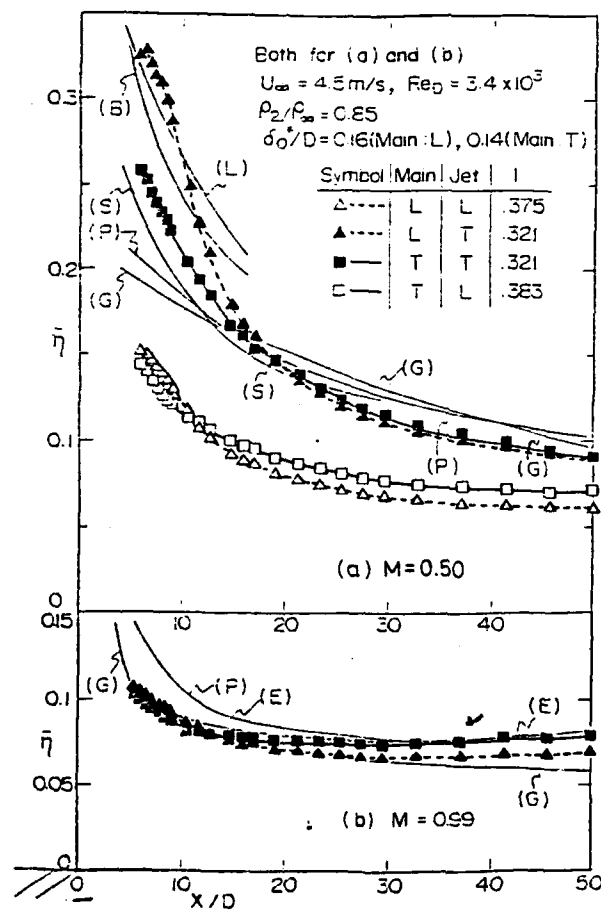


Fig. 5 Laterally-averaged film-cooling effectiveness

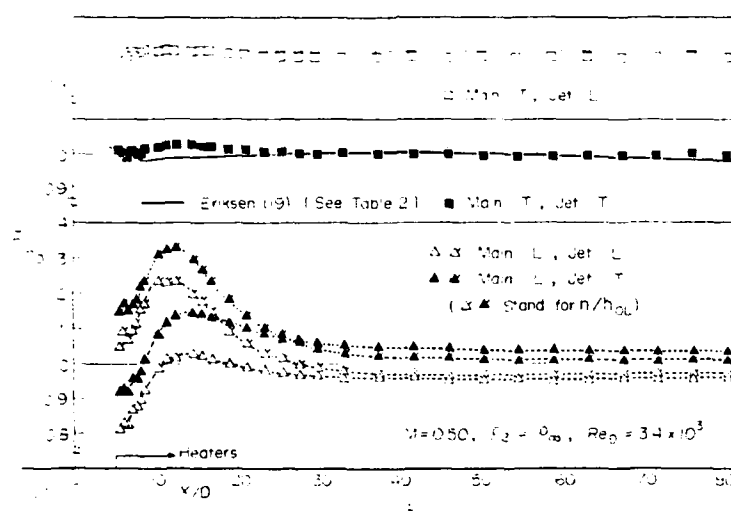
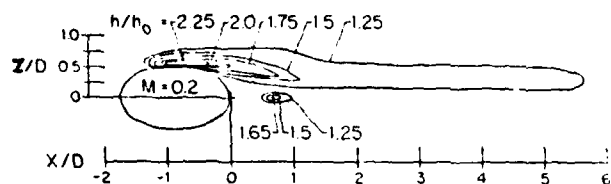
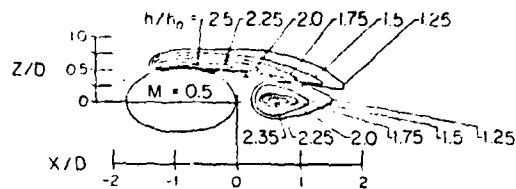


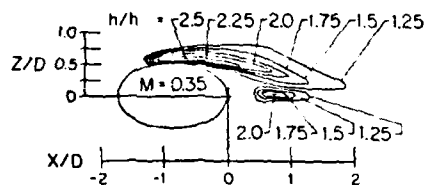
Fig. 6 Laterally-averaged heat transfer coefficient



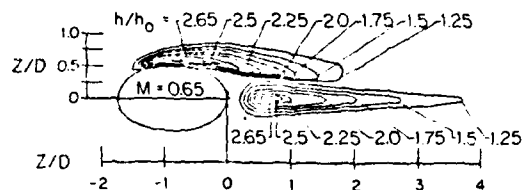
(a) at $M = 0.2$



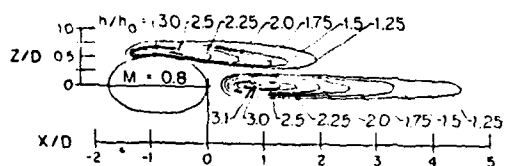
(c) at $M = 0.5$



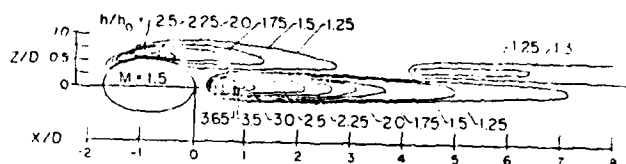
(b) at $M = 0.35$



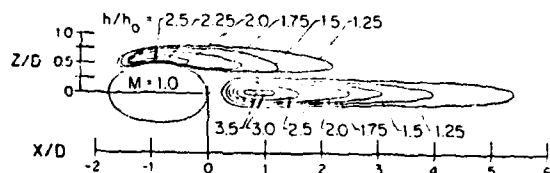
(d) at $M = 0.65$



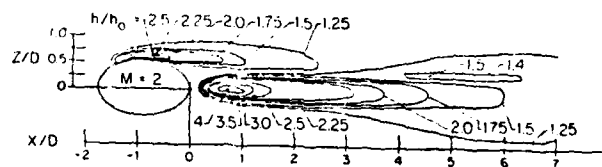
(e) at $M = 0.8$



(g) at $M = 1.5$



(f) at $M = 1.0$



(h) at $M = 2.0$

Fig. 7 Contours of h/h_0

Re-19000

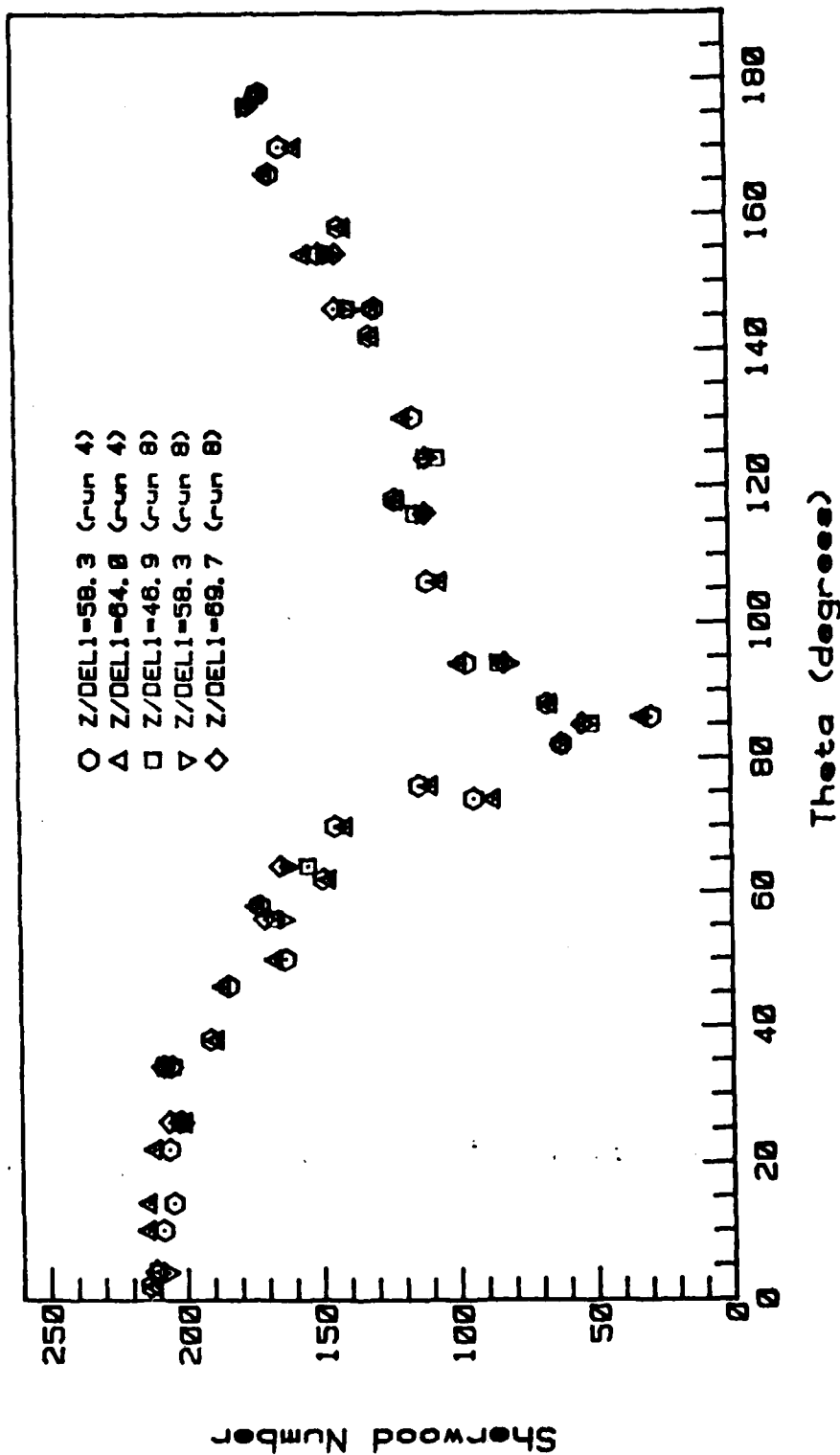
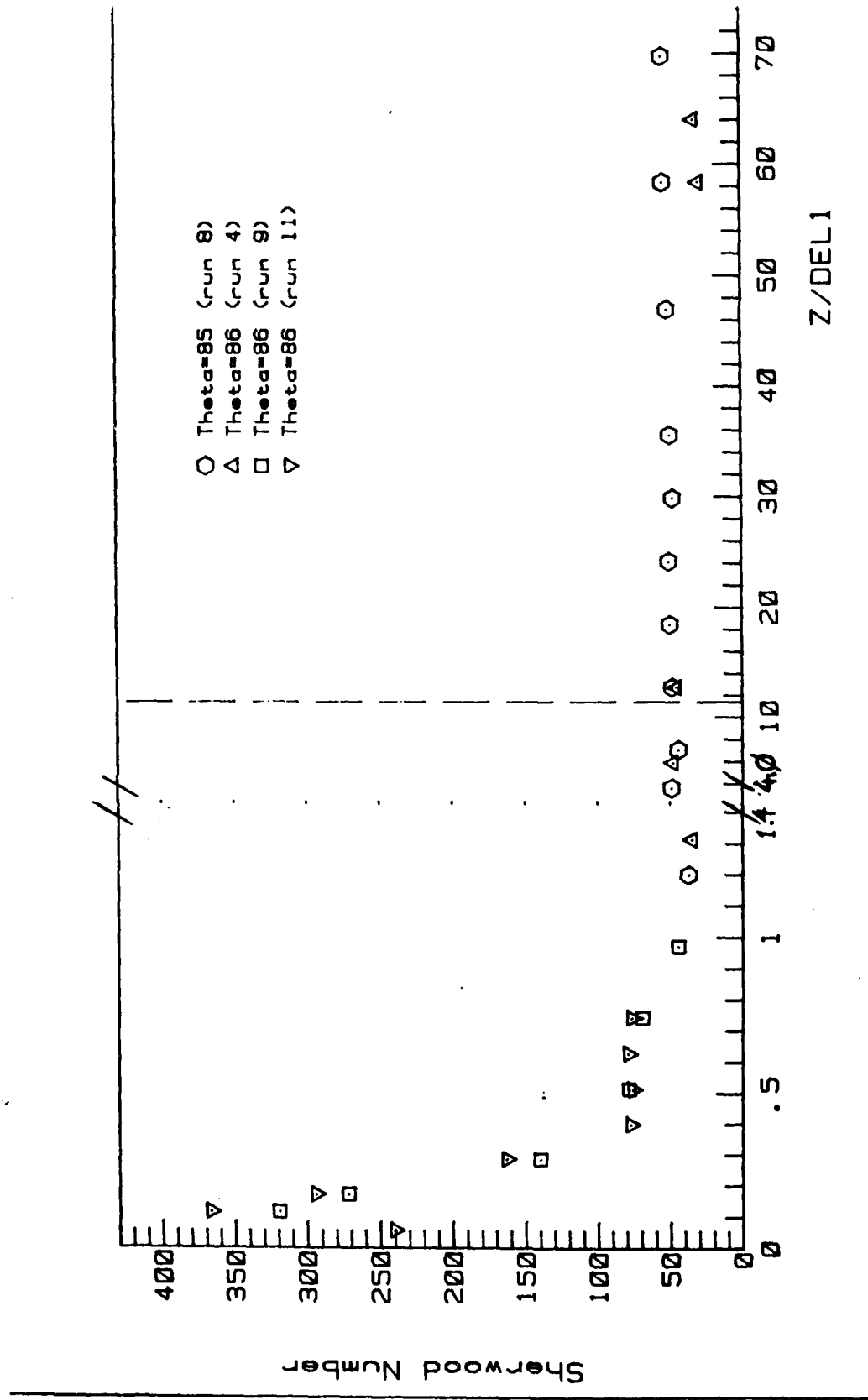


Fig. 8 Peripheral distribution of Sh



Reprinted from ENGINEERING FOR POWER, Vol. 100, No. 3, July, 1978

S. Ito¹

Research Fellow

R. J. Goldstein

Professor,
Mem. ASME

E. R. G. Eckert

Professor,
Mem. ASMEDepartment of Mechanical Engineering,
University of Minnesota,
Minneapolis, Minn.

Film Cooling of a Gas Turbine Blade

The local film-cooling produced by a row of jets on a gas turbine blade is measured by a mass transfer technique. The density of the secondary fluid is from 0.75 to two times that of the mainflow and the range of the mass flux ratio is from 0.2 to three. The effect of blade-wall curvature on the film-cooling effectiveness is very significant. On the convex wall, a near tangential jet is pushed towards the wall by the static pressure force around the jet. For a small momentum flux ratio, this results in a higher effectiveness compared with that on a flat wall. At a large momentum flux ratio, however, the jet tends to move away from the curved wall because of the effect of inertia of the jet resulting in a smaller effectiveness on the convex wall. On the concave wall, the effects of curvature are the reverse of those described for the convex wall.

Introduction

Film cooling is used to protect a solid surface from a high temperature mainstream by releasing a coolant on the surface to be protected. This secondary fluid can be considered as a heat sink for the heat flow from the hot mainstream or as an insulating layer between the hot mainstream and the surface. A summary of film cooling on flat walls is given in [1].²

Film cooling has found wide application in gas turbines where performance generally increases with turbine inlet temperature. Although the strength of the alloys at high temperature has improved, a gas turbine provides a temperature and stress environment which is beyond the limit alloys can presently achieve without cooling. In the past, convection cooling was applied to blades and vanes. More recently film cooling combined with convection cooling and/or impingement cooling is used in blades and vanes.

For design purposes, it is often required to know the relation between the heat fluxes to a wall and the temperatures of the wall surface. With film cooling, the heat transfer coefficient is customarily defined by

$$q = h(T_w - T_{aw}) \quad (1)$$

The heat transfer coefficient and the adiabatic wall temperature have often been studied independently. The present study concerns the adiabatic wall temperature, T_{aw} , or the adiabatic film-cooling effectiveness, η_T , defined by

$$\eta_T = \frac{T_{aw} - T_\infty}{T_2 - T_\infty} \quad (2)$$

A mass-heat transfer analogy is useful in studying film-cooling effectiveness. Instead of injecting heated or cooled secondary fluid, a fluid at the mainstream temperature which contains a foreign gas is injected. A local impermeable-wall effectiveness, η , is defined by

$$\eta = \frac{C_{iw} - C_\infty}{C_2 - C_\infty} \quad (3)$$

If there is no foreign gas in the mainstream

$$\eta = \frac{C_{iw}}{C_2} \quad (4)$$

The analogy of the mass transfer process to the heat transfer process holds if the turbulent Lewis number and the molecular Lewis number are unity. If the flow is sufficiently turbulent, variations in the molecular Lewis number from unity may not play an important role [1]. Pedersen [2] checked the effect of molecular Schmidt number on the impermeable-wall effectiveness. There was no apparent effect of the molecular Schmidt number of the injection gas. Strictly speaking the analogy holds if the densities at arbitrary corresponding locations are the same in the two cases. For a turbulent flow, this requires that the molar heat capacities of the injected jet and the mainstream fluids are the same or that $T_2/T_\infty \approx 1$ [3]. When the analogy holds, the relation between the adiabatic film-cooling effectiveness and impermeable-wall effectiveness is given by

$$\eta_T = \frac{\eta}{\frac{c_{p\infty}}{c_{p2}} + \left(1 - \frac{c_{p\infty}}{c_{p2}}\right) \eta} \quad (5)$$

where $c_{p\infty}$ and c_{p2} are the specific heats of the mainstream and the secondary fluid in the heat transfer situation. This relation is verified [3] by using existing experimental results for two-dimensional film cooling. If $c_{p2} = c_{p\infty}$,

$$\eta_T = \eta \quad (6)$$

¹ Presently Assistant Professor, Ikutoku Technical University, Atsugi, Kanagawa-ken, Japan.

² Numbers in brackets designate References at end of paper.

Contributed by the Gas Turbine Division of the AMERICAN SOCIETY OF MECHANICAL ENGINEERS and presented at the Tokyo Joint Gas Turbine Conference, Tokyo, Japan, May 23-27, 1977. Manuscript received at ASME Headquarters August 4, 1977.

Most studies of film-cooling effectiveness have been done using plane walls. The effects of curvature have been investigated only recently.

Rastogi and Whitelaw [4] presented a procedure for predicting mean-flow properties of laminar and turbulent two-dimensional wall jets on curved walls. The paper briefly alluded to the effect of surface curvature on film cooling—indicating a higher effectiveness with a convex wall and a lower effectiveness with a concave wall. Folayan and Whitelaw [5] recently reported an experimental and computational investigation of the influence of curvature on the effectiveness of two-dimensional film cooling. Outside the range of parameters which results in separation, they indicate that an increase in convex curvature tends to improve effectiveness and an increase in concave curvature to decrease effectiveness.

Assuming that the static pressure distribution does not change with secondary fluid injection, Nicholas and LeMeur [6] predict from the momentum equations with a two-dimensional secondary fluid on a wall surface that if there is no longitudinal pressure gradient, Archimedes type forces might either increase or decrease effectiveness depending upon the sign of the curvature of the wall and upon whether the momentum flux ratio is larger or smaller than unity. The effect of angle of injection is not included. For two-dimensional injection on a concave wall, they find good agreements with experimental results.

Hart [7] measured adiabatic film-cooling effectiveness downstream of injection through a single circular hole into a mainflow. The angle of injection was 35 deg on convex, flat, and concave walls. Up to a mass flux ratio of 0.4 to 0.5 the injection from the convex wall resulted in a higher centerline effectiveness than for the injection from the flat walls whereas on the concave wall the effectiveness was substantially lower. The curvature effect reversed at higher mass flux ratios.

Mayle, Kopper, Blair, and Bailey [8] studied curvature effects in two-dimensional film cooling. They found that the adiabatic film-cooling effectiveness was higher on a convex wall, but lower on a concave wall. This effect was attributed to the influence of curvature on Reynolds stress and the turbulent heat flux. The range of mass flux ratio was 0.5 to 0.9 at a density ratio of 0.9.

In the present paper measurements of the impermeable-wall effectiveness on convex, flat [2], and concave walls are compared. For the comparison the same ratio of boundary-layer thickness to the hole diameter would be ideal. However, though the effectiveness at the centerline of the hole is increased by decreasing the boundary layer displacement thickness [9, 10], the lateral average effectiveness is not greatly affected by the boundary displacement thickness (see [11] and [12]).

Analysis of Curvature Effects on Effectiveness

The following analysis will explain the curvature effect qualitatively and establish the important parameters.

Assumptions. The impermeable-wall effectiveness is given by equation (3) or (4). The wall gas concentration is affected by the path that the secondary (jet) flow follows as it penetrates into the primary flow. If the diffusion rates are the same for the same given conditions on walls with different curvatures, then one can expect that the jet whose height above the wall is smaller gives higher effectiveness if the velocities and the mass flow rates are the same.

The following assumptions are made in the analysis of the effect of curvature on film cooling:

- (1) The radius of curvature of the wall, r_w , is constant along the downstream direction, X -direction.
- (2) The amount of the secondary fluid is so small that the static pressure distributions are not disturbed by the secondary flow for a tangential jet.
- (3) For a tangential jet, the momentum of the jet changes from $\rho_2 U_2^2$ at $X = 0$ to $\rho_\infty U_\infty^2$ for $X \rightarrow \infty$. For a jet injected at an angle to the surface, the density times the square of the X -component of the jet velocity changes monotonically from $\rho_2 U_2^2 \cos^2 \alpha$ to $\rho_\infty U_\infty^2$ for $0 \text{ deg} \leq \alpha \leq 90 \text{ deg}$.

Jet Flow Over a Surface. Consider a jet flowing parallel to a wall. Over a flat wall the center of the jet trajectory tends to remain parallel to the wall neglecting entrainment effects near the surface of the wall. Over a curved wall the jet may move closer to or further from the wall. This tendency of the jet on a curved wall may be determined considering the balance of the forces exerted on a portion of the jet which

Nomenclature

C_{iw} = mass fraction of foreign gas at an impermeable wall
 C_2 = mass fraction of foreign gas present in secondary fluid
 C_∞ = mass fraction of foreign gas present in mainstream
 c_{p2} = specific heat of secondary fluid
 $c_{p\infty}$ = specific heat of mainstream fluid
 D = diameter of injection hole
 h = convective heat transfer coefficient
 I = momentum flux ratio, $\rho_2 U_2^2 / \rho_\infty U_\infty^2$
 K = acceleration parameter, $\frac{\nu_\infty}{U_\infty^2} \frac{dU_\infty}{dX}$
 L_c = blade chord length
 L_p = blade pitch
 M = blowing rate or mass flux ratio, $\rho_2 U_2 / \rho_\infty U_\infty$
 Ma_3 = Mach number at cascade exit
 P = local static pressure
 P_{tic} = total pressure at center of cascade inlet
 q = heat flow per unit time and area
 Re_3 = chord Reynolds number, $U_3 L_c / \nu_3$
 Re_∞ = mainstream Reynolds number based on hole diameter, $U_\infty D / \nu_\infty$
 r = radius of curvature of mainstream. (The direction of radius is the same as that of

r_w .)
 r_j = radius of trajectory of center of injected fluid
 r_w = radius of curvature of wall. (The positive direction of the radius is from the inside to the outside of the wall. $r_w > 0$ on convex wall, $r_w < 0$ on concave wall.)
 r_{w0} = radius of curvature of wall at location of injection
 T_{aw} = adiabatic wall temperature
 T_w = wall temperature
 T_2 = temperature of injected fluid
 T_∞ = mainstream temperature or recovery temperature
 t = spacing between the center lines of two adjacent injection holes
 U = local mainstream velocity in flow direction
 U_j = mean velocity of secondary fluid, downstream of an injection hole
 U_1 = mean velocity of mainstream at cascade inlet
 U_2 = mean velocity of secondary fluid at the exit of injection hole
 U_3 = mean velocity of mainstream at cascade exit
 U_∞ = mainstream velocity at location of injection

V_j = volume of a portion of secondary fluid, downstream of an injection hole
 X = distance along wall downstream from the downstream edge of injection hole
 X_n = normalized axial distance of cascade (cf. Fig. 3)
 Z = lateral distance from centerline of injection hole
 α = angle between the injection hole centerline and the direction of U_∞
 δ^* = boundary layer displacement thickness at location of injection
 η = local impermeable-wall effectiveness, equation (3)
 $\bar{\eta}$ = lateral average of impermeable-wall effectiveness
 η_T = local adiabatic film-cooling effectiveness
 ν_3 = kinematic viscosity of mainflow at cascade exit
 ν_∞ = kinematic viscosity of mainflow at injection
 ρ_j = density of a portion of a jet, downstream of an injection hole
 ρ_2 = density of secondary fluid at exit of injection hole
 ρ_∞ = density of mainstream fluid
 ϕ = positive value, $0 \leq \phi \leq 1$

is assumed to be parallel to the wall at an arbitrary location to be considered.

Consider the flow over a curved wall with no jet present. The centrifugal force on a control volume would be balanced by the static pressure difference on the volume. Thus,

$$\frac{dP}{dr} = \rho \frac{U^2}{r} \quad (7)$$

where r is the radius of curvature of the stream. The direction of r and r_w are chosen to be positive from the inside of the wall to the outside. Then, r and r_w are positive for a convex wall and negative for a concave wall. If the total pressure is constant in the radial direction, U is inversely proportional to the absolute value of the radius.

If a jet is present and close to the wall as should be true for a film-cooling jet, the radius of curvature of the flow, r , is approximately r_w and the velocity (U) is U_w . Then,

$$\frac{dP}{dr} = \rho \frac{U_w^2}{r_w} \quad (8)$$

Now consider a portion of a jet, downstream of an injection hole, which flows parallel to the wall (Fig. 1). The centrifugal force on the fluid in the control volume is in balance with the same force,

$$\frac{dP}{dr} = \rho_j \frac{U_j^2}{r_j} \quad (9)$$

In obtaining the trend of the jet trajectory we are ignoring the dynamic pressure of the mainstream on the jet which always tends to push the jet over into the direction of the mainstream.

From equations (8) and (9)

$$\rho \frac{U_w^2}{r_w} = \rho_j \frac{U_j^2}{r_j}$$

or

$$\frac{r_j}{r_w} = \frac{\rho_j U_j^2}{\rho U_w^2} \quad (10)$$

The value of $\rho_j U_j^2$ should be between the value of the entering jet $\rho_2 U_2^2$ and the value $\rho_\infty U_\infty^2$. Thus, with

$$\begin{aligned} \phi &= \frac{\rho_j U_j^2 - \rho_\infty U_\infty^2}{\rho_2 U_2^2 - \rho_\infty U_\infty^2} \\ \frac{r_j}{r_w} &= 1 + \phi(I - 1) \end{aligned} \quad (11)$$

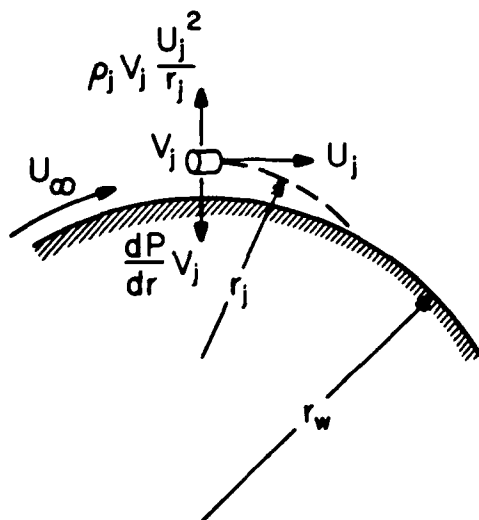


Fig. 1 The center of the trajectory of a jet flowing over a convex wall

where

$$0 \leq \phi \leq 1$$

Putting this into equation (10)

$$\frac{r_j}{r_w} = 1 + \phi(I - 1) \quad (12)$$

The relative size of r_j is dependent on the momentum flux ratio. Thus

$$\begin{aligned} |r_j| &> |r_w| \quad \text{for } I > 1 \\ |r_j| &= |r_w| \quad \text{for } I = 1 \\ |r_j| &< |r_w| \quad \text{for } I < 1 \end{aligned}$$

Considering the direction of the static pressure force over a surface, the sign of the curvature of the jet and the wall should be the same. If the absolute value of the radius of the jet is smaller than that of a curved wall, the jet comes closer to a convex wall, but moves away from a concave wall. Then, the film-cooling effectiveness on a convex wall for given conditions would be better than that on the flat or concave wall under the same conditions if $I < 1$ and worse if $I > 1$. On a concave wall, the film-cooling effectiveness for given conditions is better than that on a flat or convex wall if $I > 1$ and worse if $I < 1$.

If a film-cooling jet enters the mainflow at some angle, α , ($0 \text{ deg} \leq \alpha \leq 90 \text{ deg}$) the motion of that jet over a curved wall can be used to determine the relative film-cooling performance. For the height of a jet above a curved surface to be the same at any location as the height of a jet leaving a flat surface, the force in the radial direction due to the static pressure on the jet must balance the force to accelerate the jet in the radial direction. Then results analogous to those found above for a jet entering tangentially are found if $\rho_2 U_2^2 \cos^2 \alpha$ is used instead of $\rho_2 U_2^2$. Again we are ignoring the effect of the dynamic pressure of the mainstream. This should not affect the trend of the change in the direction and thus the trend in cooling effectiveness on walls of different curvature. When $I \cos^2 \alpha$ is less than unity the resulting jet would tend to turn more towards the surface on a convex wall than on a flat or a concave wall.

The film-cooling effectiveness on a convex wall is better than on a flat or a concave wall if $I \cos^2 \alpha < 1$ and worse if $I \cos^2 \alpha > 1$ for the same conditions. The film-cooling effectiveness on a concave wall is better than that on a flat wall if $I \cos^2 \alpha > 1$ and worse if $I \cos^2 \alpha < 1$ for $0 \text{ deg} < \alpha < 90 \text{ deg}$.

If a jet were injected upstream ($\alpha > 90 \text{ deg}$), the injected jet would tend to be turned downstream a short distance from the location of injection. Then the effect of inertia of the jet on attachment or separation from the curved surface would be small; instead, the jet is mainly influenced by the static pressure force on it. The film-cooling effectiveness on a convex wall should be then better than on a flat or concave wall at all blowing rates.

Experimental Apparatus

The present experimental study has been carried out using a low velocity wind tunnel at room temperature as shown in Fig. 2. A cascade of six blades—four solid and two hollow blades—is used. One of the hollow blades has a row of holes ($\alpha = 35 \text{ deg}$) on the suction side and the other has a row of holes $\alpha = 35 \text{ deg}$ on the pressure side. The surfaces with holes face each other. The spacing between the centerlines of two adjacent injection holes is $3D$ ($D = 0.238 \text{ cm}$). The ratio of blade span to chord length is 3.55. The rather long span is designed to avoid secondary flow and to allow use of only the central part of the span where the inlet velocity distribution is expected to be uniform. There are threaded holes in the top wall 0.76 times the chord length upstream of the leading edges of the blades to insert pitot tubes and a thermocouple. The inlet velocities, angles and temperature are measured at this section.

The shape of the blade used in the present study was supplied by the Aircraft Gas Turbine Division of the General Electric Co. The blade chord length, L_c , and the pitch, L_p , are 16.91 cm and 13.11 cm respectively. This compares to the chord length of 4.0 cm for the actual

The secondary gas is produced with the desired density from a mixture of helium or refrigerant-12 and air. The sampled gases are analyzed by a gas chromatograph. Details of the secondary and sampling systems and the analysis of sampling gases are given in [2, 3].

Figure 1 is a graph showing velocity profiles in the suction and pressure sides of a curved duct. The vertical axis is the normalized velocity $\frac{U}{U_3}$, ranging from 0 to 1.2. The horizontal axis is the normalized distance \bar{x}_n , ranging from 0 to 1.0. The upper curve represents the suction side, and the lower curve represents the pressure side. Experimental data points are shown as open circles, and the solid line represents the calculated profile (supplied by GE). Key features include the location of injection, injection velocity U_i , and various angles (44.3° , 107° , 62.7°) and distances (0.1 , 0.15 , $\bar{x}_n*1 = 14.5\text{cm}$).

At the location of injection on the suction side, the calculated boundary layer displacement thickness, δ^* , (using the approximate method due to von Kármán and Pohlhausen [13]) is 0.22 mm and δ^*/D is approximately 0.09. With this δ^* , $U_\infty \delta^*/\nu_\infty = 300$. Since the critical Reynolds number for $K = 0$ is about 660 [13], the boundary layer before the injection holes is expected to be laminar or in transition. On the pressure side, there is an adverse pressure gradient near the nose of the blade. The boundary layer at the injection hole on this surface is expected to be turbulent which is confirmed by the experiments of the aerodynamic loss of the flow in the cascade [3].

If the boundary layer is not turbulent, an additional requirement for fulfilling the mass-heat transfer analogy is that the value of the molecular Schmidt number is equal to the Prandtl number. However, even though these are different, in film-cooling the analogy may still be fulfilled because of the strong turbulent mixing of the secondary fluid with the mainstream. Also, since the gradient of the mass concentration (temperature) perpendicular to the wall should be zero on the impermeable (adiabatic) wall, the effects of the laminar region may be very small. The effects of Schmidt number on impermeable-wall effectiveness are checked [3] by using air with a tracer of helium, whose molecular weight is 4 and Schmidt number is 0.2 in the air, and refrigerant-12, whose molecular weight is 120.9 and Schmidt number is 1.7 in air [2]. The effectiveness with the different tracers was similar for similar experimental conditions on both pressure and suction surfaces—indicating that the mass-heat transfer analogy holds in the present experiments.

The effect of the mainstream Reynolds number on the lateral average impermeable-wall effectiveness on the suction (convex) side was checked by reducing the mainstream speed to about half of that normally used in the experiments. The average effectiveness depended very little on the mainstream Reynolds number.

Examples of the results of local impermeable-wall effectiveness measurements for the convex (suction) and concave (pressure) surfaces are shown in Figs. 4 and 5.

The lateral average effectiveness for the density ratio of 0.95 as a function of X/D is shown in Fig. 6 for suction side injection and in Fig. 7 for pressure side injection. On the suction side the largest effectiveness is obtained at $M = 0.5$ to 0.7. With further increase of M , the effectiveness decreases because of penetration of jets through the boundary layer. For M from 1.5 to 2.0 the effectiveness increases because of increase of the secondary mass flow even though the jets may penetrate through the boundary layer. On the pressure side the effectiveness at small M (or I) is very small. This is because the static pressure force acts on the jets in the direction to move the jets away from the surface. With high M or I for the near tangential jets the jets tend to strike the concave surface downstream resulting in relatively high effectiveness.

In Figs. 8 and 9, comparisons of the results for convex, flat, and concave walls are shown at $\rho_2/\rho_\infty = 0.95$ and $\rho_2/\rho_\infty = 2.0$ respectively. There are substantial differences for the different surfaces. The importance of $I \cos^2 \alpha$ as a parameter to correlate the curvature effect on the effectiveness was shown in the analysis. For $\rho_2/\rho_\infty = 2.0$ with $I \cos^2 \alpha = 1.3$ (see Fig. 9), the average effectiveness is smallest on the concave wall near the injection hole. At that condition, the kidney-shaped jet may just be forming. Thus, the effectiveness is very sensitive to experimental conditions. Further downstream the concave surface gives higher effectiveness.

For a better understanding of the curvature effects, the effectiveness is shown as a function of $I \cos^2 \alpha$ at $X/D = 10$ and 40 for $\rho_2/\rho_\infty = 0.95$ in Fig. 10. The lines for convex, flat, and concave surfaces cross at $I \cos^2 \alpha \approx 1$.

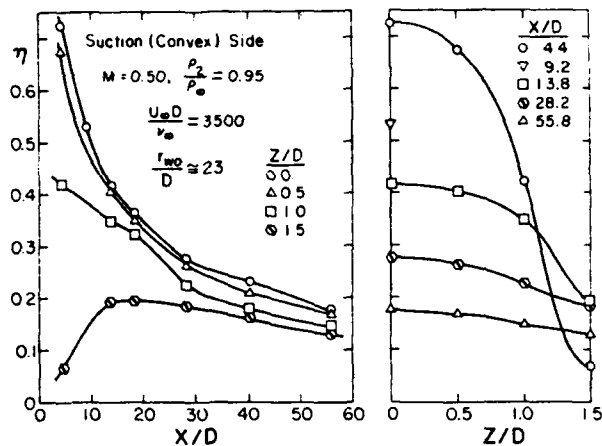


Fig. 4 Local effectiveness on convex wall, $D = 2.38 \mu\text{m}$, $\alpha = 35 \text{ deg}$, $t = 3D$, $M = 0.5$, $p_2/p_\infty = 0.95$

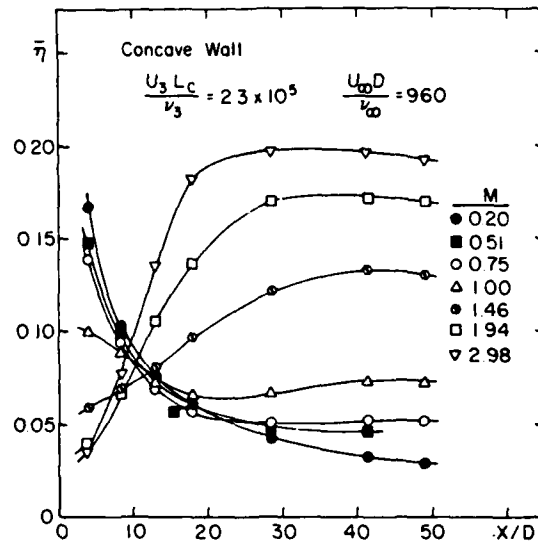


Fig. 7 Lateral average effectiveness on concave (pressure) surface, $p_2/p_\infty = 0.95$

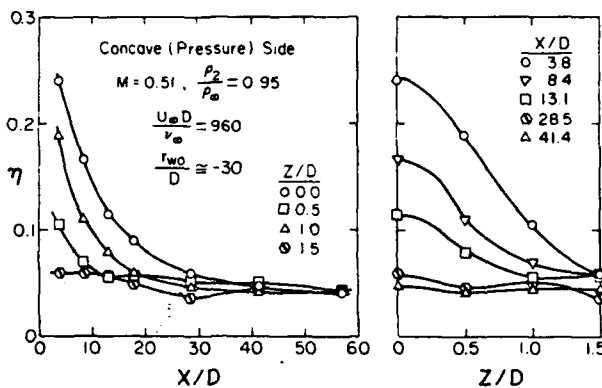


Fig. 5 Local effectiveness on concave wall, $D = 2.38 \text{ mm}$, $\alpha = 35 \text{ deg}$, $t = 3D$, $M = 0.51$, $p_2/p_\infty = 0.95$

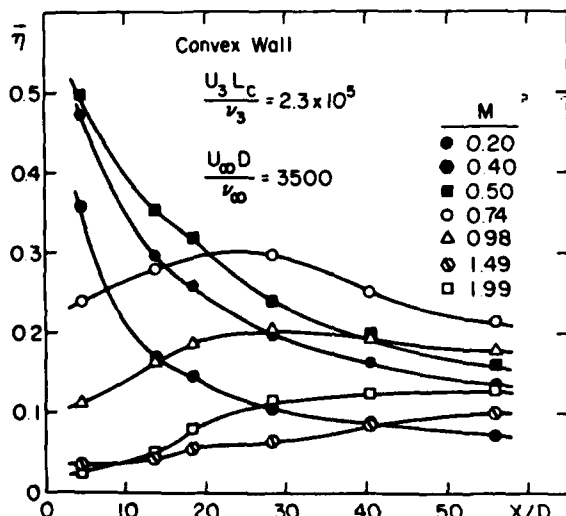


Fig. 6 Lateral average effectiveness on convex (suction) surface $p_2/p_\infty = 0.95$

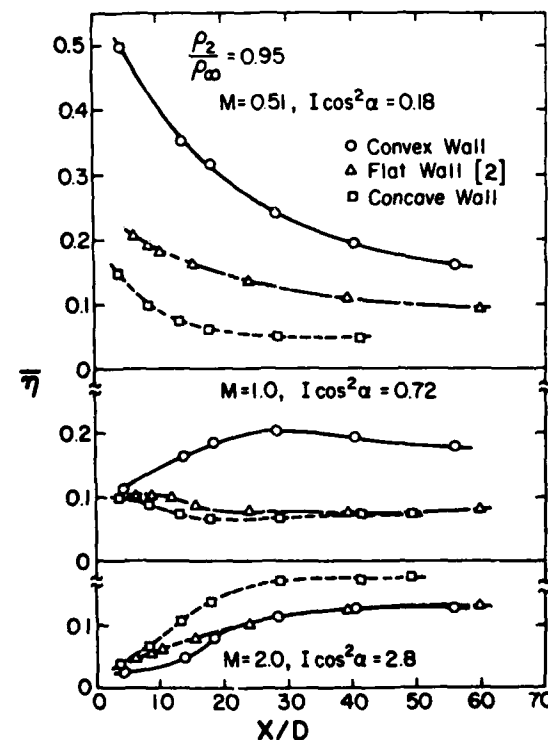


Fig. 8 Comparison of lateral average effectiveness on surfaces of different curvature, $p_2/p_\infty = 0.95$

Further downstream the effectiveness is higher at the smallest density ratio.

Conclusions

Trends in the effects of curvature on film cooling effectiveness of a jet flowing parallel to a wall can be explained by determining whether the injected fluid moves closer to or further from the wall surface. The trend of the jet trajectory can be determined by con-

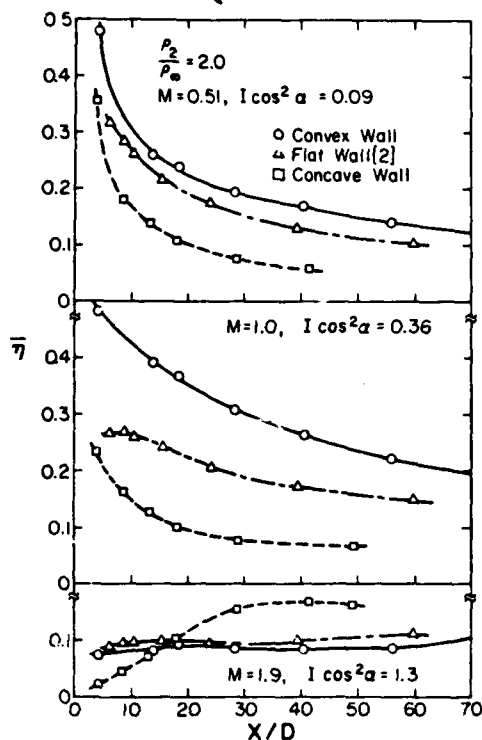


Fig. 9 Comparison of lateral average effectiveness on surfaces of different curvature, $\rho_2/\rho_\infty = 2.0$

sidering the balance of the forces exerted on the injected fluid of the jet by the static pressure and the centrifugal force along the path of the injected fluid. For a jet injected at an angle to a mainstream without a longitudinal pressure gradient, if $I \cos^2 \alpha$ is larger than unity, the effectiveness is smaller on a convex wall, but larger on a concave wall than on a flat wall for $0 \text{ deg} \leq \alpha \leq 90 \text{ deg}$. For $I \cos^2 \alpha$ less than unity the effectiveness tends to be greater on a convex surface than on a concave one.

The curvature of a surface near the injection holes or slits is particularly important to the film-cooling effectiveness. Even over a short distance downstream of the injection holes, say X/D of 5, there are substantial curvature effects on the effectiveness.

Acknowledgment

The authors would like to express their appreciation to the Power Branch of the Office of Naval Research for support under contract number N00014-76-C-0246.

References

- Goldstein, R. J., "Film Cooling," *Advances in Heat Transfer*, Vol. 7, Academic Press, New York and London, 1971, pp. 321-379.
- Pedersen, D. R., "Effect of Density Ratio on Film Cooling Effectiveness for Injection Through a Row of Holes and for a Porous Slot," Ph.D. Thesis, University of Minnesota, 1972.
- Ito, S., "Film Cooling and Aerodynamic Loss in a Gas Turbine Cascade," Ph.D. Thesis, University of Minnesota, 1976.
- Rastox, A. K., and Whitelaw, J. H., "Procedure for Predicting the Influence of Longitudinal Curvature on Boundary-Layer Flows," ASME Paper No. 71-WA/FE-37, 1971.
- Folayan, C. O., and Whitelaw, J. H., "The Effectiveness of Two-Dimensional Film-Cooling Over Curved Surfaces," ASME Paper 76-HT-31, 1976.
- Nicholas, J., and LeMueur, A., "Curvature Effects on a Turbine Blade Cooling Film," ASME Paper 74-GT-156, 1974.
- Hart, J., "Heat Transfer-Film Cooling," Ph.D. Thesis, St. John's College, Cambridge, 1974.
- Mayle, R. E., Kopper, F. C., Blair, M. F., and Bailey, D. A., "Effect of Streamline Curvature on Film-Cooling," ASME *Journal of Heat Transfer*, Vol. 98, 1976, pp. 240-44.
- Goldstein, R. J., Eckert, E. R. G., Eriksen, V. L., and Ramsey, J. W.,

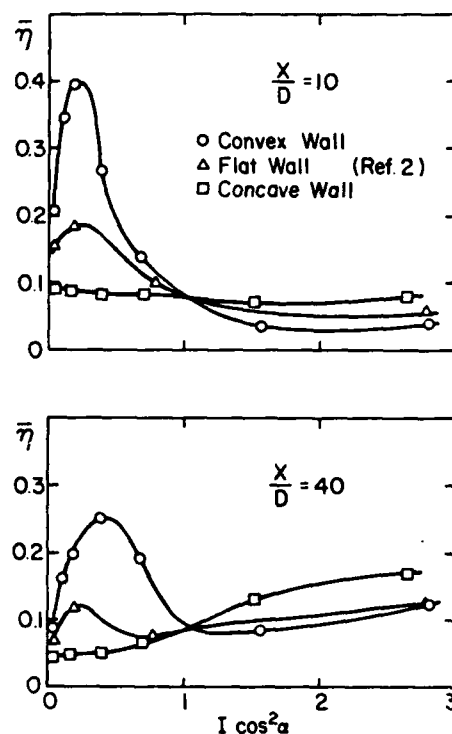


Fig. 10 Variation of lateral average effectiveness with $I \cos^2 \alpha$, $\rho_2/\rho_\infty = 0.95$

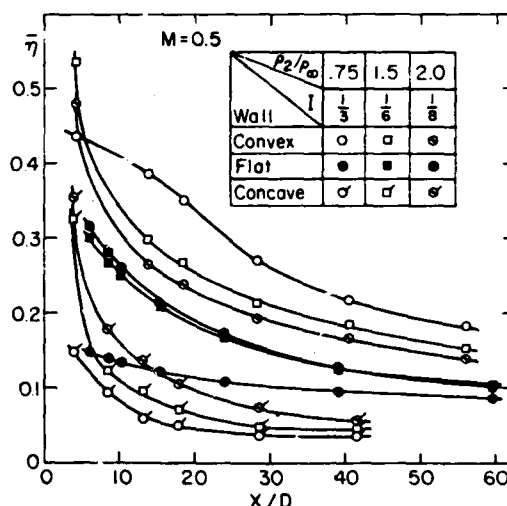


Fig. 11 Comparison of lateral average effectiveness for different density ratios on convex, flat, and concave surfaces, $M = 0.5$

- "Film Cooling Following Injection Through Inclined Circular Tubes," *Israel Journal of Technology*, Vol. 8, 1970, pp. 145.
- Eriksen, V. L., and Goldstein, R. J., "Heat Transfer and Film Cooling Following Injection Through Inclined Circular Tubes," ASME *Journal of Heat Transfer*, Vol. 96, 1974, pp. 239.
- Jabbari, M. Y., "Film Cooling and Heat Transfer with Air Injection Through a Staggered Row of Holes into an Accelerating Flow," Ph.D. Thesis, University of Minnesota, 1973.
- Kadotani, K., "Effect of Main Stream Variables on Heated and Unheated Jets Issuing from a Row of Inclined Round Holes," Ph.D. Thesis, University of Minnesota, 1975.
- Schlichting, H., *Boundary Layer Theory*, 6th Edition, McGraw-Hill, New York, 1968, pp. 192-201, pp. 470.

Appendix 2

Copy Sheet - ISRAEL ANNUAL CONFERENCE ON AVIATION & ASTRONAUTICS

FILM COOLING EFFECTIVENESS ON A TURBINE BLADE

R. J. Goldstein
Department of Mechanical Engineering
University of Minnesota

Y. Kornblum
Honeywell Avionics
Minneapolis, Minnesota

E. R. G. Eckert
Department of Mechanical Engineering
University of Minnesota

Abstract

The effectiveness of film cooling on turbine blades in a linear cascade has been measured using a mass transfer analogy. This present study examines the importance of curvature on film cooling with two rows of staggered injection holes on the pressure (concave) and suction (convex) sides of a turbine blade. Comparisons are made with earlier studies, particularly with one in which a single row of holes is used to provide the film cooling on convex and concave surfaces and another in which a flat surface was studied which had injection through two staggered rows of holes—similar to the present injection geometry. The results of the experiments indicate that curvature plays an important role in determining film-cooling effectiveness even with multiple-row injection. At low and moderate blowing rates the effectiveness is better on a convex than on a concave surface. At high blowing rates the effectiveness is not greatly influenced by the surface curvature. The influence of curvature, however, is much less than was found with injection through a single row of holes where the individual jets tend to act more independently. In general, the two rows of holes provide higher effectiveness on any of the surfaces than does a single row of holes—certainly at the same blowing rate and, in general, also for the same mass addition per unit span of the blade.

Nomenclature

D diameter of injection hole
I momentum flux ratio, $\rho_2 U_2^2 / \rho_\infty U_\infty^2$
 L_c blade chord length, see Fig. 1
 L_s blade pitch, see Fig. 1
M blowing rate or mass flux ratio, $\rho_2 U_2 / \rho_\infty U_\infty$
R density ratio, ρ_2 / ρ_∞
 Re_D Reynolds number, $\rho_\infty U_\infty D / \mu_\infty$
 Re_j injection Reynolds number, $\rho_2 U_2 D / \mu_2$
S width of equivalent two-dimensional slot (a slot having outlet area per unit span equal to that of the injection holes, $\pi D/6$)
 U_1 mean velocity of mainstream at cascade inlet

U_2 mean velocity of secondary fluid at the exit of injection hole
 U_3 mean velocity of mainstream at cascade exit
 U_∞ mainstream velocity at location of injection
X distance along wall downstream from the downstream edge of injection hole, see Fig. 2
Y distance normal to surface, see Fig. 1
Z lateral distance from centerline of injection hole
 β angle between the injection hole centerline and the direction of U_∞
 η local impermeable-wall effectiveness
 $\bar{\eta}$ lateral average of impermeable-wall effectiveness
 ρ_2 density of secondary fluid at exit of injection hole
 ρ_∞ density of mainstream fluid
 μ_∞ mainstream viscosity
 μ_2 viscosity of injected gas
 E two-dimensional film cooling parameter, $[(X + 1.909D)/MS] (Re_2 \mu_2 / \mu_\infty)^{-0.25}$ for present geometry, see Ref. 4

I. Introduction

Over the past two decades, gas turbine designs have progressed to ever higher turbine inlet temperatures as a means of decreasing specific fuel consumption. In some designs the turbine inlet temperature is of the order of the melting-point temperature of the blades. Cooling of these blades is required not only to maintain them below their melting point but at sufficiently low temperature to ensure reasonable operating life.

For aircraft engines the only coolant generally available is the working fluid—air—passing through the system. Coolant air is taken off at some stage in the compressor and thus is already at an elevated temperature. In addition, the relatively poor heat transfer characteristics of air and the temperature drop across the low con-

ductivity blade material usually indicate that internal convection cooling of a turbine blade by itself would not be sufficient. Some means must be taken to reduce the heat flow from the hot gas to the outside surface of the turbine blade. This is often done with film cooling in which relatively cool air from the compressor is introduced close to the surface of the blade. This air flows downstream along the surface, reducing the heat transfer to the blade by decreasing the temperature in the boundary layer. In typical blade configurations, injection holes are used to introduce the coolant air. One or more rows of holes are used in the stagnation region of the blade and often on both the pressure and suction surfaces of the blade.

Studies of film cooling date back to World War II. Most of the early work¹ concerned two-dimensional film cooling in which a continuous slot across the surface to be cooled is used to introduce the coolant flow. A number of studies have been reported on the use of one row of holes^{2,3} two rows of holes⁴ and many holes^{5,6} to supply coolant on a flat surface over which a mainstream flows.

Turbine blades, of course, are not flat surfaces. The pressure side is concave; the suction side is convex. On curved surfaces, a jet entering a mainstream can behave quite differently from one that is injected through a flat surface. Above a convex surface, the pressure in the mainstream flow increases with distance from the wall. A jet of low momentum, compared to the mainstream, could be "pushed" by this pressure gradient towards the wall, preventing the lift-off that might occur at the same flow rate on a flat surface. This would tend to provide better film cooling than occurs on a flat surface. However, if the jet had a high momentum flux relative to that of the free stream, the jet might tend to leave the surface on the convex wall and relatively poor film cooling performance would occur. The opposite effects would take place for film cooling on a concave surface--i.e., the jet would be moved away from the surface by the mainstream pressure gradient at low momentum flux while with a high momentum flux the jet might be expected to impinge on the surface downstream of injection.

These predicted influences of curvature were observed in experiments with injection through a single row of holes conducted in a cascade⁷. Under these circumstances, each jet can act independently, at least to some distance downstream of the row. Thus, the simple qualitative analysis describing a single jet might apply for a row of jets. It was found that on the convex surface, the film cooling was considerably better than on a flat or concave surface at low values of the momentum flux ratio, I , while at high momentum flux ratios the effectiveness on the convex wall was lower than on either a flat or concave surface.

With injection through two rows of holes the upstream jets can fill the spaces between the jets

in the downstream row. The flow of an isolated jet entering a mainstream with a pressure gradient normal to the surface might not be directly applicable in determining the trajectory of the jets nor the resulting film cooling effectiveness.

The present study is intended to demonstrate the influence of surface curvature on film cooling following injection through two staggered rows of injection holes. Both convex and concave surfaces are used. The same six-blade turbine cascade described in Ref. 7 is used in the present study with additional rows of holes on the central blades. The results on the blade can also be compared to results for injection through two rows of holes on a flat surface.

Apparatus

A linear cascade of six blades is used. The two central blades, shown in Fig. 1, have injection holes on their facing surfaces--one on the concave side, the other on the convex side. The injection holes, 2.38 mm in diameter, are placed somewhat downstream of the stagnation region, about 15-20% of the curvilinear distance from the stagnation line to the trailing edge of the blade. Two staggered rows of injection holes are used, both inclined at an angle of 35° to the blade surface at the first row (cf, Fig. 1). The injection holes are not slanted laterally. Individual holes are 3 diameters apart from their neighbors on the adjacent row as well as from the adjacent holes on the same row--cf, Fig. 2.

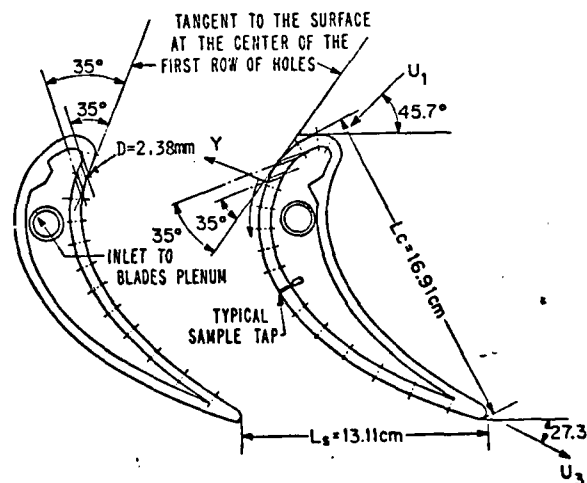


Figure 1 Central test blades in cascade

A mass transfer analogy is used in which a foreign gas is the "coolant" and local measurements of gas concentration at the impermeable wall of the blade are made. With the small size of the blades (still approximately four times actual turbine size), it would be difficult to make thermal measurements of effectiveness due to conduction errors. Previous tests on flat surfaces have shown the validity of the analogy.⁸

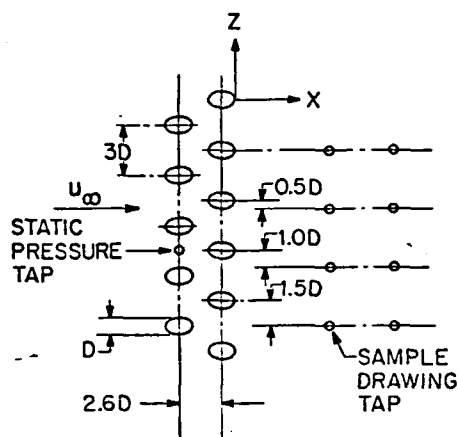


Figure 2 Injection hole geometry

The mass transfer analogy also affords an easy means of obtaining a range of values of the ratio of the density of injected flow to that of the freestream. Many early tests used density ratios close to unity while in a high-temperature turbine, the injected gas may have a density twice that of the main flow. In the present study two density ratios are used. A mixture of helium ($Sc = .235$ in air) and air provides a density ratio of 0.96 while a mixture of freon 12 ($Sc = .72$ in air) and air provides a density ratio of 2.0. In all cases the main flow is air and the entire system is close to isothermal at the ambient temperature.

The velocity of the main flow in the wind tunnel is 12 m/s as it approaches the blade cascade. At the point of injection of the first row of holes, the velocity is about 5 m/s ($Re_p = 750$) on the pressure side and 20 m/s ($Re_p = 3,000$) on the suction side. The blowing rates—defined as ratio of the mass velocity of the injected flow to that of the freestream—are 0.25, 0.5, 1.0, 1.5, and 2.0.

Calculations indicate that the pressure difference across the blade wall in the absence of main flow is much larger than that on the surface between the two rows in the absence of injection. Therefore, flow, the assumption of equal velocity of injection and film cooling parameters for the two rows should hold.

The components of the secondary flow mixture are metered separately, mixed in a plenum, and flow, via a pipe, to the inside of the blade and then through the injection holes. A sample of the

plenum mixture is drawn off in order to determine the injection mixture concentration. Small sampling holes, 0.41 mm in diameter, are located downstream of the injection holes on the surface on which film cooling takes place. An array of holding devices is connected to the sampling holes to receive a sample of the flow near the surface. These systems are connected to a vacuum pump to maintain a pressure lower than the pressure on the blade surface; this generates a flow to the sample holding devices. This flow is small, so the concentration field on the surface of the blade is not disturbed. Samples of gas from the plenum and from the region close to the wall are analyzed in a gas chromatograph. The mass concentration of gas from the sampling taps when divided by the concentration of the injected gas in the plenum before the injection holes is the impermeable wall effectiveness and, by analogy, is equivalent to the thermal film cooling effectiveness on an adiabatic surface.⁷

Procedure

The wind tunnel flow is turned on and stabilized for one hour. Sample holding devices are connected to the manifold and the suction holes. Secondary flow components are metered and time is allowed for stabilization of the concentration in the plenum. The vacuum pump is then turned on and the suction manifold pressure is established. Data, such as pressure differences and temperatures, are collected. Sample holders are clamped after 20–35 minutes of suction and then transferred to a gas chromatograph. At the chromatograph, with the aid of some known concentration samples, a calibration curve is established for each run. The plenum sample is analyzed to establish the injection concentration. Then samples from the taps are analyzed to determine the local wall concentration.

The ratio of mass concentration at the wall to that in the plenum is the local impermeable wall effectiveness, η . These values can be numerically integrated, across Z , to give the average effectiveness, $\bar{\eta}$, at a given position downstream of injection, X .

Results

Local wall effectiveness for two different blowing rates and both density ratios are shown for the suction side of the blade on Fig. 3 and from along the pressure side of the blade on Fig. 4. At moderate blowing rate of 0.5 on the suction side, there is little variation of the results with lateral position Z . At this blowing rate with the increasing pressure away from the surface, the injected flow is apparently spread out better laterally across the surface. At higher blowing rates on the suction side, there is considerable variation of effectiveness with Z until about 25 diameters downstream of injection. For both blowing rates there is considerable lateral variation of η across the pressure surface, at least to X/D of 40.

Average values of effectiveness across the span (Z direction) were obtained from numerical integration of the local measurements. It is of interest to compare these values, η with the results obtained for slot injection (two-dimensional film cooling). For two-dimensional film cooling, a parameter, ξ , has been found to correlate the data well. This parameter can be derived from a simple energy balance on the boundary layer.¹ Figure 5 shows the variation of η with ξ for both density ratios and over a range of blowing rates and positions downstream of injection. Although there is not a direct correspondence with the two-dimensional correlation, the parameter ξ can be useful in correlating the results. For the range of the present tests the effectiveness on the pressure side is generally lower than that found with the two-dimensional correlation on a flat surface, which is shown as the solid lines on the figure. On the suction side, particularly at large values of ξ , the measured effectiveness is greater than for slot injection. An earlier study² also showed that the average effectiveness for injection through two staggered rows of holes on a flat surface compared favorably with this two-dimensional film cooling correlation.

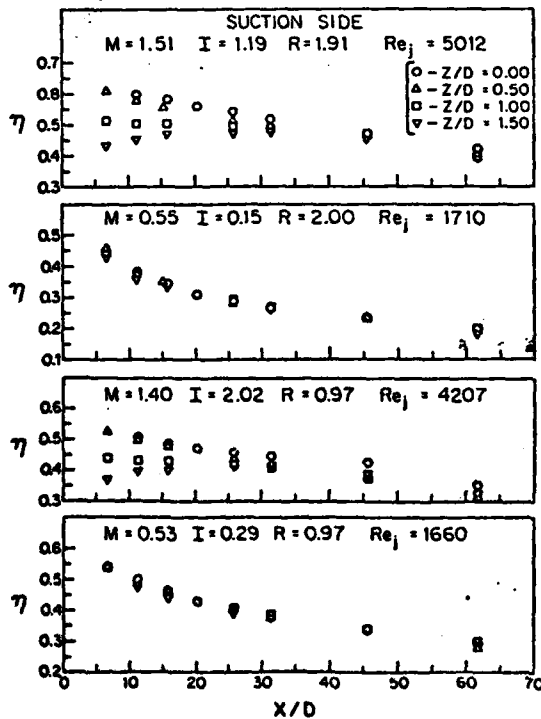


Figure 3 Local effectiveness variation on the suction side of the blade

Fig. 6 shows the variation of the local effectiveness along the centerline of an injection hole with position downstream for three different blowing rates and the two density ratios. The results are for the pressure side of the blade and indicate that there is little influence of density ratio on effectiveness along the surface at least up to a blowing rate of unity. This does not hold true on the suction side of the blade where there are much larger variations of effectiveness, and the momentum flux ratio, I , plays a more important role in determining the jet trajectory and effectiveness.

Figure 7 is a comparison of the results on the suction side of the blade with similar data from Ref. [7], in which the same cascade was used but with only a single row of holes. The hole diameter and spacing between the holes along a single row is the same for the two studies. For the same blowing rate, M , the effectiveness is much higher with the two rows of holes. This might be expected as for constant M , twice as much gas is injected per unit span across the blade because of the presence of the two rows. It is of interest to compare the results for two-row injection at a given M with those for a single row at twice that value of M ; then the injection per unit span would be the same.

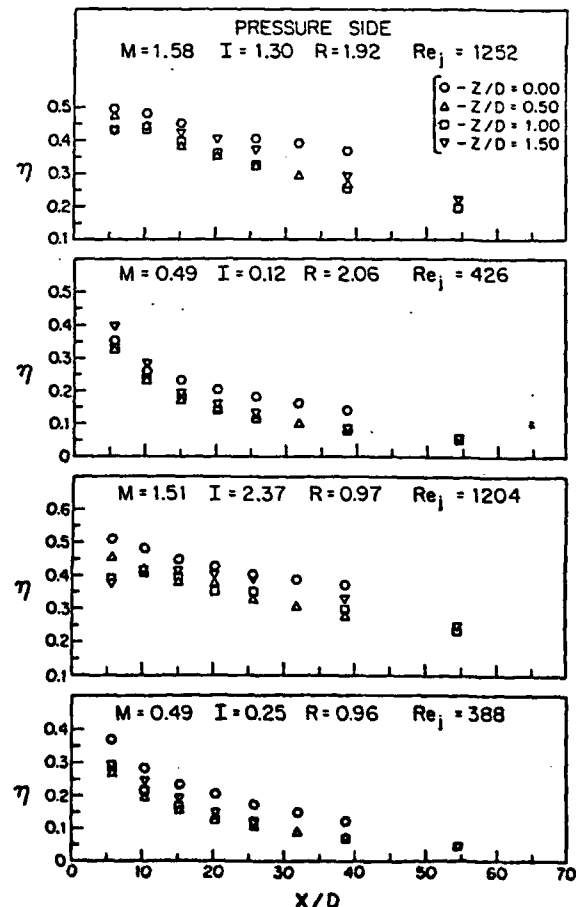


Figure 4 Local effectiveness variation on the pressure side of the blade

On the suction surface, the average effectiveness at $M = 2$ with a single row of holes is much less than that with two rows of holes and $M = 1$. Similarly, for $M = 1$ with the single row of holes and $M = 0.5$ for the two rows, at least for the density ratio near unity. However, for M approximately 0.5 with the single row of holes, the results at least at moderate and large X are close to those for M of about 0.26 with two rows of holes. Thus, at least at relatively low blowing rates some distance downstream of injection, the concept of energy balance is useful on the suction side -- i.e., a given amount of injection per unit span provides approximately the same effectiveness for single-row and two-row injection. Somewhat similar results for film cooling on a flat surface are reported in Ref. 9.

The bottom set of curves on Fig. 7 refer to results along the pressure surface of the blade. For the same mass injection per unit span the two rows-of-holes configuration provides much higher effectiveness at small X/D than does the injection through a single row of holes. However, even at large values of M , the results for the two injection configurations approach each other at large X/D , indicating that in this region the important factor for the cooling application would be the enthalpy deficit introduced by the injected fluid.

When describing the relative motion of a single jet introduced into a mainstream flowing over a curved surface, it is convenient to consider a parameter representing the momentum flux of the jet relative to the mainstream.⁷ This might be the momentum flux ratio, I , for a given angle of injection. To obtain a representation of the momentum flux in the mainstream direction, a parameter $I \cos \beta$ or $I \cos^2 \beta$ might be introduced.

Figure 8 presents the average effectiveness as a function of the parameter $I \cos^2 \beta$ at two different positions downstream of the injection holes. In addition to the results from the present study, data from Ref. [4] are shown to indicate the effectiveness on a flat surface. The data presented in Fig. 8 indicate that for small and moderate values of $I \cos^2 \beta$, the effectiveness is highest on the convex side and lowest on the concave surface and has an intermediate value on the flat surface. As $I \cos^2 \beta$ (and M) increases, the three curves appear to merge. The relative performance for the different surface curvatures is similar to that for a single row of holes⁷ at the low and moderate values of $I \cos^2 \beta$.

Fig. 9 is a comparison of the film cooling results for injection through two rows of holes and through a single row of holes. In general, the effectiveness is higher for a given surface with the two rows of holes than with the single row of holes at any value of $I \cos^2 \beta$. Perhaps the most marked differences between the results are that with a single row of holes there is a pronounced maximum of effectiveness on the convex side and then a significant fall-off as the jets penetrate into the mainstream. Only a weak maximum is present with injection through two rows of holes.

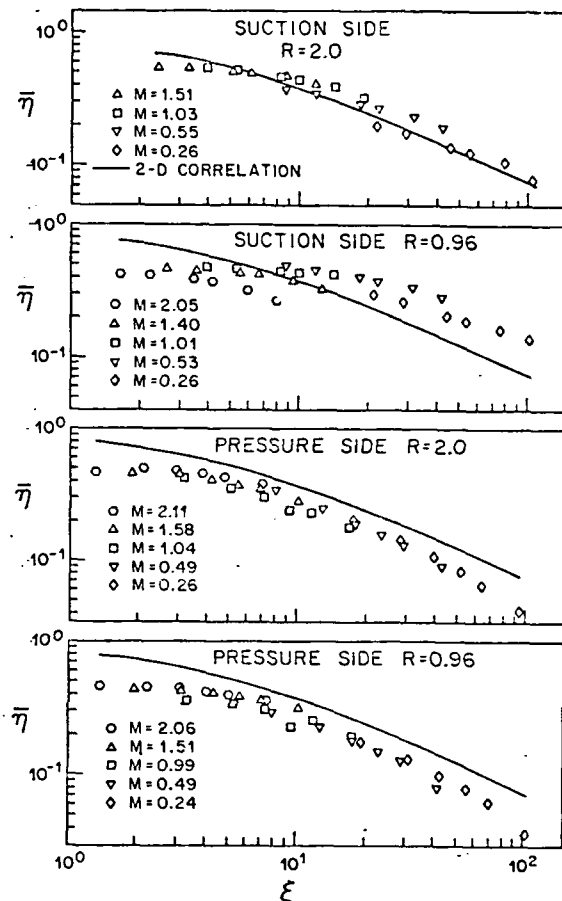


Figure 5 Average effectiveness compared with two-dimensional film cooling correlation for flat surface--solid line (Eq. 5 of Ref.4)

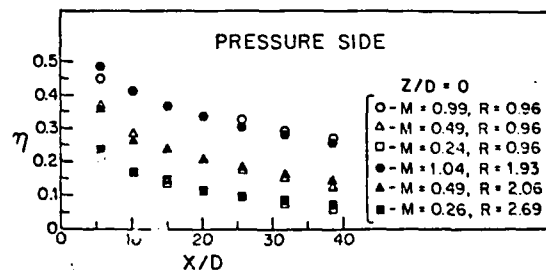


Figure 6 Centerline effectiveness of different density ratios on the pressure side

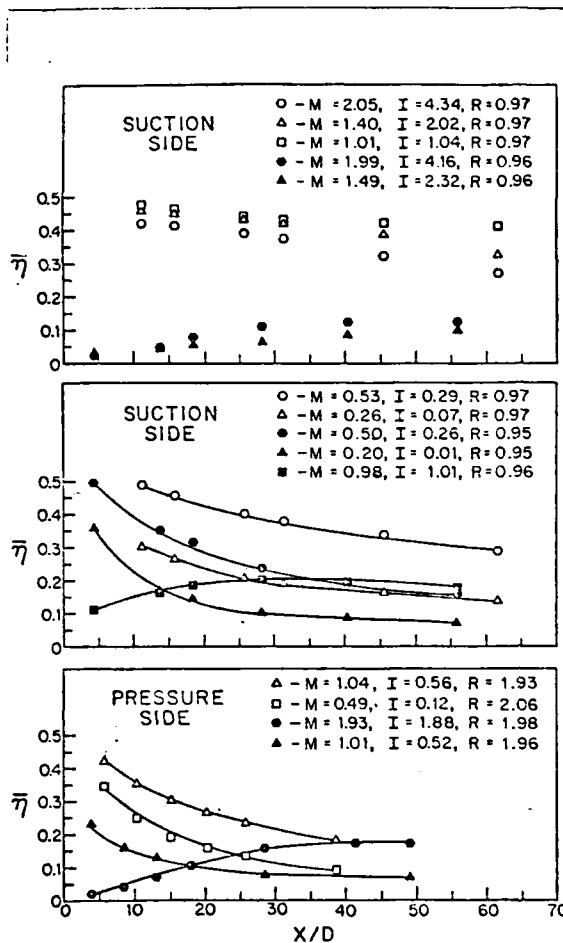


Figure 7 Comparison of average effectiveness with results for injection through one row of holes (shaded symbols--Ref. 7)

With the two rows, the effectiveness on the concave surface continually increases, approaching that of the effectiveness on the convex side. There is no significant crossover of the curves as occurs with single-row injection.

Figure 10 compares the results of the present tests using two different density ratios. The density ratio does not affect the general shapes and trends of the curves, particularly for injection on the suction side. However, on the pressure side, the blowing rate, M , actually correlates the data better (cf., Fig. 6) for the two different density ratios than does the momentum flux ratio, I , or $I \cos^2 \beta$. On the pressure side, then, the influence of the momentum flux ratio on jet trajectory does not influence the effectiveness as much as does the enthalpy or concentration deficit introduced by the injected fluid.

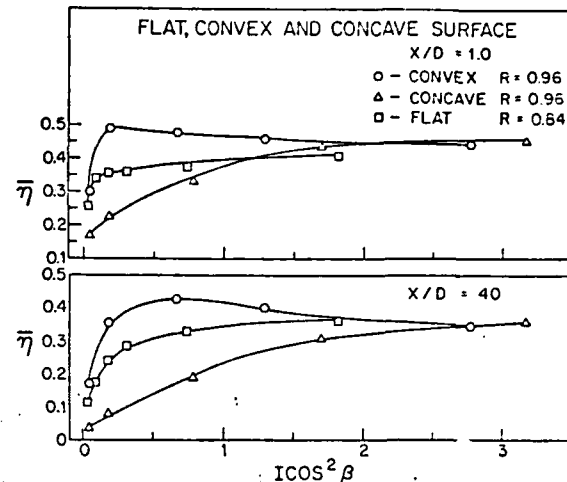


Figure 8 Comparison of average effectiveness with film cooling results obtained on a flat surface (Ref. 4)

Conclusions

The surface curvature appears to have a significant effect on film cooling performance with injection through two rows of staggered holes. The influence of curvature, however, is less than that with injection through a single row of holes where the jets tend to act more independently. With the staggered rows, the gaps between the individual holes in a row are filled in by jets from the other row with a resultant film cooling approaching the performance one might expect with two-dimensional (slot) injection. Even so, the effectiveness is considerably higher on the convex (suction) surface than on a flat or concave surface, particularly at low and moderate blowing rates. There is a slight maximum in effectiveness on the convex side as the parameter $I \cos^2 \beta$ increases, but this is weak compared to the maximum with a single row of injection holes. The average effectiveness increases monotonically with $I \cos^2 \beta$ on the concave surface, approaching the results on the convex surface at high values of $I \cos^2 \beta$.

At moderate and high blowing rates the film-cooling effectiveness with injection through two rows of holes is considerably greater than that following injection through a single row of holes--both determined for the same mass injected per unit span. This can generally be attributed to the more continuous distribution of injection across the span, tending to reduce the occurrence of lift-off or blow-off of the jets. At low blowing rate on the convex side and over a range of blowing rates on the concave side, although the injection through two rows of holes is still considerably better than for injection through a single row of holes at small values of X , the results for the two injection geometries approach

The Influence of a Laminar Boundary Layer and Laminar Injection on Film Cooling Performance

R. J. Goldstein

Department of Mechanical Engineering,
University of Minnesota,
Minneapolis, Minn. 55455
Fellow ASME

T. Yoshida

National Aerospace Laboratory
Tokyo, Japan
Assoc Mem ASME

Measurements are reported of the film cooling effectiveness and heat transfer following injection of air into a mainstream of air. A single row of circular injection holes inclined at an angle of 35 deg is used with a lateral spacing between the holes of 3 dia. Low Reynolds number mainstream and injection flow permit studying the influence of a laminar approaching boundary layer and laminar film coolant flow. Measurements of the surface heat transfer taken with no injection indicate that the hole openings can effectively trip the laminar boundary layer into a turbulent flow. The type of the approaching boundary layer has relatively little influence on either the adiabatic effectiveness or the heat transfer with film cooling. The importance of the nature of the injected flow on film cooling performance can at least be qualitatively explained by the differences in the transport mechanisms and in the penetration of the injected air into the mainstream.

Introduction

Film cooling has been used in many systems to protect solid surfaces exposed to high-temperature gas streams. The coolant injected into the boundary layer acts as a heat sink, reducing the gas temperature near the surface. Applications have been widespread, particularly in gas turbine systems where combustion chamber liners, turbine blades, and other hot parts of the engine have used air, usually taken from the exit of the engine compressor, for the film coolant.

In the leading edge region of turbine blades there is often a very high surface heat transfer. In this region, film cooling and the associated convection cooling in the coolant-injection holes have found widespread use in maintaining suitable skin temperatures. In most experiments done on film cooling, both the wall boundary layer and the flow through the injection holes have been turbulent. However, in the leading edge region and for some distance downstream, the boundary layer flow along the blade may be laminar. In addition, at low injection rates, the flow in the injection holes may be laminar.

Several investigators have considered film cooling with a laminar boundary layer along a flat surface [1-4]. In addition, experimental studies on leading edge injection have been reported using a cylindrical model [5, 6] and a flat-plate model with a circular nose [7]. There are also data on the characteristics of film-cooled turbine blades with injection holes in the leading edge region [8-13] and on full-coverage film cooling [14-17]. There has been little attention paid to a direct comparison between the film cooling results with a laminar boundary layer and with a turbulent boundary layer on the surface as well as for laminar versus turbulent flow in the injection holes. In the present work, local measurements of the adiabatic wall effectiveness and heat transfer with film cooling on a flat plate are described. By inserting or removing trips along the wall and/or in the injection tubes, laminar or turbulent flow can be obtained at approximately the same wall or tube Reynolds numbers.

Experimental Apparatus and Test Conditions

The present study has been conducted in a low-speed, open-circuit, induced-flow wind tunnel at the University of Minnesota. A sketch of the wind tunnel is shown in Fig. 1. A

detailed description of the wind tunnel is given elsewhere [18, 19]. The test section has been changed from previous studies by decreasing its length and by removing trips when a laminar approaching boundary layer is desired.

The test section floor is of low thermal conductivity material with stainless steel heater foils stretched across it. Five circular injection tubes are located at three-diameter spacing in the lateral direction and inclined at 35 deg to the mainstream flow. When a turbulent boundary layer is desired, a trip is placed on the wall as shown in Fig. 1. A thin tape may be placed across the injection holes to reduce their influence on the mainstream flow when studying the boundary layer in the absence of injection. The cross-sectional area of the test section is essentially constant and the streamwise pressure gradient is close to zero.

The freestream velocity is kept constant at 4.5 m/s. With this velocity the Reynolds number, Re_D , is of the order of magnitude of that which exists in the leading edge region of a gas turbine blade (3000 to 10,000).

The flow through the injection tubes can be changed to obtain different blowing rates. At the lowest blowing rates, the flow in the absence of any trip in the tubes is laminar. To obtain a turbulent boundary condition at low Reynolds numbers, trips 10 dia upstream of the tube exits are used. No trips are used at the high Reynolds number for which turbulent tube flow occurs naturally. In both the boundary layer and the injection tubes, velocity and turbulence measurements are obtained with a hot-film anemometer having a 0.051 mm dia by 1.0 mm long sensor.

The experiments are conducted under steady-state conditions. When measuring adiabatic wall temperature, heated air is injected to simplify the flow and measurement system. Assuming constant properties, the dimensionless adiabatic wall temperature should be the same with film "heating" as with film cooling. For the heat-transfer experiments, an approximately constant heat flux boundary condition is obtained from the foil heaters and the injected air is not heated so that it is essentially at the same temperature as the free stream (and $T_{aw} = T_\infty$).

Wall temperatures are measured by thermocouples embedded in the tunnel floor beneath the foil heaters. A correction is made for radiation from the heater and for conduction through the tunnel floor. However, no correction is made for conduction in the lateral, Z , direction; such

Contributed by the Heat Transfer Division for publication in the JOURNAL OF HEAT TRANSFER. Manuscript received by the Heat Transfer Division March 16, 1981.

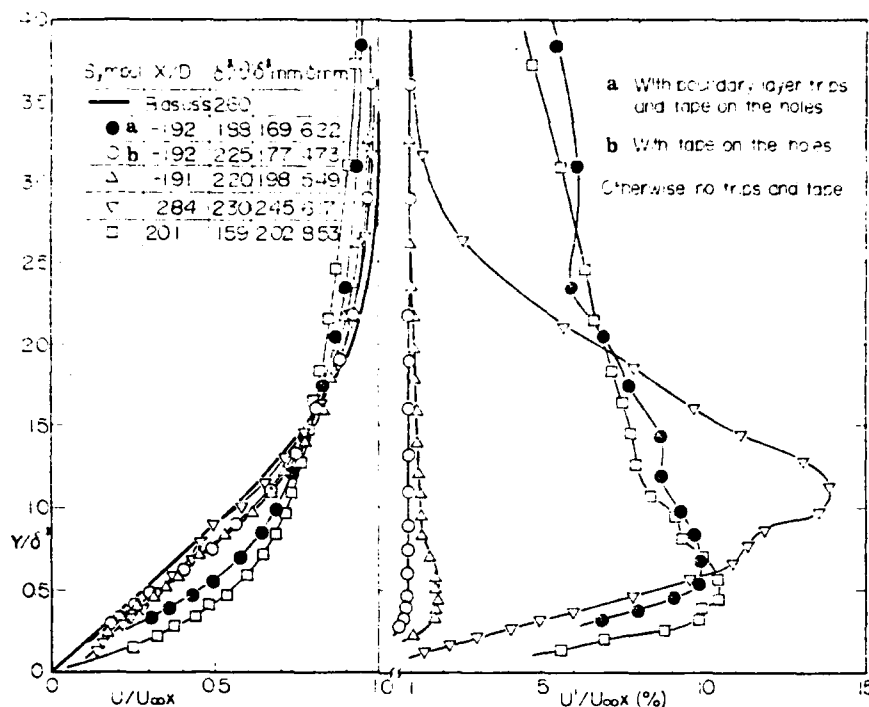


Fig. 2 Boundary layer profiles without injection

In the present study, local wall temperature measurements are made and then average values calculated.

Table 1 shows the range of test conditions in the present study.

Boundary Layer Flow Without Injection

Figure 2 shows dimensionless velocity and turbulence intensity profiles above the wall at different positions along the flow. The Blasius profile for a laminar boundary layer is indicated as a reference. The location, $X/D = -1.9$ and $Z/D = 0$, corresponds to a position 2mm upstream of the central injection hole upstream edge. At this location, in the absence of a trip, the measured profile is very close to the Blasius curve. This is true whether or not tape is used on the injection holes. The slight deviation from the theoretical curve may be due to the near-constant, cross-sectional area of the test section which produces a slight acceleration of the mainstream (see Table 1). When a trip (wire plus sandpaper roughness) is attached to the wall, the boundary layer becomes turbulent. The trips have been placed at a location to obtain approximately the same displacement thicknesses at the injection holes for the turbulent boundary layer as for the laminar boundary layer.

Somewhat downstream of injection ($X/D=2.84$), the boundary layer is still apparently laminar with open holes in the absence of trips, although some distortion in the velocity profile is evident. Further downstream, at $X/D=20.1$, the boundary layer appears to be turbulent with the open holes even in the absence of a trip. Although not shown in this figure, the boundary layer at this location is still laminar in the absence of a trip when tape is placed over the holes.

Injection Flow in the Absence of Mainstream

Figure 3 shows dimensionless velocity and turbulence intensity profiles of the flow exiting from the central injection hole ($Z/D=0$ and $Y/D=0.02$) in the absence of the mainstream. The flow is not heated. M_0 indicates a fictitious blowing rate for a density ratio of unity if the mainstream had a velocity of 4.5 m/s.

Table 1 Experimental range in the present study

Freestream mean velocity, U_∞	4.5 m/s
Freestream turbulence intensity, Tu_∞	$\approx 1\%$
Blowing rate, M	0.2, 0.35, 0.5
	1.0, 1.50, 2.0
Momentum flux ratio, I	0.060 - 5.1
Density ratio, ρ_2/ρ_∞	0.85, 1
Reynolds number, $Re_D (= \rho_\infty U_\infty D/\mu_\infty)$	3.4×10^3
Reynolds number, $Re_\tau (= \rho_2 U_2 D/\mu_2)$	$6.0 \times 10^2 - 6.7 \times 10^3$
Normalized displacement thickness 2mm upstream of leading edge injection hole, δ_0^*/D	0.16—laminar 0.14—turbulent
Acceleration parameter, K	1.2×10^{-2}

At low Reynolds number ($Re_\tau \sim 1.5 \times 10^3$), the velocity profile, in the absence of a trip, is close to that of a fully developed laminar pipe flow. The turbulence intensity is less than 0.4 percent everywhere across the flow. At the same Reynolds number, when the trip ring is attached on the inner surface of the tube, 10 dia upstream of the tube exit, the profile is similar to that for fully developed turbulent tube flow [20]. At larger Reynolds numbers no trip ring is used, and the velocity profile is close to that of a fully developed turbulent flow.

Film Cooling Effectiveness

The variation of the laterally averaged, film-cooling effectiveness with downstream position is shown in Fig. 4 for two different blowing rates. Curves representing results of some previous studies are shown for comparison. The key to the upper case letters, indicating the source of the earlier data for this and later figures, is contained in Table 2.

The most notable variation among the results from the present experiment occurs for a blowing rate of 0.5. The average effectiveness with laminar injection is considerably lower than with turbulent injection. This is true for either the laminar or turbulent boundary layer along the wall. It is known [18] that the film cooling effectiveness with $\beta=35$ deg reaches a maximum with variation in blowing rate near

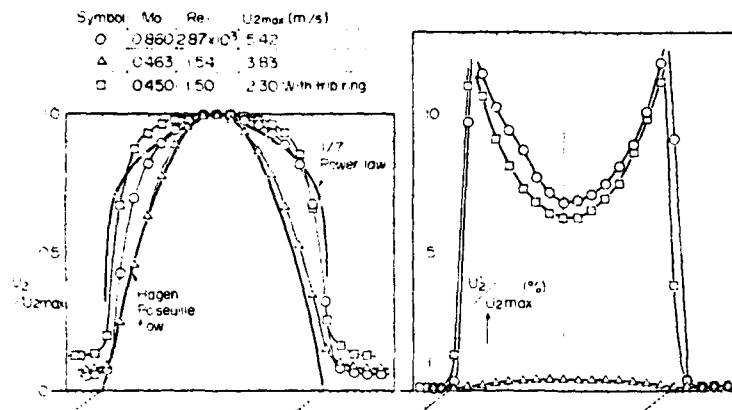


Fig. 3 Injection flow without mainstream

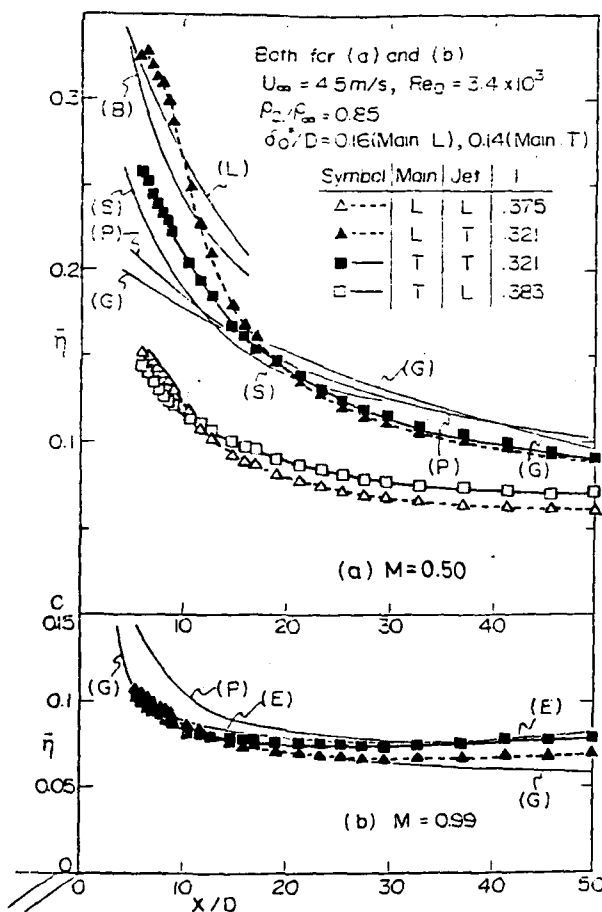


Fig. 4 Laterally averaged film-cooling effectiveness (see Table 2 for key to letters designating results from other studies)

$M=0.5$ for a density ratio close to unity. It is at this blowing rate that there is the greatest sensitivity to potential lift-off of a jet flowing from a film-cooling hole. When the jet penetrates into the mainstream its "cooling" influence on the wall is reduced; the enthalpy deficit it provides is no longer near the surface but rather is dissipated in the core of the primary flow.

In many of the earlier studies, done with turbulent injection or with a very short injection tube, the coolant entering the

mainstream has a relatively blunt profile so that the maximum velocity is close to the mean velocity. With developed laminar tube flow, the peak velocity is considerably greater than the average velocity. Thus, the mean momentum flux at the exit plane for laminar tube flow would be greater than the mean momentum flux at the same blowing rate, M , for a turbulent or plug-type flow.

At the same mean velocity, or M , the value of the mean square velocity for fully developed laminar tube flow is about 30 percent greater than the mean square velocity for 1/7 power law turbulent flow. Actually, the measured values of the momentum flux ratio, I , for the laminar jet were only about 18 percent greater than for the turbulent jet. A greater value of I at a given value of M could lead to greater penetration of the jet into the mainstream. The film-cooling effectiveness would be particularly sensitive to this effect at injection rates close to those yielding the maximum effectiveness.

With turbulent injection, the influence of the nature of the boundary layer approaching the injection holes is most pronounced close to the injection holes. The effectiveness is higher with a laminar boundary layer at $M=0.5$. The flow in the turbulent boundary layer with its greater fluctuations tends to dilute the influence of the injected fluid. Further downstream the curves cross and a slightly higher effectiveness occurs with a turbulent boundary layer, particularly with the laminar jets. This may be due to the turbulence causing the jet to mix more and diffuse back towards the wall.

The trends of most of the other investigations are close to the present ones for turbulent jets entering a turbulent boundary layer. The differences that occur may be due to uncertainty in experimental measurements and differences in the Reynolds number. Other influences may be the very blunt injection profile in reference [1] and the slightly smaller inclined angle and closer spacing in reference [2].

At a blowing rate close to unity there is a relatively good agreement with earlier studies that were performed in this laboratory, though not always with the same apparatus. The results of [21] indicate somewhat higher effectiveness, but in those tests the density ratio (ρ_2/ρ_∞) was somewhat higher than in the other studies.

Lateral distributions of the film cooling effectiveness at different downstream locations are presented in Fig. 5. When the approaching mainstream boundary layer is turbulent, a relative maximum appears near the region $Z/D=1$. This may be due to a pair of vortex flows and the resulting high turbulence which have been observed there. The adjacent minimum has been described [2] as due to the pumping effect

Table 2 Earlier works for film cooling effectiveness used for comparison

Worker	M	$Re_D \times 10^4$	ρ_2/ρ_∞	δ_0^*/D	Research
(B) Bergeles [2]	0.5	3.3	1.0	0.095	Spacing = $2.67D$ $\beta = 30$ deg mass transfer
(E) Eriksen, V. L. [19]	0.493 0.976	4.4	0.842 0.848	0.149	For heat transfer $M = .496$ $\rho_2 = \rho_\infty$
(G) Goldstein, Eckert, Eriksen, and Ramsey [22]	0.5 1.0	2.2	0.85	0.124	
(K) Kadorani and Goldstein [23]	0.5	1.1 4.4	0.85	0.245 0.175	(K1) (K2)
(L) Liess, C. [1]	0.57	1.5	0.79	0.087	Main: L Jet: E*
(P) Pedersen, Eckert and Goldstein [21]	0.513	1.1	0.960	0.162	Mass transfer
(S) Sasaki, Takahara, Kumagai and Hamano [24]	0.537	1.5	0.94	0.10	$\beta = 45$ deg Jet: E

* Jet: E means not fully developed turbulent but entrance region at the exit of injection holes.

Unless specified:
spacing = $3D$
 $\beta = 35$ deg
main: T and Jet: T
smooth surface, free stream turbulence intensity $\leq 1.5\%$
 η from wall temperature measurements

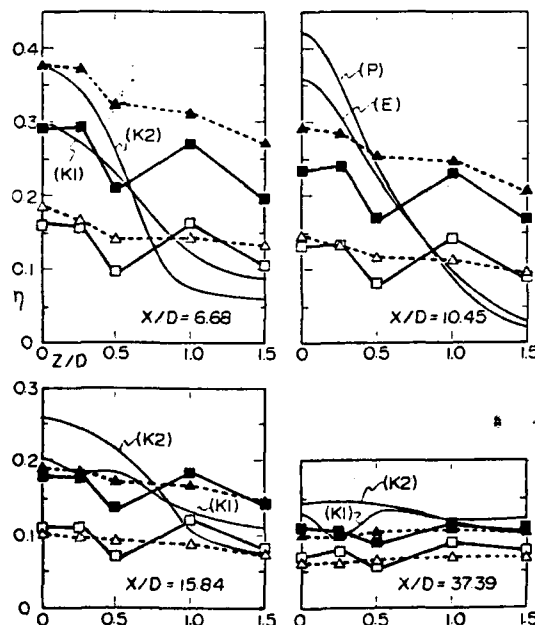


Fig. 5 Lateral distributions of effectiveness at $M = 0.5$ (see Table 2 for key to letters designating results for other studies; symbols for flow conditions are the same as in Fig. 4)

of the pair of rotating vortices. There is considerable difference in the lateral variation in the present study compared to the earlier ones shown in the figure. The present results indicate more uniform effectiveness in the Z direction. This may be partially due to the smoothing out of the results by conduction in the wall in the present work, but perhaps of more importance is the large difference in Reynolds number. The present results were taken at Reynolds number

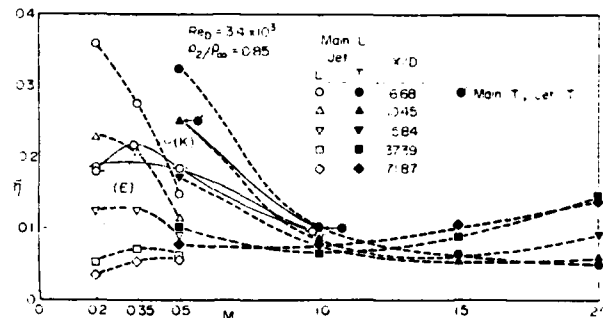


Fig. 6 Laterally averaged effectiveness versus blowing rate (see Table 2 for key to letters designating results from other studies)

$\rho_\infty U_\infty D / \mu_\infty$, about one-tenth of those used in the earlier studies for the turbulent boundary layer and turbulent jet flow. This is also borne out by comparison of curve K1 to K2. These results are obtained on the same apparatus but the data for curve K1 are at lower Re than for K2.

Figure 6 shows the variation of the average effectiveness with blowing parameter at different downstream locations. At blowing rates greater than 0.5, the injected flow is turbulent and the curves show the familiar decline of effectiveness with increasing M . As M is increased still further, above 1.0 or 1.5, the jets merge together and their influence is felt down on the wall, especially at large X .

At low blowing rates ($M < 0.5$), the flow in the injection holes is laminar. The maximum of η occurs at considerably lower values of M with laminar injection than with turbulent injection. It is also noteworthy that η for the laminar jet at low values of M can be higher than the peak η for turbulent injection. This is probably due to the relatively small amount of mixing (with the mainstream) of the laminar jet; at low M , when the jet does not leave the wall, this can result in high effectiveness. It should be noted, too, that the present results

for turbulent boundary layer and turbulent injection indicate a higher mean effectiveness than was found in [19] and [23] at $M=0.5$. This may be due to the higher (~three times) mainstream and jet Reynolds numbers in those earlier works.

The variation of centerline effectiveness, η_{cl} , with M is shown in Fig. 7. As observed in the previous figures, the effectiveness at a given M is considerably lower with the laminar injection. At moderate values of M , the centerline effectiveness for turbulent injection is somewhat higher with the laminar mainstream. The centerline effectiveness measured in the present study is less than that observed in [19], [22], and [23] for similar conditions of turbulent injection and turbulent boundary layer. This difference is apparently due to the lower Reynolds numbers during the present tests.

Heat-Transfer Coefficient

Figure 8 shows the spanwise-average, heat-transfer coefficient at various downstream locations in the absence of injection. A linear average of the local values measured at $Z/D=0, 0.75$, and 1.5 is used. Two sets of data were obtained with the holes covered by a thin layer of tape to prevent them from introducing a cavity-type roughness which could disturb the flow. In the other two runs the holes were open, as would occur when injection takes place, although there is no net throughflow of gas. For both the open- and closed-hole conditions there is a set of data when the boundary layer trips were placed on the wall and another set when there were no trips.

When the holes are closed, there is little variation (approximately 3 percent) of the heat-transfer coefficient in the lateral direction. With open holes in the presence of trips this variation is approximately 5 percent. With no trip, the open holes can initiate transition and this leads to a significant variation of h_{av} across the span; the maximum value of h_{av} occurs at $Z/D=0$, except very close to the downstream edge of the holes. The variation of the heat-transfer coefficient from the mid-point of the holes to the region half-way between the holes ($Z/D=1.5$) averages about 10 percent for these open holes without trips and has a maximum of 17 percent.

Note in Fig. 8, with taped-over holes in the absence of trips the heat transfer closely follows the equation (1) which represents heat transfer along a flat plate with a laminar boundary layer. Far downstream, the measured points rise somewhat above the predicted curve, perhaps due to transition. The other three sets of data appear to be represented, at least some distance downstream, by the heat-transfer correlation (equation (2)) for a turbulent boundary layer on a flat plate. When the trips are present there is virtually no difference between the measured results for the closed and open holes. In the absence of trips with the holes open, there is a transition region downstream from the start of heating. This is indicated by the somewhat lower heat transfer results for this flow condition till approximately 20 dia downstream of the injection hole location. Further downstream there appears to be little difference between this and the data obtained with a boundary layer trip.

Figure 9 shows the variation of the average heat-transfer coefficient with downstream position for a blowing rate of 0.5 and different conditions of mainstream and injected flow. At this blowing rate with the turbulent boundary layer there is very good agreement with an earlier study [19]. The average heat-transfer coefficient is increased little over that without injection.

When the boundary layer is initially laminar, the injection has a bigger effect on the heat transfer. With the laminar boundary layer, for both laminar injection and turbulent injection, two curves are plotted on Fig. 9. In one, the reference heat-transfer coefficient is the same as for the

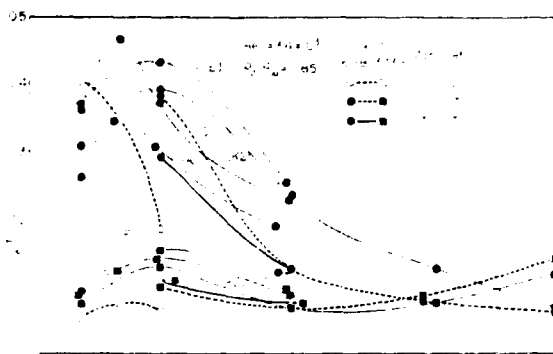


Fig. 7 Centerline effectiveness versus blowing rate (see Table 2 for key to letters designating results from other studies)

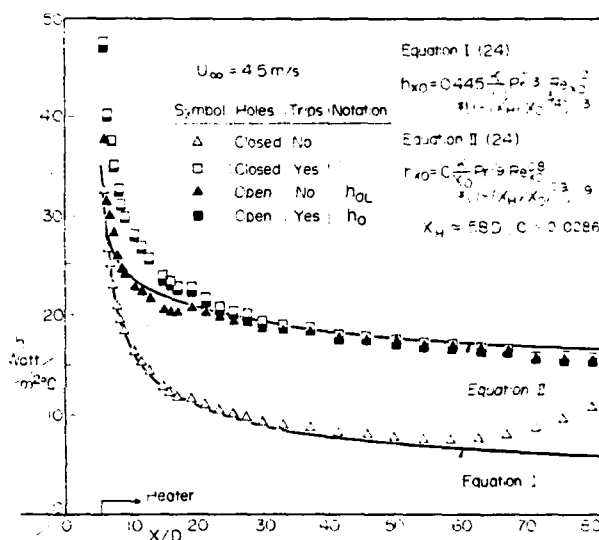


Fig. 8 Laterally averaged heat-transfer coefficient without injection

turbulent boundary layer studied and is taken from the data in the present experiment with the trip, as was true for the plots with the turbulent boundary layer in the top portion of Fig. 9. It should be noted that this is a somewhat arbitrary reference state—used only for comparison with the other data—as the boundary layer flow for these runs was laminar upstream of injection. With this reference value (in the denominator of the ratio), we see that there is not a great variation from the heat-transfer coefficient for a turbulent boundary layer without injection other than close to the holes. There, laminar flow injection results in lower heat-transfer coefficients (smaller transport coefficients); with turbulent injection, the eddies along the wall give an increase in the heat-transfer coefficient.

The other two curves for the initially laminar boundary layer case refer to the data (h_{ref}) from Fig. 8 for open holes in the absence of a trip. Compared to this case, which had a somewhat lower heat-transfer coefficient than when the trip was present, the injection increases the heat transfer to a maximum of 20–30 percent over that without injection. In the absence of injection there are still essentially laminar patches along the wall with relatively small heat transport. Injection results in eddies which make the heat-transport coefficient greater than that with the laminar patches. Far downstream at this blowing rate, the heat-transfer coefficient is little altered by the injection and, of course, is little different from the heat transfer with the turbulent boundary layer in the absence of injection.

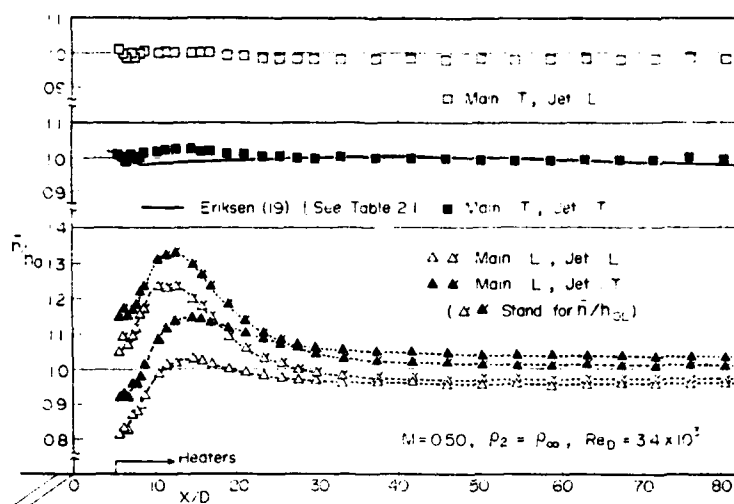


Fig. 9 Laterally averaged heat-transfer coefficient

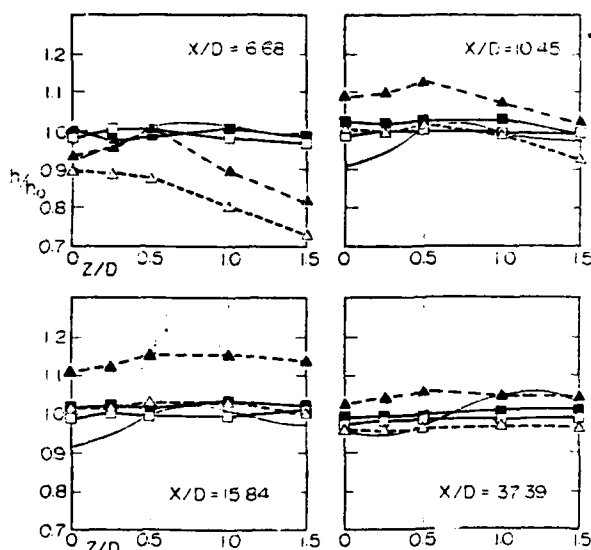


Fig. 10 Lateral distributions of heat-transfer coefficient (symbols and experimental conditions are the same as those described in Fig. 9)

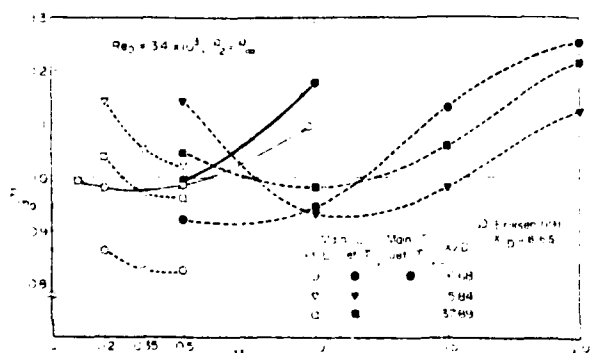


Fig. 11 Laterally averaged heat-transfer coefficients versus blowing rate

Figure 10 shows the spanwise variation of the heat-transfer coefficient—in all cases compared to the heat-transfer coefficient for the turbulent boundary layer with the trip in the absence of injected flow. There is little variation with Z

other than close to injection. With an initially laminar boundary layer, h is relatively small between the holes at $X/D=6.68$, where one might expect incomplete transition to turbulence. Relatively low h also occurs in a laminar boundary layer in this region when there is no injection yet open holes.

Figure 11 shows the variation of the average heat-transfer coefficient with blowing rate at three different downstream locations. Some results from [19] are included for comparison. The results for laminar injection and a laminar boundary layer should be noted. The ratio, \bar{h}/h_0 , is less than unity at small X/D over the range of M for which experiments could be run. If the denominator of this ratio were the heat transfer with a laminar boundary layer and no injection (even with the holes open), the three points would be close to or above unity. Further downstream, the ratio is near or above unity. With laminar injection the heat-transfer coefficient decreases with increasing M in the range studied. The turbulent jets are still attached to the wall at $M=0.5$ and lead to a somewhat higher heat transfer than do the laminar jets.

There is a decrease in \bar{h}/h_0 as M increases for the case of the turbulent jet in an initially laminar boundary layer due to jet penetration. At higher blowing rates the heat transfer coefficient increases with M , as had been shown in an earlier study [19] for the turbulent boundary layer and turbulent jet combination. Under those conditions, the turbulent jet flow tends to dominate the transport characteristics in the mainstream.

Conclusions

The major influence of the character of the boundary layer and of the injection jets for film cooling in the geometry studied is in the differing results for laminar jet flow versus turbulent jet flow. With laminar jets the maximum in film cooling effectiveness occurs at relatively small values of the blowing parameter M . This is due to the greater penetration of the laminar jets at a given value of M as compared to turbulent jets. The fuller the velocity profile of the jet, the greater is the blowing rate before the jet tends to lift off the surface. In this regard, it should be noted that flow through a short entrance section occurs in many applications and will often result in a blunt velocity profile.

The nature of the boundary layer seems to play a bigger role when the jet is turbulent, at least in terms of the film-cooling effectiveness. Thus, there is a higher effectiveness with the laminar boundary layer and turbulent jets, at least close to injection, as compared to the turbulent boundary layer with

the turbulent jet. With the laminar jet, the nature of the boundary layer does not greatly influence the effectiveness.

In terms of heat transfer with the turbulent boundary layer, both the turbulent and laminar jets appear to have similar influences. For the initially laminar boundary layer the most important effect of injection is its influence on transition to turbulence.

Acknowledgment

The support of the U.S. Army Office of Research under Grant DAA29-79-C-0117 is gratefully acknowledged. Early portions of the study were supported by the Power Branch of the Office of Naval Research.

References

- 1 Liess, C., "Experimental Investigation of Film Cooling with Ejection From a Row of Holes for the Application to Gas Turbine Blade," *ASME Journal of Engineering for Power*, Vol. 97, 1975, pp. 21-27.
- 2 Bergeles, G., "Three-Dimensional Discrete-Hole Cooling Processes. An Experimental and Theoretical Study," Ph.D. thesis, Imperial College, University of London, 1976.
- 3 Pavri, R. and Tabakoff, W., "An Analytical Solution of Wall-Temperature Distribution for Transpiration and Local Mass Injection Over a Flat Plate," *ASME Paper No. 72-HT-57*, 1972.
- 4 Nilson, R. H. and Tsuei, Y. G., "Film Cooling by Oblique Slot Injection in High-Speed Laminar Flow," *AIAA Journal*, Vol. 13, 1975, pp. 1199-1202.
- 5 Luckey, D. W., Winstanley, D. K., Hanus, G. J., and L'Ecuyer, M. R., "Stagnation Region Gas Film Cooling for Turbine Blade Leading-Edge Applications," *J. Aircraft*, Vol. 14, 1977, pp. 494-501.
- 6 Russell, L. M., "Flow Visualization of Discrete-Hole Film Cooling with Spanwise Injection Over a Cylinder," *NASA TP 1491*, 1979.
- 7 Sasaki, M., Takahara, K., Sakata, K., and Kumagai, T., "Study on Film Cooling of Turbine Blades," *Bulletin of the JSME*, Vol. 19, 1976, pp. 1344-1352.
- 8 Hiroki, T. and Katsumata, I., "Design and Experimental Studies of Turbine Cooling," *ASME Paper No. 74-GT-30*, 1974.
- 9 Muska, J. F., Fish, R. W., and Suo, M., "The Additive Nature of Film Cooling from Rows of Holes," *ASME Journal of Engineering for Power*, Vol. 98, 1976, pp. 457-464.
- 10 Yoshida, T., Minoda, M., Sakata, K., Nouse, H., Takahara, K., and Matsuki, M., "Low- and High-Speed Cascade Tests of Air-Cooled Turbine Blades," *ASME Paper No. 76-GT-40*, 1976.
- 11 Hanus, G. J. and L'Ecuyer, M. R., "Leading-Edge Injection for Film Cooling of Turbine Vanes," *Journal of Energy*, Vol. 1, 1977, pp. 44-49.
- 12 Nouse, H., Takahara, K., Yoshida, T., Yamamoto, A., Sakata, K., Inoue, S., Mimura, F., and Usui, H., "Aerodynamic and Cooling Performances of a Film-Cooled Turbine," *Proceedings of the 1977 Tokyo Joint Gas Turbine Congress*, 1977, pp. 206-214.
- 13 Sakata, K., Usui, H., and Takahara, K., "Cooling Characteristics of Film Cooled Turbine Vane Having Multi-Row of Ejection Holes," *ASME Paper No. 78-GT-21*, 1978.
- 14 Metzger, D. E., Takeuchi, D. I., and Kuenstler, P. A., "Effectiveness and Heat Transfer with Full-Coverage Film Cooling," *ASME Journal of Engineering for Power*, Vol. 95, 1973, pp. 180-184.
- 15 Mayle, R. E. and Camarata, F. J., "Multi-Hole Cooling Film Effectiveness and Heat Transfer," *ASME Paper No. 74-HT-9*, 1974.
- 16 Crawford, M. E., Kays, W. M., and Moffat, R. J., "Full Coverage Film Cooling on Flat, Isothermal Surfaces: A Summary Report on Data and Predictions," *NASA CR-3219*, 1980.
- 17 Launder, B. E. and York, J., "Discrete-Hole Cooling in the Presence of Free Stream Turbulence and Strong Favourable Pressure Gradient," *International Journal of Heat and Mass Transfer*, Vol. 17, 1974, pp. 1403-1409.
- 18 Goldstein, R. J., Eckert, E. R. G., and Ramsey, J. W., "Film Cooling with Injection Through a Circular Hole," *NASA CR-54604*, University of Minnesota HTL TR No. 82, 1968.
- 19 Eriksen, V. L., "Film Cooling Effectiveness and Heat Transfer with Injection Through Holes," *NASA CR-72991*, University of Minnesota HTL TR No. 102, 1971.
- 20 Laufer, J., "The Structure of Turbulence in Fully-Developed Pipe Flow," *NACA TR-1174*, 1954.
- 21 Pedersen, D. R., Eckert, E. R. G., and Goldstein, R. J., "Film Cooling with Large Density Differences Between the Mainstream and the Secondary Fluid Measured by the Heat-Mass Transfer Analogy," *ASME JOURNAL OF HEAT TRANSFER*, Vol. 99, 1977, pp. 620-627.
- 22 Goldstein, R. J., Eckert, E. R. G., Eriksen, V. L., and Ramsey, J. W., "Film Cooling Following Injection Through Inclined Circular Tubes," *Israel Journal of Technology*, Vol. 8, 1970, pp. 145-154.
- 23 Kadotani, K. and Goldstein, R. J., "On the Nature of Jets Entering a Turbulent Flow, Part B: Film Cooling Performance," *ASME Journal of Engineering for Power*, Vol. 101, 1979, pp. 466-470.
- 24 Sasaki, M., Takahara, K., Kumagai, T., and Hamano, M., "Film Cooling Effectiveness for Injection from Multirow Holes," *ASME Journal of Engineering for Power*, Vol. 101, 1979, pp. 101-108.
- 25 Hartnett, J. P., Eckert, E. R. G., Birkebak, R., and Sampson, R. L., "Simplified Procedures for the Calculation of Heat Transfer to Surfaces with Non-Uniform Temperatures," *University of Minnesota HTL TR No. 10*, 1956.



The Society shall not be responsible for statements or opinions advanced in papers or in discussion at meetings of the Society or of its Divisions or Sections, or printed in its publications. Discussion is printed only if the paper is published in an ASME Journal. Released for general publication upon presentation. Full credit should be given to ASME, the Technical Division, and the author(s). Papers are available from ASME for nine months after the meeting.
Printed in USA

MASS TRANSFER IN THE NEIGHBORHOOD OF JETS ENTERING A CROSSFLOW

R. J. GOLDSTEIN

Professor and Head

Department of Mechanical Engineering

University of Minnesota

Minneapolis, Minnesota

Fellow, ASME

J. R. TAYLOR

Member, Technical Staff

The Aerospace Corporation

Los Angeles, California

The mass transfer coefficient downstream of a row of jets entering a cross flow is determined by measuring the local sublimation rate from a naphthalene surface. This mass transfer relates directly to the heat transfer that would occur on a film-cooled wall. Mass transfer is used to study film cooling because of better control of the boundary conditions and greater precision in the local measurements than would occur with a heated surface. The experiments indicate that jets significantly increase the transfer coefficient in the neighborhood of the holes through which the jets emanate--in particular, immediately adjacent to the holes and some distance downstream of the centerline of the holes.

NOMENCLATURE

D	injection tube inner diameter, 11.7 mm
h	heat or mass transfer coefficient
h_H	heat transfer coefficient, Eq. 2
h_M	mass transfer coefficient, Eq. 3
M	blowing parameter or blowing rate; ratio of mass flux of injected air to mass flux of free stream
\dot{m}	mass flux of naphthalene from surface
Pr	Prandtl number
q	wall heat flux
Sc	Schmidt number
Sh	Sherwood number
St	Stanton number
T_{aw}	adiabatic wall temperature
T_r	free stream recovery temperature
T_2	film coolant temperature
X	downstream distance from downstream edge of injection holes
Z	lateral distance across span measured from center of injection holes

Greek Symbols

ρ_w	density of naphthalene at surface
ρ_{iw}	density of naphthalene at an impermeable surface
η	film cooling adiabatic wall effectiveness, Eq. 1

INTRODUCTION

Film cooling continues to be a widely-used yet not fully understood technique to prevent overheating of surfaces exposed to high-temperature gas streams. The emphasis in terms of applications is towards gas turbine systems--both aircraft and land-based--where higher gas temperatures can lead to significant improvements in economy and output.

In film cooling, a fluid (usually a gas) is injected from and along the surface to be protected from a high-temperature mainstream. The film coolant tends to act as an insulating layer separating the surface from the high-temperature flow. Alternately, one can consider the injected fluid as a dilutant which reduces the temperature in the boundary layer. Early film cooling studies [1] concentrated on two-dimensional flows with the coolant introduced continuously across the span of the surface to be protected. In many applications, however, a discontinuous injection system usually with one or more rows of discrete holes along the surface is used. This latter method of injection, often called three-dimensional film cooling, is usually not as effective as two-dimensional film cooling because of the opportunity of the hot mainstream to flow underneath the jets of coolant that emanate from the discrete holes. Recently, full two-dimensional arrays of injection holes along the surface have been studied. This full-surface film cooling tends to approach transpiration cooling in the limit as the spacing between the injection holes decreases.

In studying either two-dimensional film cooling from a single slot or three-dimensional film cooling from a single row or even several rows of holes, a convenient means of analyzing the problem has been to consider the adiabatic wall temperature and the heat transfer coefficient as separate quantities to be determined. The adiabatic wall temperature can be put in a convenient dimensionless form as a film cooling effectiveness

$$\eta = \frac{T_{aw} - T_r}{T_2 - T_r} \quad (1)$$

In the idealized limit, the effectiveness would be unity near injection and far downstream the effectiveness would approach zero as the adiabatic wall temperature approaches the freestream recovery temperature. It should be borne in mind that although the latter is generally true, the effectiveness -- particularly with three-dimensional film cooling -- is usually well below unity even close to injection.

Use of the adiabatic wall temperature permits the definition of a well-behaved heat transfer coefficient

$$q = h_h (T_w - T_{aw})$$

or

$$h_h = \frac{q}{T_w - T_{aw}} \quad (2)$$

Note that when the temperature difference ($T_w - T_{aw}$) is zero, q goes to zero without any special requirement on h_h . In addition, some distance downstream from injection, the heat transfer coefficient should approach the value that would occur on a similar surface with similar mainstream flow and no injected flow.

The present study is concerned with measurements that would lead to prediction of the heat transfer coefficients downstream of a single row of injection holes with air as the film coolant and with a mainstream of air. Although a number of different geometries for the injection holes are possible, a system is chosen that approximates one used in many applications. This is a row of circular holes inclined at 35° to the surface and spaced apart, center to center, by 3 diameters. Figure 1, which shows part of the test apparatus, gives an indication of this geometry.

PREVIOUS STUDIES

A number of studies have been made on three-dimensional film cooling. Many of these, however, have been concerned primarily with the determination of adiabatic wall effectiveness. Heat transfer is much more difficult to determine, particularly when close to the injection holes, at least in part due to thermal conduction to or from the injected flow through the wall over which the mainstream flows.

Most measurements of heat transfer with film cooling have been done using a system in which averages are taken at least across the span of the tunnel. This includes studies by Metzger and Fletcher [2], Metzger, Kuenstler, and Takeuchi [3], Liess [4], and Mayle and Camarata [5].

Crawford, Kays and Moffat used heat transfer gauges to study the heat transfer with full-surface film cooling [6]. Heat transfer has been studied in high-speed tunnels using transient heat flux gauges by Schultz, Oldfield and Jones [7] and Louis [8].

Local measurements of heat transfer on a film-cooled surface with a single row of injection holes have been reported by Erikson and Goldstein [9] and Jabbari and Goldstein [10]. In these studies, a uniform wall heat flux boundary condition was approximated by having a thin heater stretched across an almost adiabatic surface. Heat transfer coefficients were determined from local measurements of the wall temperature. These studies indicated an increase in the heat transfer close to the injection location relative to that on an equivalent surface without injection. The heat transfer coefficients increased as the amount of injected gas was increased and tended to decrease some distance downstream of the injection hole, eventually approaching the values observed without injection. For a hole geometry similar to that in the present experiment, the closest to the holes that measurements could be made was approximately 5.57 diameters downstream. The problem with measurements closer to the holes, in these as in other studies, is the error introduced by wall conduction as well as the difficulty in having a heated surface extremely close to the injection region.

The present study was initiated to obtain information on heat and mass transfer very close to injection holes over a range of flow conditions. The geometry chosen was similar to that of Ref. [9], a single row of holes inclined at 35° to the mainstream with 3-diameter center-to-center spacing between the holes. To avoid problems encountered with heat conduction in the wall, a mass transfer technique was used.

MASS TRANSFER SYSTEMS

A mass transfer analogy has been used in a number of studies on film cooling. With two-dimensional film cooling, local impermeable wall concentrations have been compared to adiabatic film cooling effectiveness for some time [11, 12]. The validity of this mass transfer analogy for injection through a row of discrete holes was demonstrated in Ref. [13]. The advantages of the mass transfer analogy for measuring wall effectiveness are that a large range of densities can be obtained without having large temperature differences and the problems due to wall conduction are avoided.

A different application of the mass transfer analogy is used in determining the influence of injection on the heat transfer. Naphthalene sublimation has been used to determine average mass transfer coefficients by determining the mass of naphthalene that is sublimed in either a forced or natural convection system [14]. With this technique a naphthalene surface is cast in the particular geometry desired. With a forced flow across that surface, mass will be continually lost due to diffusion and convection in a similar manner to heat transferred from a surface. The analogy between the mass transfer and heat transfer processes is direct, taking into account differences in properties and assuming the turbulent transport and boundary conditions are similar for the mass transfer and heat transfer systems.

One boundary condition in an isothermal air-naphthalene system would be constant naphthalene vapor pressure and vapor concentration at the surface which is equivalent to an isothermal wall heat transfer boundary condition. The only significant difference in boundary conditions appears to be in the velocity at the wall. The finite sublimation of naphthalene gives a normal component of velocity

which is absent in most convective heat transfer studies. In general, this component of velocity is small enough that it does not significantly alter the sublimation rate.

A mass transfer coefficient, h_M , is defined by

$$\dot{m} = h_M (\rho_w p_{1w}) \quad (3)$$

In the present study the concentration of naphthalene vapor in both the freestream and in the injected gas is zero and Eq. (3) reduces to

$$\dot{m} = h_M \rho_w \quad (4)$$

This is analogous to Eq. 2.

The analogy indicates that the Sherwood number is equivalent to the Nusselt number if the Schmidt number and the Prandtl numbers are equal. This implies not only equal diffusion coefficients but equal turbulent transport coefficients as well.

The Schmidt number (approximately 2.5 at ambient temperature for naphthalene diffusing in air) has a different value from the Prandtl number of air (~0.7). The comparison of mass transfer and heat transfer results is often put in the form

$$Sh/Nu = (Sc/Pr)^n \quad (5)$$

where n is typically of the order of 0.4.

The validity of the analogy has been demonstrated by Sogin [15]. Local measurements of mass transfer were made by Lee and Barrow [16] and Kan, Miwa, Morishita, Munakata and Nomura [17].

EXPERIMENTAL APPARATUS AND PROCEDURE

The experiments were conducted in the University of Minnesota Heat Transfer Laboratory Wind Tunnel. The tunnel cross section is 0.355 m high, 0.61 m wide, and 2.5 m long. Sidewalls for the present experiment reduced the width of the channel to about 0.20 m. These walls were set to diverge slightly to maintain a uniform free stream speed of the air in the tunnel. A wire trip followed by sand paper was placed about 0.41 m upstream of the naphthalene plate. The main-stream velocity and the boundary layer profiles were determined using a total pressure probe and static pressure wall taps. With the normal free stream speed of 15 m/s, the boundary layer displacement thickness at the upstream edge of the injection holes was about 2.2 mm. The Reynolds number based on this velocity and D was 11×10^3 . Extrapolation of the boundary layer thickness upstream indicated that the effective starting point of the boundary layer was 155 mm upstream of the trip wire.

Air was injected through six tubes, with three-diameter spacing placed across the span. These tubes are essentially the same as those used in an earlier study [18]. They have an 11.7 mm ID, a 14.3 mm OD, and are long enough to assure fully-developed turbulent flow at the exit in the absence of a mainstream flow. The flow injected through the tubes could be controlled by needle valves. The overall injected flow was determined by measuring the pressure drop across an orifice plate. Three of the tubes were cut off and the extensions to the plate surface were part of the injection system included in the naphthalene

plate shown in Fig. 1. The injection tube Reynolds number was 2300 at $M = 0.2$ and about 23,000 at $M = 2$.

The removable section (Fig. 1) consists of the naphthalene test plate, its support, and three injection tubes as well as temperature-measuring instrumentation. The main body of the naphthalene test plate is made of aluminum. The opening in the tunnel floor in which the plate sits is 241 mm long by 170 mm wide. The actual naphthalene surface within this plate is 184 mm long by 95 mm wide. Thermocouples are embedded in the test plate to measure the temperature at the naphthalene surface. The tip of the center injection tube near which measurements were made was beveled to reduce the metal exposure so that mass transfer measurements within 0.1 D of the tube could be made. When the test plate is in the tunnel floor, the three tubes are connected to the lower portion of the injection system through tight plastic sleeves.

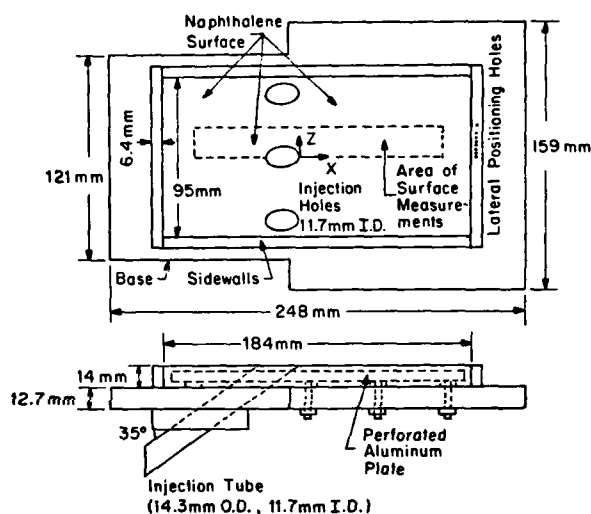


Fig. 1 The naphthalene test plate

In preparing the naphthalene mold, the test plate was placed in an inverted position on a lapped stainless steel plate. The perforated plate within the system (cf, Fig. 1) was heated to about 80°C, somewhat below the melting point of naphthalene. After pouring in the molten naphthalene, the system was allowed to cool. When the outer naphthalene surface reached about 40°C, it was freed by a sharp blow to the stainless-steel plate.

Measurements of the naphthalene surface profile were taken before and after exposure in the wind tunnel. For these measurements, the test plate was placed on a lathe bed which can be translated in the X and Z directions. A mechanical depth gauge accurate to approximately 5×10^{-4} mm with a range of 0.2 mm was used to determine surface profiles from measurements at 370 locations in the area shown in the rectangle on Fig. 1. Only differences in naphthalene height or thickness are required. However, after exposure in the wind tunnel, the test plate could not be replaced in exactly the same location on the measuring bed as it had been when the first surface measurements were taken. Therefore, at each Z location, measurements were taken at reference points on the aluminum frame

of the test plate. Thus, the displacement of a point on the surface from a line connecting these reference points both before and after exposure in the wind tunnel could be determined. The amount of naphthalene sublimed varied from ~ 0.05 mm to ~ 0.18 mm.

Due to the great sensitivity of the naphthalene vapor pressure to temperature, care was taken to be sure the system was isothermal. Temperatures were measured continuously using thermocouples embedded close to the naphthalene surface, along the injection tubes, and in the mainstream. Usually, the naphthalene surface could be maintained within 0.25°C of the free stream and the injected air within 0.15°C of the free stream.

Measurements of the surface temperature gave naphthalene vapor pressure and density or concentration. These measurements were taken every five minutes and an average concentration was used to determine the value over the period of the test. At the lowest blowing rate the naphthalene surface was exposed for approximately 90 minutes. At the highest blowing rate the test runs lasted about 60 minutes.

Knowing the change of depth and the density of solid naphthalene, the local mass transfer over the period of exposure in the wind tunnel could be obtained. From this and the surface concentration, the mass transfer rate and the Sherwood number were determined. The measurements were corrected for sublimation during the time profiles were being measured, the time to set up the test plate in the tunnel, and the time for remounting it in the measuring apparatus. The total correction was typically of the order of 6.5% of the smallest sublimation depth.

MASS TRANSFER RESULTS

The first measurements of mass transfer were made on a flat uninterrupted surface of naphthalene. From the measurements Sherwood numbers and Stanton numbers for mass transfer were calculated. These results compare favorably to a correlation for heat transfer from a flat surface to a turbulent boundary layer of air taking into account an "un-heated" starting length and using Eq. 5. The experimental points are about 2% above the prediction line and have an almost identical slope.

The measurements on the continuous naphthalene surface indicated the validity of the mass transfer analogy for studying heat transfer. They also gave the reference point for mass transfer coefficients on an undisturbed surface, h_0 , to which the results with injection are compared.

The influence of injection through the tubes on mass transfer is presented in terms of the ratio of the mass transfer coefficient with and without injection h/h_0 . Note that h_0 is determined in the absence of the injection tubes as well. Figure 2 contains plots of the relative mass transfer with distance downstream at different lateral positions, Z . Each part of the figure is for a different blowing rate. The position $X = 0$ corresponds to the downstream edge of the injection holes and $Z = 0$ to the center of a hole.

The results are also plotted in contour form in Figure 3 for different blowing rates. These contours were obtained from cross plots of the data shown in Fig. 2. The ellipses in Figure 3 represent the in-

side surface of the injection hole in the plate of the naphthalene. Contours for h/h_0 less than 1.25 are not drawn as they tend to spread out over large areas.

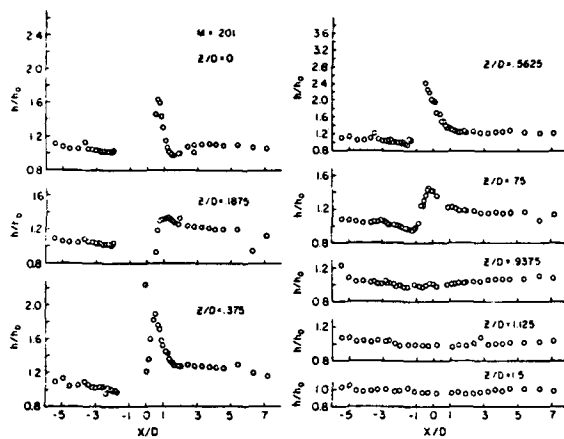
Several special comparison tests were made. One was for $M = 0$; for this experiment the lower portion of each injection tubes was plugged. These results essentially show the effect of the tube opening without any net outflow. A test with the top of the injection hole plugged to give a smooth surface gave results which were very close to that of a continuous surface of naphthalene. The slight difference observed could be explained by the different concentration boundary condition at the plugged hole.

We had postulated that the jets, especially at high blowing rate, might act very much like solid rods blocking the mainstream flow and produce eddies similar to that around a tube in a crossflow. To examine this, another set of mass transfer data was obtained with aluminum rods placed into the injection holes to provide some solid blockage of the mainstream crossflow. The rod extended up into the flow a distance of 50 mm past the downstream end of the naphthalene surface.

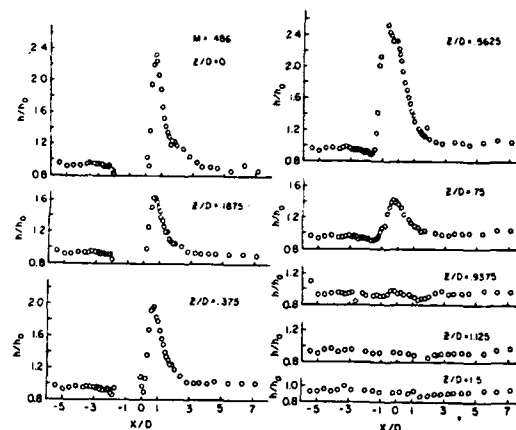
There are few earlier tests that show the effect of injection on heat and mass transfer close to an injection hole. For a row of inclined holes, heat transfer data were obtained [9] no closer than $X/D \sim 5.5$. In that study, there was concern for the effect of heat conduction close to injection. The present results give reasonably good agreement with Ref. [9], particularly at large Z/D . Close to the centerline, somewhat higher values of h/h_0 were found in the present results. This may be due to the difference in Reynolds number, the effect of heat conduction in the tests of Ref. [9], or the lower values of h_0 at a given X/D due to an active surface upstream of the injection holes for this study vs no upstream heating in Ref. [9].

The results shown in Figs. 2 and 3 can perhaps best be described by considering different regions on the surface around an injection hole. Referring to Figure 4, A corresponds to the region upstream of the injection hole, B to a region midway between two holes, C to the region immediately downstream of a hole where a low transfer coefficient was observed, D to the region of high mass transfer coefficient immediately adjacent to an injection hole, E to the region of high transfer coefficient downstream of the injection hole, and F to a region of relatively high transfer coefficient some distance downstream of the injection hole which occurs at the highest blowing rates.

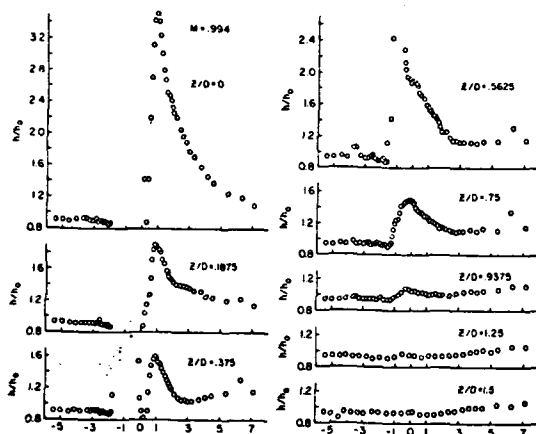
Upstream of the injection hole (region A), the mass transfer is little affected by the presence of the jet. At intermediate blowing rates there is slight decrease of mass transfer, probably due to the slowing down of the mainstream fluid by the jet. At small M there is not enough flow to slow down the mainstream air, while at large M the downstream velocity component of the jets is close to that of the mainstream fluid. With the solid bar (Fig. 2), there is an increase in the mass transfer coefficient close to the bar. This is probably due to secondary flow similar to that observed near cylinders maintained normal to a solid surface. The flow induced by the boundary-layer cylinder interaction sweeps out a re-



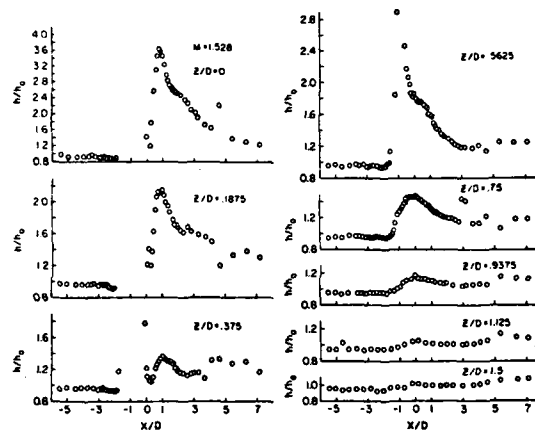
(a) at $M = .2$



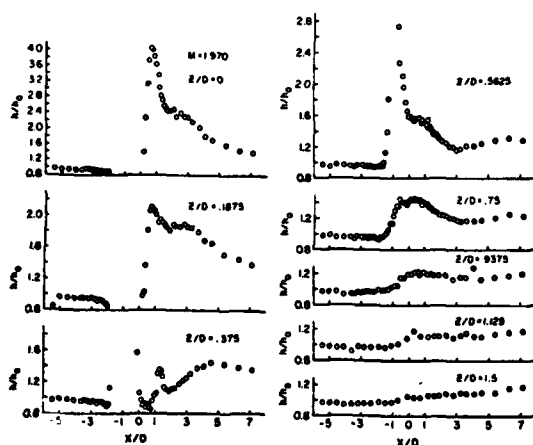
(b) at $M = .49$



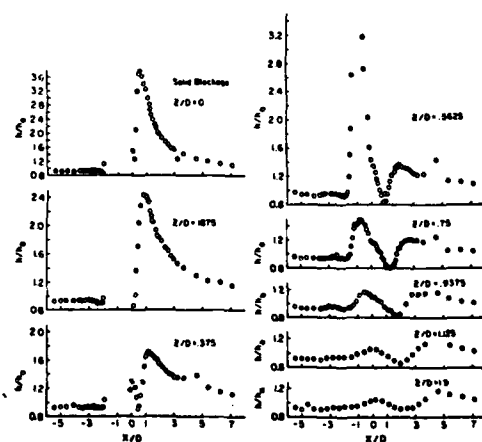
(c) at $M = 1.0$



(d) at $M = 1.53$

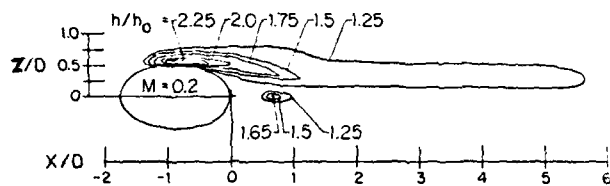


(e) at $M = 1.97$

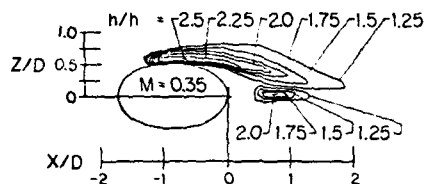


(f) for solid blockage

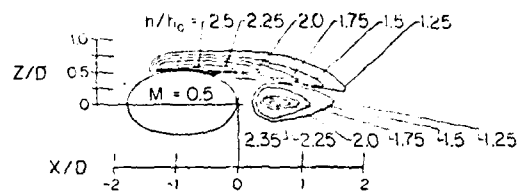
Fig. 2 Mass transfer coefficients



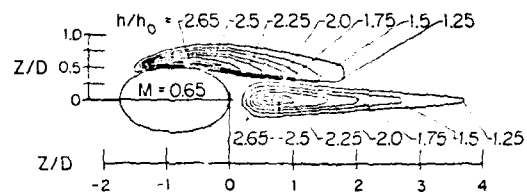
(a) at $M = 0.2$



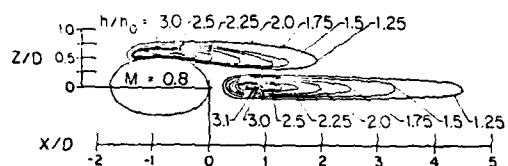
(b) at $M = 0.35$



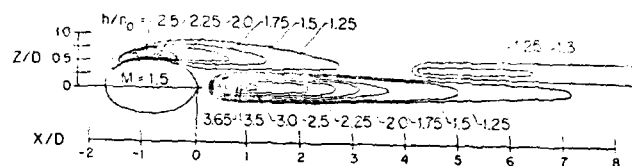
(c) at $M = 0.5$



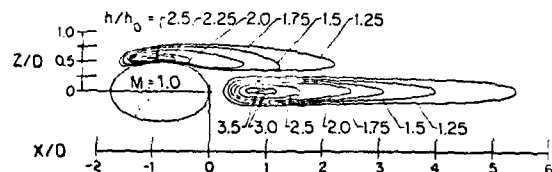
(d) at $M = 0.65$



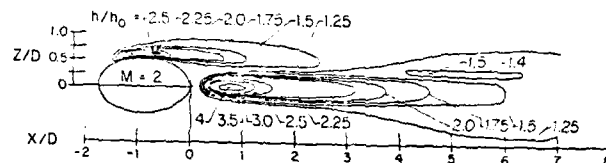
(e) at $M = 0.8$



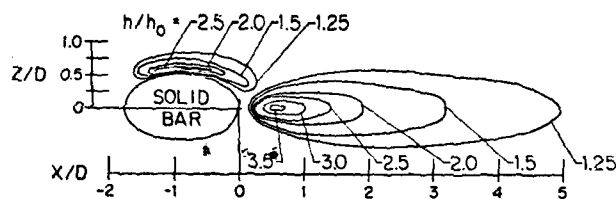
(g) at $M = 1.5$



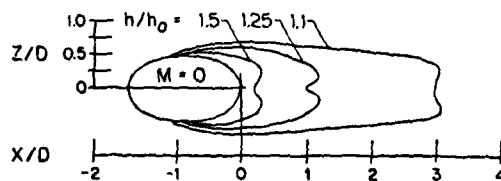
(f) at $M = 1.0$



(h) at $M = 2.0$



(i) for solid blockage



(j) for $M = 0$

Fig. 3 Contours of h/h_0

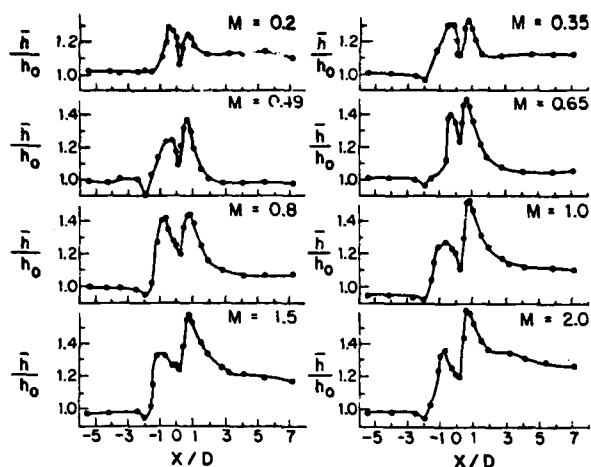


Fig. 5 Average values of h/h_0 at $M = 0.2$ to 2.0

REFERENCES

- Goldstein, R. J., Film Cooling, in Advances in Heat Transfer, eds. T. Irvine and J. P. Hartnett, vol. 7, 1971, pp. 321-379, Academic Press, New York.
- Metzger, D. E. and Fletcher, D. D., Evaluation of Heat Transfer for Film-Cooled Turbine Components, J. Aircraft, vol. 8, 1971, pp. 33-38.
- Metzger, D. E., Kuenstler, P. A., and Takeuchi, D. I., Heat Transfer with Film Cooling Within and Downstream of One to Four Rows of Normal Injection Holes, ASME Paper No. 76-GT-83, 1976.
- Liess, C., Experimental Investigation of Film Cooling with Ejection from a Row of Holes for the Application to Gas Turbine Blades, J. Engr. Power, vol. 97, 1975, pp. 21-27.
- Mayle, R. E. and Camarata, F. J., Multihole Film Cooling Effectiveness and Heat Transfer, J. Heat Transfer, vol. 97, 1975, pp. 534-538.
- Crawford, M. E., Kays, W. M., and Moffat, R. J., Full-Coverage Film Cooling on Flat Isothermal Surfaces: A Summary Report on Data and Predictions, Report No. HMT-30, Dept. of Mech. Engr., Stanford University, 1979.
- Schultz, D. L., Oldfield, M. L. G., and Jones, T. V., Heat Transfer Rate and Film Cooling Effectiveness Measurements in a Transient Cascade, AGARD-CPP-281, 1980.
- Louis, J. F., Shock Tunnel Studies of Heat Transfer and Film Cooling Effectiveness, Proceedings of the 10th Int. Shock Tube Symposium, Kyoto, Japan, vol. 5, 1975, pp. 452-471.
- Eriksen, V. L. and Goldstein, R. J., Heat Transfer and Film Cooling Following Injection through Inclined Circular Tubes, J. Heat Transfer, vol. 96, 1974, pp. 239-245.
- Jabbari, M. Y. and Goldstein, R. J., Adiabatic Wall Temperature and Heat Transfer Downstream of Injection through Two Rows of Holes, J. Eng. Power, vol. 100, 1978, pp. 303-307.
- Goldstein, R. J., Rask, P. B., and Eckert, E. R. G., Film Cooling with Helium Injection into an Incompressible Flow, Int. J. Heat Mass Transfer, vol. 9, 1966, pp. 1341-1350.
- Kacker, S. C. and Whitelaw, J. H., The Dependence of the Impervious Wall Effectiveness of a Two-Dimensional Wall-Jet on the Thickness of the Upper Lip Boundary Layer, Int. J. Heat Mass Transfer, vol. 10, 1967, pp. 1623-1624.
- Pedersen, D. R., Eckert, E. R. G., and Goldstein, R. J., Film Cooling with Large Density Differences Between the Mainstream and the Secondary Fluid Measured by the Heat-Mass Transfer Analogy, J. Heat Transfer, vol. 99, 1977, pp. 620-627.
- Christian, W. J. and Kezios, S. P., Experimental Investigation of Mass Transfer by Sublimation from Sharp-Edged Cylinders in Axisymmetric Flow with Laminar Boundary Layer, 1957 Heat Transfer Fluid Mechanics Institute, 1957, pp. 359-381, Stanford University Press, Stanford.
- H. H. Sogin, Sublimation from Disks to Air Streams Flowing Normal to Their Surfaces, Trans. ASME, vol. 80, 1958, pp. 61-69.
- K. Lee and H. Barrow, Transport Processes in Flow Around a Sphere with Particular Reference to the Transfer of Mass, J. Heat Mass Transfer, vol. 11, 1968, pp. 1013-1026.
- Kan, S., Miwa, K., Morishita, T., Munakata, Y., and Nomura, M., Heat Transfer of a Turbine Blade, JSME-30, 1971.
- Saboya, F. E. M. and Sparrow, E. M., Local and Average Transfer Coefficients for One-Row Plate Fin and Tube Heat Exchanger Configurations, J. Heat Transfer, vol. 96, 1974, pp. 265-272.
- Ramsey, J. W. and Goldstein, R. J., Interaction of a Heated Jet with a Deflecting Stream, J. Heat Transfer, vol. 93, 1971, pp. 365-373.

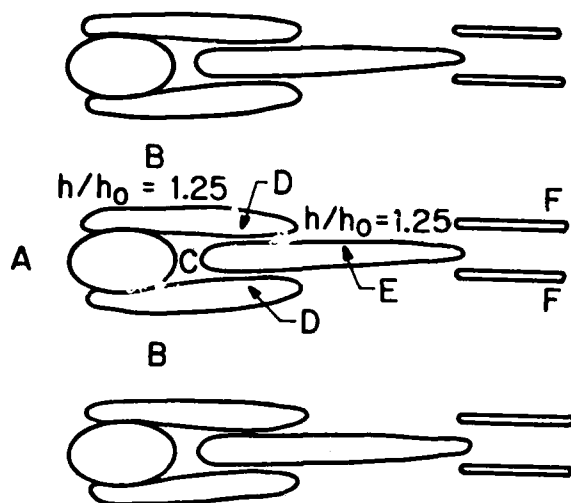


Fig. 4 The pattern of high transfer areas around the injection holes

gion upstream of the cylinder. The effect would be smaller with a cylinder inclined downstream.

In the central area between the holes (region B), injection has little effect on the mass transfer coefficient except at the highest blowing rates. Even then the increase is only of the order of 10%, which may be due to mainstream acceleration caused by jet blockage.

Immediately downstream of the injection hole (region C), relatively low mass transfer rates occur. The minimum occurs at 0.2 to 0.3 diameters downstream for most M . For zero blowing rate, however, there is actually a maximum value at the edge of the injection hole downstream edge. The reduced mass transfer in region C for most M can be explained by the action of the jets creating a stagnation region immediately downstream of injection. The blowing rate has little effect on this region.

For all flow rates other than $M = 0$, there is an area (region D) of very high mass transfer coefficient along the sides of the injection hole which extends some distance downstream (cf., Fig. 3). This high mass transfer results from the jet mainstream interaction in large shear stresses and eddies at the edges of the jets. A similar result occurs with solid blockage.

Region D (defined by the $h/h_0 = 1.25$ contour) extends from $X/D \approx -1.2$ to $X/D \approx 6$, at $M = 0.2$. At $M = 0.5$, this length is considerably smaller but gradually increases as M is increased above this point. The minimum in the extent of region D may be due to lift-off of the jet from the surface. The maximum value of h/h_0 along the sides of the injection holes is between 2.5 and 3.0 for most M . This maximum usually occurs between X/D of -1 and -0.5 . The narrow width of the high mass transfer coefficient region suggests the scale of the eddies created by the jet-mainstream interaction. This region of high mass transfer extends considerably further downstream with the jets as contrasted to solid blockage.

Downstream of the injection hole (region E), the maximum mass transfer occurs at $X/D \approx .75$ for most values of M and at $X/D \approx 0.55$ for solid blockage. The maximum of h/h_0 in this region increases from 1.65 at $M = 0.2$ to 4.0 at $M = 2.0$; it is 3.5 for solid blockage. As M increases from 0.2 to 0.5, the width of the region (defined by $h/h_0 = 1.25$ contour) increases and then remains about the same at higher M . The length of the region increases from 1.5 to 3.8 diameters downstream as M increases from 0.5 to 0.65. Further increases in M lengthen the region out to $X/D \approx 7.0$ at $M = 1.5$ and past the edge of the naphthalene plate ($X/D = 7.16$) at $M = 2$. The shape of this region is affected by separation of the jet from the surface which begins to occur at $M \approx 0.5$. With separation, the mainstream flow penetrates beneath the jet and forms large eddies which increase the mass transfer. At small M the jet remains attached to the surface and the increase in mass transfer is quite small. At high M the pattern of mass transfer due to the jets is similar to that with solid blockage except that in the former case the downstream region of high mass transfer is narrower.

At high M , (1.5 and 2.0), two areas of high transfer coefficient (region F) are present downstream of injection. This region, symmetrical about the line $Z = 0$, apparently results from the partial reattachment of the jet to the surface. A jet entering a cross stream can form a kidney-shaped cross section with two symmetrical lobes that extend close to the surface [19]. When the flow in these lobes touches the surface some distance downstream of injection, increased wall shear and mass transfer coefficient can occur.

It is also of interest to see how the mass transfer averaged across the span of the plate varies with position and blowing rate. For Fig. 5, averages were obtained by numerically integrating the local mass transfer coefficient measurements across the span. Considering only the area where there was an active surface and not the open area of the injection hole, a characteristic of these plots is the presence of two maxima. One is due to the high transfer coefficients in region D and is at X/D between -1 and -0.5 . The second peak at X/D between 0.5 and 0.9 is chiefly due to the high mass transfer in region E directly downstream of the hole. As the blowing rate increases, the magnitude of the upstream peak stays approximately constant at about 1.35 while the value of the second maximum increases.

SUMMARY

The mass transfer coefficient on a surface near a row of holes through which air is injected has been measured. The measurements indicate large increases in the mass transfer close to the sides of the injection holes (region D) and some distance downstream of the holes (region E). The results also indicate that the influence of the jets at high blowing rates on the mass transfer is similar in many respects to the effect of solid blockage that occurs if a solid rod is placed into the injection hole and extended out into the mainstream.

HEAT TRANSFER IN HIGH-TEMPERATURE GAS TURBINES: Film Cooling and Impingement Cooling

R. J. Goldstein
Mechanical Engineering Department, University of Minnesota
Minneapolis, Minnesota 55455, U.S.A.

ABSTRACT

Film cooling and impingement cooling as used in modern gas turbine systems are described. Both processes lead to three-dimensional turbulent flows which are complex and difficult to analyze. Different experimental techniques, including the use of mass transfer analogies, have been used in studying such flows to permit more accurate measurements and to avoid the necessity of going to a high-temperature hostile environment in the laboratory. The present paper primarily describes research that has been performed in the Mechanical Engineering Department of the University of Minnesota.

NOMENCLATURE

D	= injection hole diameter
h	= heat transfer coefficient
h_0	= heat transfer coefficient in absence of injection
I	= momentum flux ratio
K	= acceleration parameter
M	= blowing rate ($\rho_2 u_2 / \rho_\infty u_\infty$)
Nu	= Nusselt number
Re_D	= Reynolds number ($u_\infty D / \nu_\infty$)
Re_j	= $u_2 D / \nu_2$
S	= spacing between injection holes
T	= temperature
T_{aw}	= adiabatic wall temperature
T_r	= recovery temperature of mainstream
T_w	= wall temperature
T_2	= temperature of injected fluid
T_∞	= temperature of mainstream
u_2	= velocity of injected (coolant) fluid
u_∞	= velocity of mainstream
X	= distance downstream from trailing edge of injection hole
Y	= distance normal to surface
Z	= position along span, measured from center of injection hole
α	= angle between injected flow and mainstream
δ^*	= momentum thickness of boundary layer
ρ_2	= density of injected fluid
ρ_∞	= density of mainstream fluid
η	= film cooling effectiveness
η_{CL}	= film cooling effectiveness at $Z=0$
$\bar{\eta}$	= film cooling effectiveness averaged over the span
θ	= $(T - T_\infty) / (T_2 - T_\infty)$

ν_2 = viscosity of injected fluid
 ν_∞ = viscosity of mainstream fluid

INTRODUCTION

Gas turbine engine designs have progressed to higher and higher temperatures at the inlet to the turbine section. In some systems, this inlet temperature is higher than the melting point of the turbine blades. Thus, some means must be provided to protect the blades and maintain them at temperatures not only below their melting point but sufficiently low to ensure long operating life in the face of extreme temperature gradients and the potential of stress rupture and creep.

On stationary gas turbine systems, various coolants may be employed to maintain moderate temperatures on the exposed surfaces. One design under consideration uses water cooling. If the blade is only cooled internally, however, the temperature drop across the blade skin—even with ideal cooling—may be so high that the external temperature of the blade surface may be at an unacceptable value. With water-cooling systems, a very thin skin is used and relatively low temperature water serves as the coolant.

For an aircraft engine, the only coolant generally available is the air that flows through the engine. This usually is taken off at some stage of the compressor, often at the last stage, and thus is already at a somewhat elevated temperature. In addition, because of the relatively poor heat transfer characteristics of air, internal convection cooling may not be sufficient. Often some means must be taken to reduce the heat flow from the hot gas to the outside surface of the blade itself.

Figure 1 shows a high-performance turbine blade for a modern engine [1]. Rather than a simple solid blade, the inside is a complex geometry of flow passages to provide different types of cooling. Near the leading edge region of the blade the external heat transfer is very high: an impingement system provides an array of jets which strike the inside surface in this region. These jets provide a relatively high internal convection heat transfer coefficient. The spent air from the jets can then flow out through film cooling holes. The injected (or coolant) air provides considerable heat transfer during its flow

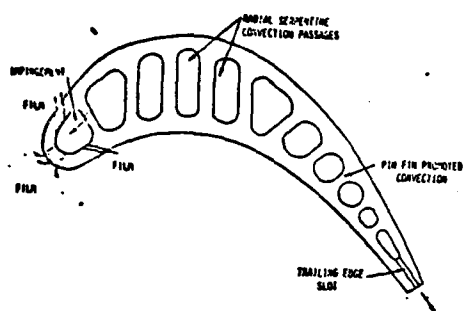


Figure 1 Typical High Pressure Turbine Blade Using a Combination of Film, Impingement, and Promoted Convection Cooling [1]

through the skin of the blade, particularly in the leading edge region. In terms of film cooling action upon injection to the external flow, the coolant should be kept close to the surface where it serves as an insulating layer between the surface and the hot gas flowing over it. In addition to the leading edge region, film cooling holes are often provided on both the pressure and suction sides of the blade. In the aft region of the blade, internal convection cooling includes the use of pin fins. These promote the heat transfer in the trailing edge region of the blade.

The air that is used for cooling is supplied by the compressor. If not used for cooling, it could flow through the compressor and turbine stages, providing more engine output. Design practice calls for using as little cooling air as possible to maximize the throughflow to the combustor and turbine. In addition, the air injected by film cooling or out the trailing edge of the blades should not decrease too greatly the aerodynamic efficiency of the turbine.

The work to be described primarily concerns film cooling research conducted at the Mechanical Engineering Department at the University of Minnesota. Developments to measure film cooling effectiveness and heat transfer following coolant injection are described. Research has also been done on impingement cooling in the presence of crossflow, either from a separate air stream or from an upstream set of injection holes.

FILM COOLING

If only internal air cooling is used, the temperature drop across the skin of a gas turbine blade may be too high. Thus, in many systems, some means of reducing the heat flow to the outside of the turbine blade must be provided. This can be done with film cooling, in which relatively cool air is injected close to the surface of the blade. This air flows downstream along the surface, acting as an insulating layer and separating the hot gas stream

from the turbine blade. Another way of looking at the film coolant is that it tends to decrease the temperature in the boundary layer and thus reduces the heat flow to the blade surface. The flow through injection holes also provides more internal cooling of the blade skin. This is particularly important in the leading edge holes which are often designed to have a fairly large length-to-diameter ratio.

Different injection systems have been used for film cooling [2]. In what has come to be called two-dimensional film cooling, a continuous slot (across the span of the system) is used to inject fluid. Various types of step-down slots, angled injection, and flow through porous regions along a wall have been used (Figure 2). These two-dimensional systems are usually quite effective, as the continuous flow of coolant across the span is, essentially, impressed down upon the wall by the mainstream flow, providing effective protection of the surface. However, such geometries are not feasible in many systems—such as in gas turbine blades. In these, a series of discrete injection holes is required for the proper structural characteristics; either a single row or multiple rows of holes can be used. With full surface film cooling there is a two-dimensional array of injection holes along the surface of the blade, a system that approaches transpiration cooling.

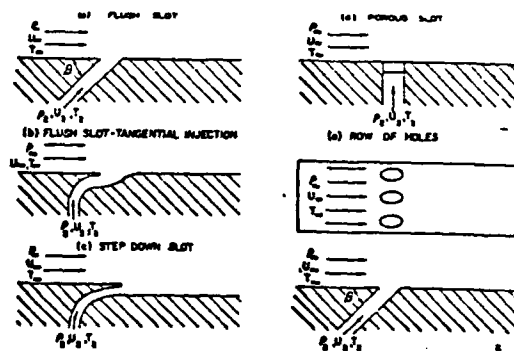


Figure 2 Film Cooling Geometries

With discrete hole injection—for example, through a single row of angled injection holes—the film cooling performance is often far worse than with a continuous slot. The resulting three-dimensional flow (three-dimensional film cooling) can permit individual jets of injected fluid to penetrate through the boundary layer into the mainstream. The injected fluid, then, is not close to the surface which it is intended to protect. Mainstream flow can go around the jet and heat or overheat the surface which it is supposed to protect.

Figure 3 is a representation of the flow following injection at relatively high blowing rate, M —in this case, through a

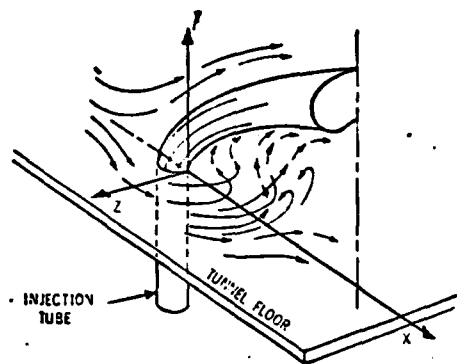


Figure 3 Sketch of Half-Jet Based on Tuft Observations

single hole normal to the surface. The jet takes on a kidney-like shape with mainstream flow going around and under the jet.

Figure 4 shows the temperature profiles downstream of a single normal jet [3]. Note that when the flowing rate is fairly small, the jet appears to remain very close to the surface. As the blowing rate increases, the jet lifts away from the surface, with the center of the jet considerably elevated and rising continually as it goes downstream. Figure 5 shows contours of constant temperature at various positions downstream of a single injection hole [3]. Note the kidney-shaped profile of the isothermal lines. From these profiles, high blowing rate injection would not be expected to provide good film cooling performance because the coolant is away from the surface.

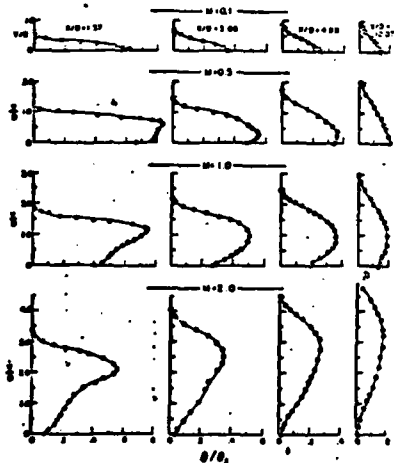


Figure 4 Temperature Profiles for 90 Deg Injection Angle, $Z/D=0$

The interaction of a jet entering at some angle to the mainstream can result in very large eddies of the order of size of the jet diameter or greater. This large-scale interaction makes analytical prediction of the flow and heat transfer along the wall quite difficult. Figure 6 shows the flow interaction of a jet entering normal to a

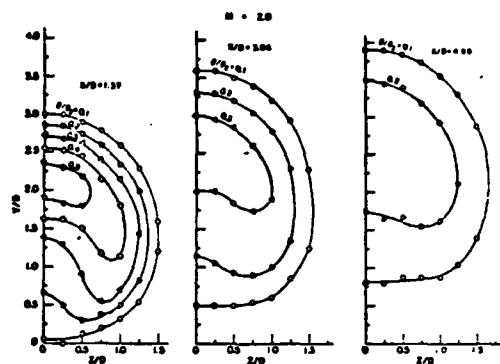


Figure 5 Constant-Temperature Contours for 90 Deg Injection Angle, $M=2.0$

fluid stream [4]. Greater penetration is observed at the large blowing rates. The short-time exposure photos show the large scale of the eddy motion of the flow. It is not apparent from the picture that there is an actual "lift-off" of the jet at high blowing ratio as is indicated in Figs. 3-5. Lift-off does occur, although at times the eddies from the jet do touch down upon the surface.

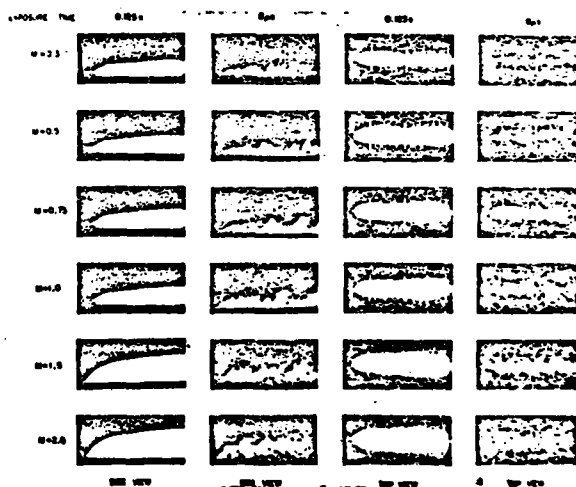


Figure 6 Photographs of Jet in Crossflow with Normal Injection

Many of the figures shown previously represent flow from a single jet entering a mainstream. In practice, of course, at least a row of jets is used in film cooling. In addition, the injection is generally not normal but inclined as close to the wall as possible. This tends to keep the jet closer to the surface. Design limitations, however, often preclude the jets being at angles smaller than 30 or 35 degrees from the surface.

In determining the effectiveness of protection that film cooling affords, different parameters can be used. A common and convenient one is a measure of the adiabatic

wall temperature, T_{aw} . This is the temperature of a wall downstream of film cooling, assuming the wall is truly adiabatic, without any heat passing through it. It is the limiting temperature that the wall would reach and permits the use of a simple and convenient dimensionless parameter, the "film cooling effectiveness",

$$\eta = \frac{T_{aw} - T_r}{T_2 - T_r} \quad (1)$$

The adiabatic wall temperature provides a reference that can be used in defining a heat transfer coefficient,

$$q = h (T_w - T_{aw}) \quad (2)$$

Far downstream the dimensionless film cooling effectiveness would generally approach zero while near injection, at least with two-dimensional film cooling, T_{aw} is close to the injection temperature and the effectiveness is close to unity.

The film cooling effectiveness is a function of many variables, including the geometry of the injection system, the properties of the mainstream and injection fluids (in particular, the density difference if the two are the same chemical composition), the position along the surface, and the blowing parameter, M , or the momentum flux ratio, I .

Though not the only possible definition for h , the one given by Equation 2 is convenient. When the wall temperature approaches the adiabatic wall temperature, h maintains its finite value. Far downstream the heat transfer coefficient should approach that due to the mainstream flow alone. This latter property has often been found to be the case, even relatively close to injection for small and moderate blowing rates.

Figure 7 shows the variation of the adiabatic wall temperature (film cooling effectiveness) with blowing rate for injection through tubes inclined at an angle of 30 degrees to the wall surface [5]. The effectiveness is determined along a line downstream of the center of an injection hole ($Z=0$). Note the maximum effectiveness occurs at a blowing parameter of approximately 0.5. There is relatively close agreement between the results for single hole injection and for a row (across the span) of holes, at least at low and moderate blowing rates and small distances downstream. As more mass is injected through the injection holes (M larger), one might expect more flow along the surface to act as an insulating layer or more mass to reduce the temperature in the boundary layer. However, at sufficiently high blowing rates the jet tends to leave the surface, resulting in poor effectiveness. With a row of holes at high blowing rates, the jets can merge together some distance downstream and be partially turned towards

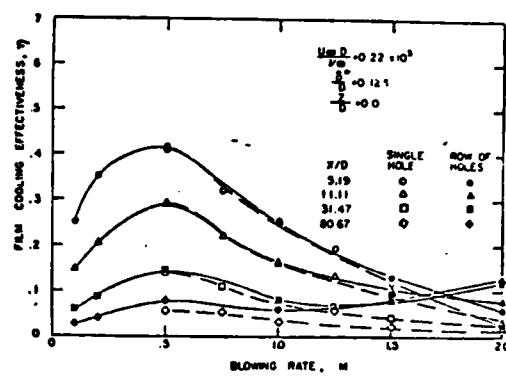


Figure 7 Effect of Blowing Rate on Centerline Film Cooling Effectiveness for Single Hole and Multiple Hole Injection at an Angle of 35 Deg with the Flow

the wall, resulting in an increase of effectiveness with M at large X .

Strictly speaking, the results shown in Fig. 7 are only valid for a density ratio, p_2/p_∞ , close to unity. To study the influence of larger variations in the density of injected gas compared to that of the mainstream, an injection temperature very different from that of the main flow could be used. This is what occurs in many applications where the absolute temperature of an air-free stream may be 1-1/2 to 2-1/2 times that of injected coolant air, resulting in very large density differences. The use of a mass transfer analogy permits a study of the effect of density ratio on film cooling at moderate (room) temperature. With this system [6], instead of injecting a hotter or colder gas through the injection holes, air mixed with another gas—either a tracer, to have a density ratio of approximately unity, or a large concentration of the other gas, to have a density higher or lower than that of air—is used. Downstream of injection, a wall concentration, rather than a wall temperature, is measured. This wall concentration leads to an impermeable wall effectiveness which can be shown to be equivalent to the film cooling (thermal) effectiveness [6,7].

The effect of density on film cooling can be observed in Figure 8 [6]. For varying injection rate, the maximum of effectiveness appears to occur at a fixed ratio of the velocity of the injected fluid to that of the mainstream fluid. Note that the figure shown is specific to the injection geometry used, a single row of holes inclined at approximately 35 degrees to the mainstream.

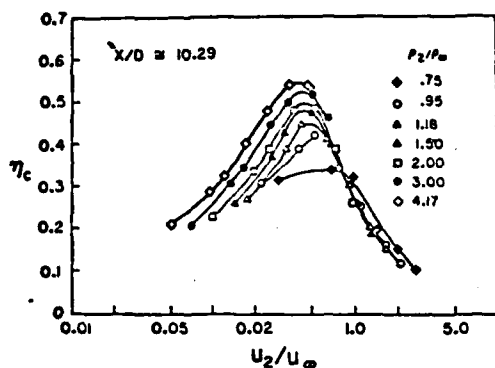


Figure 8 Effect of Injection Velocity On the Center-Line Effectiveness for Injection Through a Row of Inclined Holes, $Z/D=0$

An important goal is reducing the effect of blow-off on film cooling effectiveness. Essentially this means preventing, or delaying, blow-off so that it does not occur at the values of blowing rate or velocity ratio used in many applications. At least two designs to prevent or reduce blow-off have been tried. One involves the use of multiple rows of holes. With two staggered rows of holes, as shown in Figure 9, the jets emanating from the upstream row tend to fill the space between the jets from the downstream row. This provides more blockage across the span of the tunnel by the jets, affording less possibility for the mainstream fluid to go around and underneath the jets. The jets are essentially pressed down, maintaining the coolant flow along the wall. The resulting improvement in effectiveness is shown in Figure 10, where the film cooling performance of a single row of holes is compared to that of two staggered rows [8].

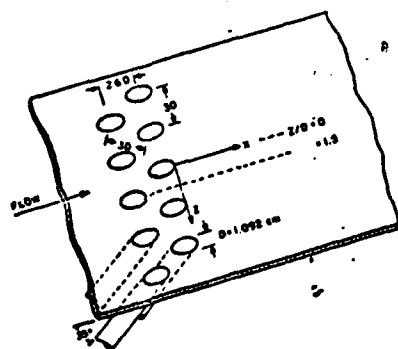


Figure 9 Film Cooling Injection with Two Staggered Rows of Holes

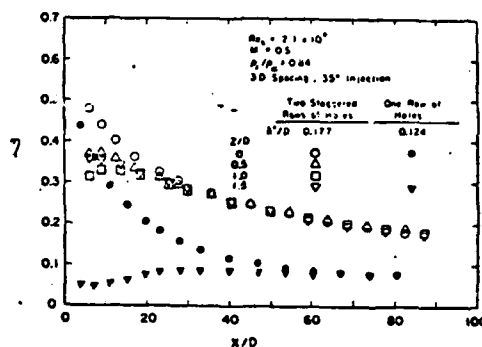


Figure 10 Local Distribution of Effectiveness for $M=0.5$

Another means of having the injected jets stay close to the wall and not penetrate into the mainstream involves changing the simple geometry of a round tube. The tubes are widened near their exit and a fairly straight lip is used as the downstream edge of the hole. This is to simulate the geometry that produces a two-dimensional jet where, in the absence of a mainstream, a Coanda-type effect might cause the injected flow to follow more closely the surface downstream of injection [9]. Figure 11 shows flow following injection through a round cylindrical hole and through the special widened or shaped hole. Note that both in the absence and presence of a crossflow or mainstream flow, the jet leaving the shaped hole tends to stay closer to the surface, which should give better film cooling performance. Figure 12 shows that, indeed, superior film cooling performance occurs with the shaped hole, particularly at the high blowing rates, where the jets from the straight holes tend to lift off the surface [9].

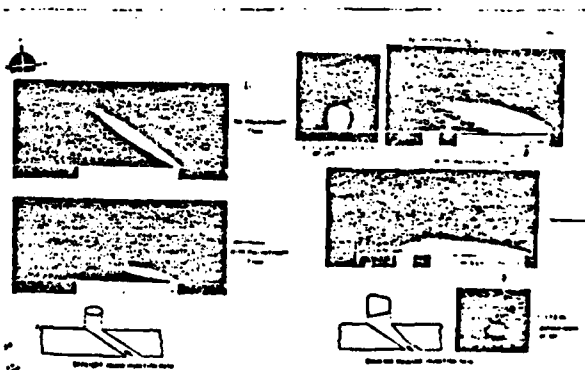


Figure 11 Flow Visualization Study of Jets Leaving a Cylindrical or Shaped Channel

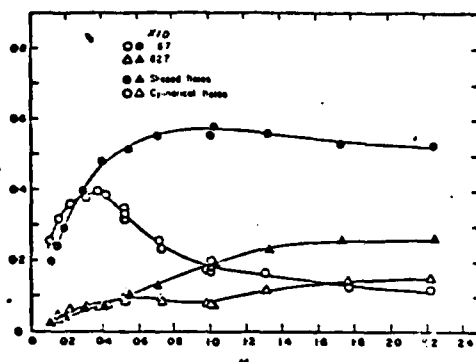


Figure 12 Centerline Effectiveness As a Function of Blowing Rate For Injection of Air Through Straight Round Holes and Shaped Holes, Row of Holes on 3 D Spacing

The results for film cooling described above refer to a flat surface at and downstream of injection. However, in many applications, including those on a turbine blade, the mainstream flows over a curved surface. There might be little difference in the film cooling on such a surface following a two-dimensional slot. With flow through discrete holes, however, film cooling is strongly affected by surface curvature.

Consider the flow of a jet along with a mainstream around a curved surface. For simplicity, assume the velocity of the jet is in the same direction as the mainstream. Above a convex surface, the pressure in the mainstream flow increases with distance from the wall. Thus, a jet of relatively low momentum (compared to the mainstream) might be pushed by this pressure gradient towards the wall, tending to provide good film cooling. If the jet had a high momentum flux relative to that of the free stream, the jet might tend to leave the surface on the convex wall, giving relatively poor film cooling. Just the opposite would be expected to occur on a concave wall, where, at relatively low velocity or momentum flux, the jet could be "pushed" away from the surface by the higher pressure near the surface. At high momentum flux ratios on the concave surface, the jet might be expected to impinge on the surface downstream of injection, yielding good film cooling.

Experiments were performed with a turbine cascade in which the geometry of the blades corresponded to a current design [10]. The mass transfer analogy was used to obtain an impermeable wall effectiveness on the pressure (concave) and suction (convex) sides of a blade. A comparison of these results with results obtained previously for film cooling on a flat surface is given in Figure 13. Note that at low blowing rates (actually, momentum flux ratio in

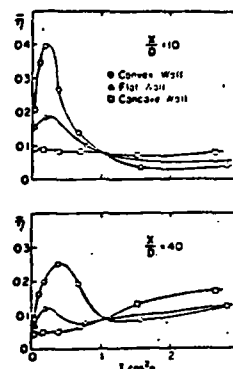


Figure 13 Average Film-Cooling Effectiveness As a Function of $I \cos^2 \alpha$ for $\rho_2/\rho_\infty = 0.95$

mainstream direction), there is considerably better film cooling performance on the convex surface than on the flat surface, while at higher blowing rates, where the jet would tend to move away from the surface, the convex surface gives the poorer film cooling performance. Just the opposite occurs on the pressure (concave) side of the blade, where, at a low momentum flux ratio, the jet is "pushed" by the pressure gradient away from the surface, giving relatively poor film cooling effectiveness.

The influence of curvature on film cooling is very important with a single jet or a single row of jets. This has not always been considered when predicting cooling performance on turbine blades. Curvature would not be expected to have as great an influence on film cooling from two staggered rows of holes where the jets tend to merge and act more like a continuous slot.

Other parameters that have been studied relative to their influence on film cooling include freestream acceleration [11], freestream turbulence [12], and the laminar versus turbulent nature of both the injected coolant flow and the boundary along the surface [13]. Modest acceleration of the mainstream flow does not have a great effect on film cooling. At low blowing rates, high turbulence mixing decreases somewhat the effectiveness along the center line of the injection hole. Freestream turbulence intensity does not significantly alter the lateral distribution of effectiveness, while changing the turbulence scale does affect it considerably. When the coolant flow in the injection hole is laminar, the effectiveness is lower than that following turbulent injection. This lower effectiveness, particularly at blowing rates near where lift-off tends to occur, is apparently due to the peaked nature of the velocity profile with laminar flow.

The influence of coolant injection on the heat transfer coefficient is shown in Figure 14, where the heat transfer coefficient is compared to that which would occur in the absence of blowing [14]. Note that at low blowing rates, the heat transfer coefficient is close to that found for zero blowing, as is also true some distance downstream, even at quite high blowing rates. The results on this figure were taken with actual heating of the surface downstream of injection. With heating, it is difficult to get accurate values of the surface heat flux close to the injection hole through which the coolant flows. Thermal conduction through the wall can lead to significant errors in measurement of the local heat transfer at small distances downstream of injection.

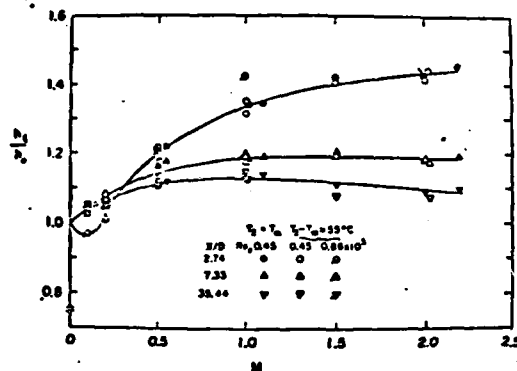


Figure 14 Variation of the Center-Line Heat Transfer Coefficient With Blowing Rate

As an alternate technique, a mass transfer analogy using the sublimation of naphthalene was used [15]. Measurements of the relative mass transfer rate close to injection can then be taken. Figure 15 shows the high mass transfer coefficients that occur in the vicinity of the injection hole. Values many times that obtained in the absence of injection occur both immediately adjacent to the hole and immediately downstream of the hole. It is important to know the heat transfer coefficients in this region because of their influence on the thermal stresses that are produced by temperature gradients along the surface.

IMPINGEMENT COOLING

In many applications, very high local heat transfer can be obtained with impingement of one or more jets onto a surface. Such impingement heat transfer is used in cooling of many systems, including the leading edge region of a turbine blade (cf. Fig. 1).

The high heat transfer in the impingement region is primarily due to the high velocity and thin boundary layer that occur there. Much of the early work on impinge-

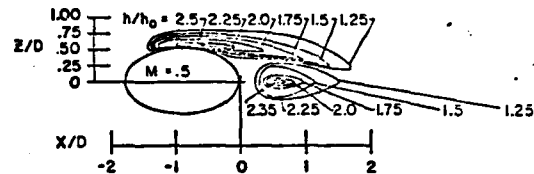


Figure 15 Contours of Constant Values of h/h_0 for $M = 0.5$

ment heat transfer was concerned with flow from a single round jet or from a two-dimensional slot into a still atmosphere. The influence of crossflow on impingement heat transfer, however, is important in many applications. Figure 16 shows the flow of an impinging jet with various crossflows at right angles to the jet [16]. At low values of the crossflow (high values of the flow parameter, M), the jet impinges almost directly across from its exit hole. As the jet flow relative to the main flow decreases, it is turned in the downstream direction until at sufficiently low jet velocity it appears not to impinge at all on the opposing surface.

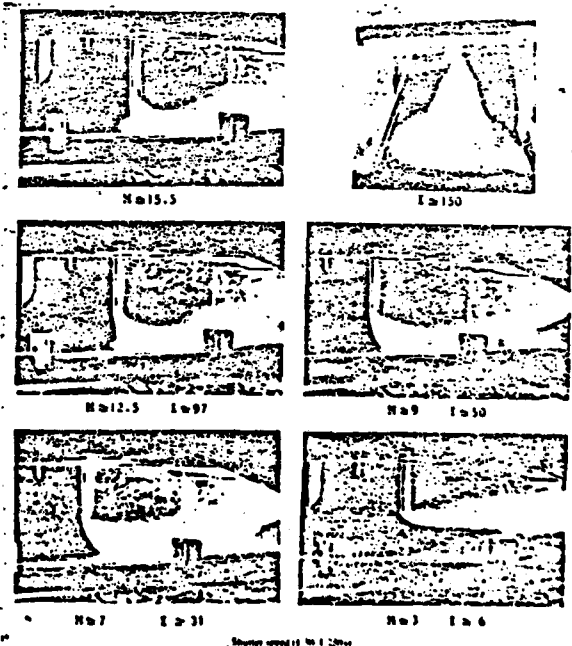


Figure 16 Impinging Jet flow for Jet-to-Wall Spacing of Six Diameters

In measuring heat transfer with an impinging jet, care must be taken because of the high rates of heat transfer and, therefore, small temperature differences that occur in the region of impingement. In addition, the recovery temperature along the wall is not easy to predict. Recovery factors, both greater and less than unity, are measured in the impinging region. The heat transfer coefficient should be defined using the temperature of the wall minus the recovery temperature.

Figure 17 shows the influence of crossflow on impingement heat transfer [16]. At relatively low crossflow, or high jet velocity, the maximum heat transfer is directly opposite the center of the injection hole. As the injection velocity decreases for a fixed mainstream flow, the peak heat transfer decreases and the location of the peak moves in the downstream direction.

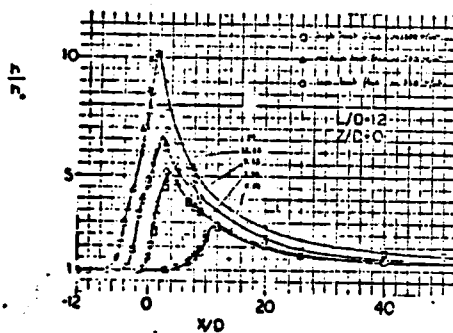


Figure 17 Heat Transfer Coefficient For Jet Impingement With Crossflow

In many applications, a row of jets, or perhaps a two-dimensional array of jets is used to cool a surface. With a two-dimensional array there is often a crossflow from the spent air of the upstream jets. The heat transfer from one such two-dimensional array made up of five rows of holes is shown in Figure 18 [17]. With this array the crossflow is produced by the upstream rows of jets. The maximum heat transfer at the first row of holes is somewhat less than at the second and third rows, while the peak heat transfer for the fourth or fifth row is considerably smaller. In addition, there is a displacement of the maxima in the downstream direction which is readily apparent for the downstream holes. There is also considerable variation of the heat transfer between the holes of an individual row.

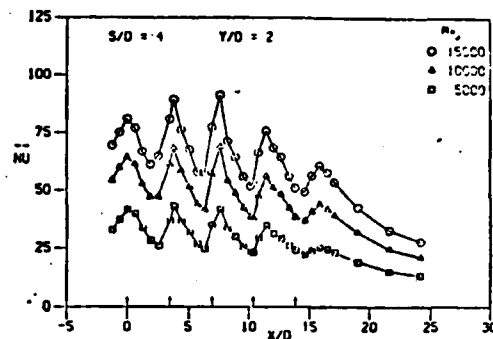


Figure 18 Spanwise Average Nusselt Number For Impingement From An Array of Jets

CONCLUDING REMARKS

We have briefly surveyed studies on film cooling and impingement heat transfer that have been conducted at the University of Minnesota. Flow phenomena related to the interaction of discrete jets with a mainstream are quite complex and far from fully understood. Because of the large structure of the eddies and the resulting complex interactions, it is difficult to develop good analytical or numerical predictions for such flows. Several semi-empirical techniques using turbulent eddy diffusivities have been used and are convenient for developing correlations. These are described in earlier works. Considerably more experimental and numerical work is necessary to fully take into account the influence of such things as surface curvature and injection jet geometry on adiabatic wall temperature and local heat transfer.

ACKNOWLEDGMENT

Support from the Office of Army Research during the writing of this survey is gratefully acknowledged.

REFERENCES

1. Elovic, E. and Koffel, W. K., Proceedings of the 1979 International Joint Gas Turbine Congress and Exhibition, Paper No. G-1(97) (1979).
2. Goldstein, R. J., Advances in Heat and Mass Transfer, vol. 7, pp. 321-379 (1971).
3. Ramsey, J. W. and Goldstein, R. J., J. Heat Transfer, 93, 365 (1971).
4. Goldstein, R. J., Eriksen, V. L., and Ramsey, J. W., Heat Transfer 1978, vol. 5, pp. 255-260 (1978).

5. Goldstein, R. J., Eckert, E.R.G., Eriksen, V. L., and Ramsey, J. W., Israel J Technology, 8, 145 (1970).
6. Pedersen, D. R., Eckert, E.R.G., and Goldstein, R. J., J. Heat Transfer, 99, 620 (1977).
7. Ito, Sadasuke, University of Minnesota Ph.D. Thesis, December 1976.
8. Jabbari, M. Y. and Goldstein, R. J., J. Engr. Power, 100, 303 (1978).
9. Goldstein, R. J., Eckert, E.R.G., and Burggraf, F., Int. J. Heat Mass Transfer, 17, 595 (1974).
10. Ito, S., Goldstein, R. J., and Eckert, E.R.G., J. Engr. Power, 100, 476, (1978).
11. Jabbari, M. Y. and Goldstein, R. J., Heat Transfer 1978, vol. 5, pp. 249-254 (1978).
12. Kadotani, K. and Goldstein, R. J., J. Engr. Power, 101, 466 (1979).
13. Yoshida, Toyooki, University of Minnesota M.S. Thesis, December 1977.
14. Eriksen, V. L. and Goldstein, R. J., J. Heat Transfer, 96, 239 (1974).
15. Taylor, J. R. and Goldstein, R. J., To Be Published.
16. Bouchez, J.-P. and Goldstein, R. J., Int. J. Heat Mass Transfer, 18, 719 (1975).
17. Behbahani, A. and Goldstein, R. J., To Be Published.